Illinois U. Library.

The American Mineralogist

Journal of the Mineralogical Society of America

Vol. 41 MAY-JUNE, 1956 Nos. 5 and 6

Contents

The alkali feldspars. III. An optical and *x*-ray study of high-temperature feldspars . . . . . W. S. MacKenzie and J. V. Smith 405

Physical properties of end-members of the garnet group . . . . . Brian J. Skinner 428

The absorption and refraction corrections and the lattice constant of chromium . . . . . M. E. Straumanis and C. C. Weng 437

An interpretation of the law of Donnay and Harker . . . . . P. Hartman and W. G. Perdok 449

On the composition of some Indian chromites . . . . . P. D. Malhotra and G. H. S. V. Prasada Rao 460

Occurrence and age of chevkinite from the Devil's slide fayalite-quartz syenite near Stark, New Hampshire . . . . . Howard W. Jaffe, Howard T. Evans, Jr., and Randolph W. Chapman 474

Jadeite-bearing metagraywackes in California . . . . . T. W. Bloxam 488

A regularly interstratified chlorite-vermiculite clay mineral . . . . . W. F. Bradley and C. E. Weaver 497

Notes and news: A note on some properties of synthetic montmorillonites . . . . . Rustum Roy and L. B. Sand 505

Optical anomalies in arfvedsonite from Greenland . . . . . Th. G. Sahama 509

Unit cell and space group of barylite . . . . . J. C. Smith 512

Contamination of the characteristic *x*-radiation of copper by Fe, Cr, and Ni radiation . . . . . J. A. Kohn and A. A. Levinson 514

A chart for measurement of optic axial angles . . . . . A. C. Tobi 516

An easy method to obtain *x*-ray diffraction patterns of small amounts of material . . . . . S. A. Hiemstra 519

A joint-free sample splitter . . . . . Charles R. McKinney and Leon T. Silver 521

Validity of "Vegard's law" . . . . . E-an Zen 523

The curved-crystal *x*-ray spectrometer, a mineralogical tool . . . . . Isidor Adler and J. M. Axelrod 524

Incorporation of impurities in synthetic quartz crystals . . . . . J. M. Stanley and S. Theokritoff 527

Book reviews 530

New mineral names 536

EDITOR: WALTER F. HUNT

ASSISTANT EDITOR: LEWIS S. RAMSDELL

BOARD OF ASSOCIATE EDITORS:

IAN CAMPBELL
WILLIAM F. BRADLEY
E. WM. HEINRICH
BRIAN MASON (1956)
FRANCIS J. TURNER (1956–57)
CHARLES L. CHRIST (1956–58)

Published bi-monthly by the Society

Mineralogical Society of America

ASSOCIATED WITH THE GEOLOGICAL SOCIETY OF AMERICA

President: **Clifford Frondel,** Harvard University, Cambridge, Mass.
Vice-President: **D. Jerome Fisher,** University of Chicago, Chicago, Illinois.
Secretary: **C. S. Hurlbut, Jr.,** Harvard University, Cambridge 38, Massachusetts.
Treasurer: **Earl Ingerson,** U. S. Geological Survey, Washington 25, D. C.
Editor: **Walter F. Hunt,** University of Michigan, Ann Arbor, Michigan.
Councillors: **C. Osborne Hutton,** Stanford University, Palo Alto, California.
Felix Chayes, Geophysical Laboratory, Washington, D. C.
Leonard G. Berry, Queen's University, Kingston, Ontario, Canada.
Chester B. Slawson, University of Michigan, Ann Arbor, Mich.
Alfred O. Woodford, Pomona College, Claremont, California.
Harry H. Hess, Princeton University, Princeton, New Jersey.

The enlarged issues of this journal for 1956 are made possible by a grant from the Penrose Fund of the Geological Society of America.

The American Mineralogist—Journal of the Mineralogical Society of America

A journal containing articles on mineralogy, crystallography, petrography, and allied sciences, is issued every two months. Contributions are invited from everyone.

Office of Publication, Mineralogical Laboratory, Ann Arbor, Michigan.

The general conduct of the journal is in the hands of the editor, **Walter F. Hunt,** Ann Arbor, Michigan, to whom all manuscripts should be submitted. To assist the editor the council of the Mineralogical Society has appointed **Lewis S. Ramsdell,** Ann Arbor, Michigan, assistant editor, and the following board of associate editors:

William F. Bradley, Illinois State Geological Survey, Urbana, Illinois.
Ian Campbell, California Institute of Technology, Pasadena 4, California.
Charles L. Christ, U. S. Geological Survey, Washington 25, D. C.
E. Wm. Heinrich, Dept. of Mineralogy, Univ. of Michigan, Ann Arbor, Mich.
Brian H. Mason, American Museum of Natural History, New York, N. Y.
Francis J. Turner, University of California, Berkeley 4, California.

It will expedite publication if two copies of each manuscript are submitted to the editor.

REPRINT PRICE SCALE

Pages	*1–4*	*5–8*	*9–12*	*13–16*	*17–20*	*21–24*	*25–28*	*29–32*	*Covers*
Copies									
25	$6.60	$ 8.80	$ 9.70	$12.00	$14.20	$17.20	$18.80	$19.60	$ 7.60
50	7.00	9.60	11.00	13.40	15.90	19.10	21.00	21.90	8.40
75	7.40	10.40	12.20	14.80	17.60	21.00	23.10	24.20	9.20
100	7.80	11.20	13.50	16.20	19.30	22.90	25.30	26.50	10.00
Add. 100s to 500	3.00	5.00	7.00	8.00	10.00	12.00	13.00	14.00	3.20

Extra charges: Refolioing—$.60 per page; Remaking—$1.25 per page; Cover composition—$3.50 per page; Title page composition—$3.50 per page; Reimposition—$1.00 per page.

Reprint prices for inserts available subject to special quotation. Copies in excess of 500 are subject to special quotations.

Postage is additional in all reprint orders.

Sent to all members and fellows of the Mineralogical Society of America. Membership dues $4.00 annually, fellowship dues $5.00 annually. Subscriptions for libraries, colleges, institutions, companies and similar organizations $6.00 annually.

Entered as second class matter at the post office at Menasha, Wis., under Act of March 3, 1879. Acceptance for mailing at the special rate of postage provided for in section 1103, Act of Oct. 3, 1917, paragraph 4 section 429 P. L. & R. authorized March 13, 1922.

Notice of change of address, orders, and remittances should be sent to Dr. Earl Ingerson, U. S. Geological Survey, Washington 25, D. C.

Printed by the George Banta Company, Inc., Menasha, Wisconsin
Printed in the United States of America

THE AMERICAN MINERALOGIST
JOURNAL OF THE MINERALOGICAL SOCIETY OF AMERICA

Vol. 41 MAY-JUNE, 1956 Nos. 5 and 6

THE ALKALI FELDSPARS. III. AN OPTICAL AND X-RAY STUDY OF HIGH-TEMPERATURE FELDSPARS

W. S. MacKenzie and J. V. Smith,* *Geophysical Laboratory, Carnegie Institution of Washington, Washington, D. C.*

Abstract

A series of high-temperature alkali feldspars has been studied both optically and by *x*-rays. Almost all the specimens appear under the microscope to be optically homogeneous, but *x*-ray studies show that those in the composition range $Or_{60}Ab_{40}$–$Or_{25}Ab_{75}$ are unmixed to some extent. Single-crystal *x*-ray photographs of the unmixed specimens enable the separate phases to be studied, and in some cases the reciprocal lattice angles α^* and γ^* of the sodium feldspar phase can be measured. The values obtained for these angles correspond well with those of single-phase, high-temperature sodium-rich feldspars.

The effect on the mean value of the optic axial angle of heating at 900° C. for 24 hours has been studied and reveals a possible discontinuity in the series near the composition $Or_{60}Ab_{40}$, which has not been previously noted.

Introduction

It has thus far proved impossible to synthesize alkali feldspars with properties corresponding to those of the natural low-temperature[1] minerals, and therefore the complete phase relations in the system $KAlSi_3O_8$-$NaAlSi_3O_8$ have not been determined experimentally. However, field studies supplemented by more detailed laboratory investigations of the natural minerals may make it possible to deduce the sub-solidus relations in this system. Because of the complexity of these relations it has been found necessary to treat separately feldspars from differing geologic environments, and the optical and *x*-ray investigations reported in this paper are part of this systematic study.

Paper I of this series was devoted to a study of the orthoclase-microperthites, the name generally given to optically monoclinic feldspars from supposedly moderate temperature environments. The present paper is concerned with feldspars from high-temperature environments and consists of an optical and x-ray study of twenty chemically analyzed or partially analyzed specimens.[2] The first-named author is responsible for the optical studies and part of the x-ray work, while the contribution of the second author is mainly in the interpretation of the single-crystal x-ray photographs.

---

* Now at the Department of Mineralogy and Petrology, Cambridge University, England.

[1] The use of the term low-temperature implies that, although the feldspar may have crystallized initially at high temperature, it has cooled sufficiently slowly to invert to a low-temperature form. Rapid cooling in a volcanic rock would quench the feldspar in its high-temperature form.

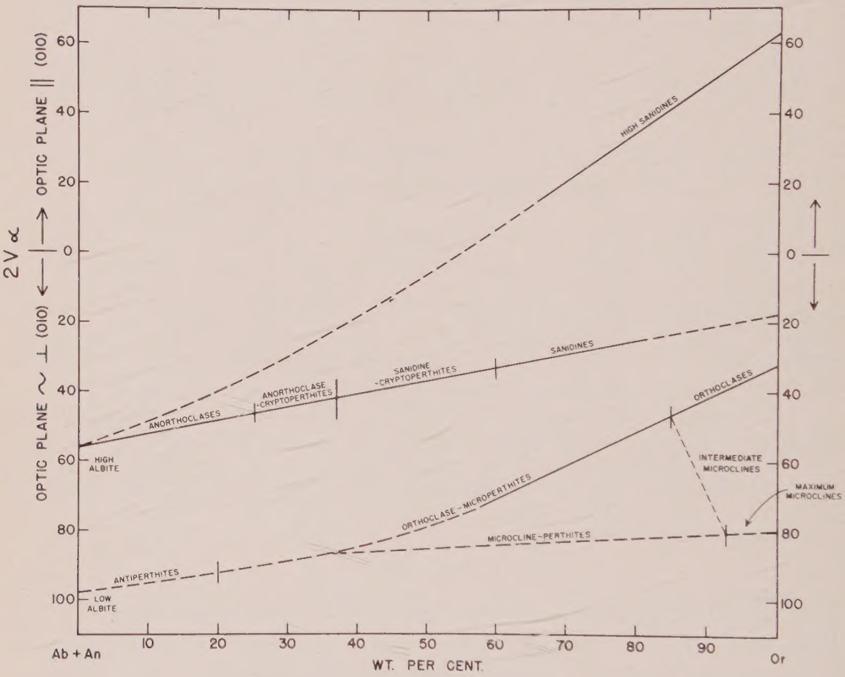

FIG. 1. Diagram showing the relation between optic axial angle and chemical composition in the four series of alkali feldspars (modified after Tuttle, 1952). The parts of each series in which homogeneous specimens occur are separated from those in which the specimens are generally unmixed.

Tuttle (1952) divided the alkali feldspars into four series on the basis of the size of the optic axial angle and the orientation of the optic plane for a known chemical composition. Tuttle's curves relating optic axial angle with chemical composition have been adopted to define four series of feldspars and a slightly modified form of Tuttle's diagram, which was

[2] Two of the specimens studied here (Nos. 16 and 20) are not identical with those on which the chemical analyses were performed but were collected from the same localities as the analyzed samples.

given in paper I of this series, is reproduced again here (Fig. 1) since it is considered the only satisfactory method of classifying the alkali feldspars. Most of the specimens studied belong to the sanidine-anorthoclase-high-temperature albite series. When homogeneous the monoclinic members of this series are known as sanidines and the triclinic members are anorthoclases.[3] The vertical line in Fig. 1 at the composition $Or_{37}(Ab+An)_{63}$ separates the monoclinic from the triclinic feldspars.

The refractive indices of the alkali feldspars vary very slightly both with chemical composition and from one form to another. If the refractive indices are to be used in a study of the alkali feldspars they must be determined with much greater accuracy than is normally achieved.[4] In addition, the small amounts of other elements present, chiefly calcium, affect the refractivity to some extent. Spencer (1937) showed that heating orthoclase-microperthites at 850° C. may cause changes in refractive indices of as much as 0.002 with only very slight or no change in optic axial angle. It is clear from the work of Spencer (1937) and Tuttle (1952) that the most useful optical property for a study of the alkali feldspars is the optic axial angle.

Dr. O. F. Tuttle (personal communication) found that many natural sanidines and anorthoclases showed considerable variation in optic angle in different crystals from the same rock specimen. He also noted that this variation was in some cases reduced by heating the sample at 900° C. for a few hours. To make a more careful study of these effects, values of the optic angle were determined on a series of specimens both in their natural state and after heating at 900° C. for about 24 hours. At least five crystals from each sample were examined to obtain some indication of the variation in optic axial angle both in the heated and the unheated samples.

Many of the specimens studied showed a pale blue schiller in cleavage fragments, although under the microscope they appeared optically homogeneous. *X*-ray powder and single-crystal studies were made of most of the specimens to determine whether or not they were unmixed.

---

[3] A great deal of confusion exists in the literature as to the precise meaning of the term anorthoclase. It is proposed to use the term here to denote a high-temperature alkali feldspar, more sodium-rich than $Or_{37}(Ab+An)_{63}$, which when heated inverts from triclinic to monoclinic symmetry and reinverts to the triclinic form even on rapid quenching. This definition makes possible a distinction between potassium-bearing albites and oligoclases on the one hand and calcium-bearing alkali feldspars on the other hand (see MacKenzie, 1952).

[4] The accuracy of ± 0.001, quoted by some workers for their refractive index determinations can be obtained only if very careful attention is given to control of temperature. In the sanidine-anorthoclase-high-temperature albite series the total change in n_β from $KAlSi_3O_8$ to $NaAlSi_3O_8$ is about 0.011 (Tuttle, 1952).

In all cases the unmixed specimens could be rendered homogeneous by heating at 700° C. for an hour or two and in some cases a few minutes were sufficient. In this respect the high-temperature feldspars differ from the orthoclase-microperthites of intermediate composition, some of which require prolonged heating at 1050° C. before they can be homogenized. The single-crystal *x*-ray photographs permit a more detailed study of the separate phases than do the powder photographs. Measurements made from the single-crystal photograph enable a high-temperature sodium feldspar phase to be distinguished readily from a low-temperature sodium feldspar phase and it has been found that all the sanidine- and anorthoclase-cryptoperthites studied here have a high-temperature sodium feldspar phase, as might be expected. Orthoclase-microperthites generally have a sodium feldspar phase corresponding to low-temperature albite (MacKenzie and Smith, 1955).

METHODS

X-ray powder methods. A Norelco high-angle *x*-ray diffractometer was used for the powder diffraction studies. From the *x*-ray patterns it is possible to determine whether or not a feldspar is unmixed, since unmixed specimens generally have two or more peaks between $2\theta = 21°$ and 22° (approx.) (Cu$K\alpha$ radiation) representing the $\bar{2}01$ reflections for the separate phases (Bowen and Tuttle, 1950).[5] Unmixed specimens were homogenized by heating at 900° C. for approximately 24 hours and then the orthoclase content of each specimen was determined from the spacing of the $\bar{2}01$ reflection (Bowen and Tuttle, 1950). The position of the $\bar{2}01$ reflection was determined using a vein quartz from Lake Toxaway as an internal standard. The $10\bar{1}0$ reflection of quartz at $2\theta = 20.876°$ (Cu$K\alpha$) is suitable for specimens having more than 20% by weight of sodium feldspar in their bulk composition; for more potassium-rich specimens the $\bar{2}01$ reflection of a sample of Amelia albite, Virginia, previously calibrated against quartz was used. The scanning of the *x*-ray diffractometer was set to give a change in 2θ of 0.25° per minute, and the recorder produced a chart in which 2 inches was equivalent to 1° in 2θ. The part of the *x*-ray diffraction pattern required was scanned four times, and the mean value of the angle between the $\bar{2}01$ reflection of the feldspar and the $10\bar{1}0$ reflection of quartz was determined. In the case of unmixed specimens the positions of the $\bar{2}01$ reflections for the separate phases were also obtained where possible. The measurements were reproducible to ±0.02° in 2θ.

---

[5] Tuttle (1952) found that some cryptoperthites show only one $\bar{2}01$ reflection in the powder diffraction pattern, but Laves (1952) noted that this does not necessarily mean that this or other reflections might not be observed by single-crystal techniques. Very slight unmixing may not be detected from the powder pattern and may only be revealed by single-crystal methods.

From the powder diffraction patterns the symmetry of homogeneous feldspars of composition near $Or_{37}Ab_{63}$ can be readily determined since the 111 and $1\bar{1}1$ reflections are coincident for monoclinic symmetry and separate for triclinic symmetry (Donnay and Donnay, 1952).

X-ray single-crystal methods. Single-crystal x-ray oscillation photographs were made from most of the specimens, using a Unicam oscillation camera. Each photograph was taken in the same orientation so that they could be readily compared. Although many alkali feldspars consist of two phases, morphologically they appear as single monoclinic crystals, and the morphology may be used for alignment of the crystals in the x-ray camera. A b-axis oscillation photograph with the (001) cleavage set parallel to the x-ray beam in the center of a 15° oscillation arc was chosen as the standard orientation. Full details of the interpretation of the oscillation photographs and of a rapid method of determining the reciprocal lattice angles α^* and γ^* of the sodium feldspar phase are given in paper II of this series (Smith and MacKenzie, 1955).

Unmixing can be readily detected by the appearance of two or more reflections where a homogeneous monoclinic feldspar would show single reflections. If the unmixing is very slight, indistinct streaks on the x-ray photographs parallel to the layer lines are associated with each reflection.[6] Because of the simplicity of both the crystal setting and the interpretation of the x-ray photograph, the taking of single-crystal photographs has been used as a routine operation in the study of the feldspars.

Optical methods. Optical determinations were made on a Leitz five-axis universal stage. The conoscopic method was used to locate the postion of the optic plane and measure the size of the optic angle. The interference figure was observed using the Bertrand lens, and to obtain the full aperture of the objective a Leitz U. T. 5 sub-stage condenser was employed. The optic angle measurements were made in sodium light, except in a few cases where the optic angle was very small and the greater intensity obtainable with white light was necessary. In every case the optic angle was measured directly, the crystal fragments having been selected so that each showed the points of emergence of both optic axes and both cleavages well developed, i.e. the a crystallographic axis was approximately vertical. Both 45° positions were used in measuring the size of the optic angle, as proposed by Fairbairn and Podolsky (1951), and there is no doubt that this precaution reveals an inaccurate setting of the optic plane. Readings on the outer E–W axis of the universal stage were made three times in each of the 45° positions and the mean value was taken. Optic axial angle measurements given here are reproducible to ±0.5°.

---

[6] Crystals removed from thin sections frequently give diffuse streaks centered on the sharp reflections. These streaks are the result of misorientation of the surface layers caused by grinding and may be distinguished from streaks due to unmixing, since the former lie on curves of constant θ.

A parting approximately perpendicular to the *a*-axis is frequently developed in these high-temperature feldspars and this makes it possible to select crystals which are parallel sided and lie flat on the glass slide although both cleavages are vertical. Crystals of the order of 0.1 mm. in thickness or greater yield very good interference figures on the universal stage.

UNMIXING IN NATURAL HIGH-TEMPERATURE ALKALI FELDSPARS

Table 1 gives a list of the specimens studied with their compositions as calculated from chemical analyses.[7] The orthoclase content of each specimen after homogenization, as obtained from the $\bar{2}01$ spacing, is given for comparison with the results obtained from chemical analyses. In the case of unmixed specimens the orthoclase contents of the separate phases, as obtained from the $\bar{2}01$ spacings, are also given.

All the specimens studied here which contain between 60% and 25% of potassium feldspar in their bulk composition are unmixed to some extent as found in nature; two specimens of composition about $Or_{23}(Ab+An)_{77}$ are also unmixed. It may be noted here that in the low-temperature feldspars it was found that specimens ranging in composition from 84.5% to 19.5% of potassium feldspar were unmixed (MacKenzie and Smith, 1955). In the anorthoclase from Quatre Ribeiras, Azores (No. 15), which was almost certainly derived from a glassy rock (Fouqué, 1883), and in specimen S. C. XX (No. 6) from an obsidian in the San Juan Mountains (Larsen and Larsen, 1938) very slight unmixing was detected only from the single-crystal photographs. The anorthoclase from Grande Caldeira, Azores (No. 14), showed three $\bar{2}01$ reflections in the powder diffraction pattern, indicating the presence of three phases, one of which was found to correspond to the bulk composition of the specimen. This suggests either that the individual phenocrysts are only partially unmixed or, more likely, that some phenocrysts have unmixed more readily than others. The difference in properties of individual crystals from the same rock specimen has been noted frequently in the study of feldspars and will be mentioned further in this paper.

The graph relating the spacing of the $\bar{2}01$ planes with the orthoclase content of alkali feldspars was constructed by Bowen and Tuttle (1950) for a series of synthetic feldspars. Comparison of the orthoclase contents of these natural feldspars as given by chemical analyses with the values obtained using the curve of Bowen and Tuttle, reveals that in fourteen out of twenty specimens the *x*-ray results are within 2% of those given by chemical analyses. Since the chemical analyses are themselves liable to error the agreement may be considered fair. In the case of low-temperature feldspars, however, considerable caution must be taken in using this *x*-ray method to find the orthoclase content, since many perthites can be homogenized only after prolonged heating at 1050° C. and erroneous results may be obtained if the specimens are not completely homogeneous.

---

[7] All compositions are given as weight % of orthoclase, albite and anorthite, and where necessary celsian.

TABLE 1. CHEMICAL COMPOSITION OF FELDSPARS EXAMINED

	Chemical comp.			Comp. from *x*-ray method			Notes on powder diffraction patterns of unmixed specimens
	Or.	Ab.	An.	Bulk Or-content	Separate phases Or.	Or.	
1. Eifel	77.8	21.3	0.9	82.0	homogeneous		
2. Kokomo	72.5	24.0	3.5	76.5	homogeneous		
3. Alder Creek	72.0	25.0	3.0	72.5	homogeneous		
4. Mineral Creek	66.7	30.8	2.5	65.5	homogeneous		
5. Grant County	59.0	40.7	0.3	60.0	82.0	0	
6. S. C. XX	62.0	35.0	3.0	59.5	slight unmixing		
7. Pine Creek Mesa	61.2	36.0	2.8	57.5	72.0	—	No $\bar{2}01$ reflection for sodium phase
8. Nathrop	60.4	37.5	2.1	57.5	81.5	0	
9. Sparling Gulch	49.2	47.0	3.8	48.0	87.0	0	
10. Spring Creek	44.3	52.2	3.5	44.0	86.0	0	
11. Mitchell Mesa	42.9	56.3	0.8	44.0	92.0	0	
12. Old Baldy Mt.	41.5	55.5	3.0	42.5	95.0	0	
13. Cebolla Creek	40.3	57.6	2.1	39.0	88.0	0	
14. Grande Caldeira	31.7	66.5	1.8	31.5	56.0	8.0	In the unmixed specimen a third $\bar{2}01$ reflection gives a composition of Or_{31}
15. Quatre Ribeiras	31.9	64.7	3.4	30.5	slight unmixing		
16. Mt. Franklin	24.9	67.5	7.6	25.0	homogeneous		
17. Victoria	23.3	75.5	1.2	23.0	—	5.5	No $\bar{2}01$ reflection seen for potassium phase
18. Brownhills	25.7	70.8	3.5*	22.5	homogeneous		
19. Ropp	23.0	69.2	7.8†	21.0	—	8.0	No $\bar{2}01$ reflection seen for potassium phase
20. Mt. Anakie	18.2	75.1	6.7	19.5	homogeneous		

* Includes 0.8% Cs.

† Includes 0.3% Cs.

References

Specimens 1, 2, 5 and 17, Kracek and Neuvonen (1952).
Specimens 3, 4, 6, 7, 10, 12 and 13, Larsen and Larsen (1938).
Specimens 11 and 14, Tuttle (1952).
Specimen 9, Spencer (1930).
Specimen 15, Fouqué (1883).
Specimen 16, The specimen used here was not from the analyzed sample. Edwards (1938).
Specimen 19, Joyce and Game (1952).
Specimen 20, The specimen used here was not from the analyzed sample. Osten (1951).

THE SEPARATE PHASES OF HIGH-TEMPERATURE CRYPTOPERTHITES

A review of the status of knowledge of the structure of perthites as revealed by *x*-rays was given in the first paper in this series (MacKenzie and Smith, 1955), so that little need be added here. In the study of orthoclase-microperthites it was found that these consisted of two or more phases: a monoclinic potassium feldspar phase or a monoclinic and a triclinic potassium feldspar phase together with one or two sodium feldspar phases generally having lattice angles near those of low-temperature albite or oligoclase. The single-crystal *x*-ray studies of sanidine- and anorthoclase-cryptoperthites show that these usually con-

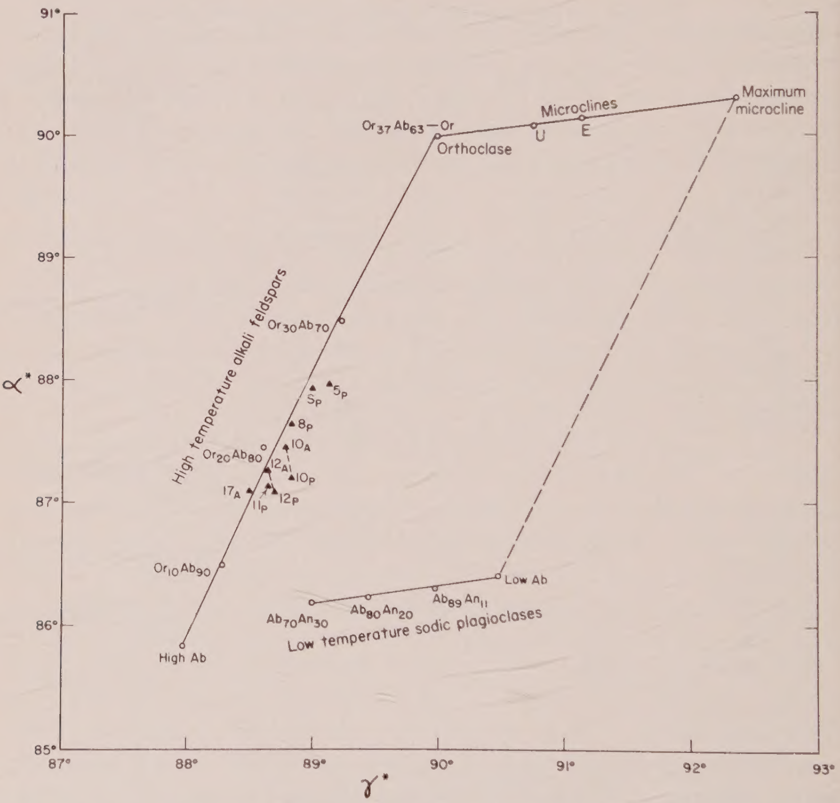

FIG. 2. Plot of the reciprocal lattice angles α^* and γ^* for triclinic alkali feldspars and three low-temperature plagioclase feldspars; a point representing monoclinic feldspars is also given. A point representing the sodium feldspar phase of each of seven high-temperature cryptoperthites is plotted; the numbers refer to the specimens listed in Table 1 and the subscripts *A* and *P* to the type of twinning (albite or pericline) from which the measurements of α^* and γ^* were made. *S* refers to specimen *P* of Spencer (1937).

sist of only two phases. The potassium-rich phase is generally monoclinic and, in contrast with the low-temperature specimens, there is no evidence of a triclinic phase with lattice angles similar to those of microcline. The sodium feldspar phase may be untwinned, pericline twinned, albite twinned, or both pericline and albite twinned. In sanidine-cryptoperthites pericline twinning of the sodium-rich phase is most frequently found, and in specimens having both types of twinning the intensity of the pericline-twinned reflections is greater than that of the albite-twinned reflections. When the sodium feldspar phase is untwinned it appears to have monoclinic symmetry; this will be discussed more fully in a following section.

When the sodium feldspar phase is twinned the reciprocal lattice angles α^* and γ^* may be measured from the oscillation photograph by the method described by Smith and MacKenzie (1955). This has been done for six of the specimens studied here. The chemical compositions of the separate phases in cryptoperthites are not known, and in order to compare the reciprocal lattice angles of these specimens with each other and with those of single-phase feldspars the method of plotting α^* against γ^* has been adopted.

TABLE 2. RECIPROCAL LATTICE ANGLES OF SODIUM-RICH PHASE OF CRYPTOPERTHITES

No.	Specimen	Albite twinning		Pericline twinning	
		α^*	γ^*	α^*	γ^*
5	Grant County			87° 58′	89° 8′
8	Nathrop			87° 39′	88° 50′
10	Spring Creek	87° 27′	88° 47′	87° 12′	88° 50′
11	Mitchell Mesa			87° 8′	88° 39′
12	Old Baldy Mt.	87° 16′	88° 39′	87° 5′	88° 41′
17	Victoria	87° 6′	88° 30′		
S	Spencer's specimen *P* (Spencer, 1937)			87° 56′	89° 0′

Figure 2 is constructed by plotting α^* against γ^* for the following feldspars: high-temperature albite and synthetic high-temperature alkali feldspars of composition $Or_{10}Ab_{90}$, $Or_{20}Ab_{80}$, $Or_{30}Ab_{70}$ (Donnay and Donnay, 1952); low-temperature albite and three natural low-temperature plagioclases of composition near $Ab_{89}An_{11}$, $Ab_{80}An_{20}$, $Ab_{70}An_{30}$ (Smith, 1956). Points representing a maximum microcline, two intermediate microclines (MacKenzie, 1954) and orthoclase are also plotted. On this diagram are plotted points representing the sodium feldspar phases of six of the high-temperature cryptoperthites studied here and one high-temperature cryptoperthite described by Spencer (1937), specimen *P*. The reciprocal lattice angles α^* and γ^* for the sodium feldspar phase of these specimens are given in Table 2. The subscripts *A* and *P* refer to the type of twinning, albite or pericline, from which the measurements were made. In specimens 10 and 12 both albite and pericline twinning are present and the angles determined from both types of twinning show good agreement in each case.

The proximity of the points representing the sodium-rich phase of the cryptoperthites to the curve showing the variation of α^* and γ^* with chemical composition for the high-temperature synthetic feldspars is striking. In addition the points are spread out along this curve, and both these facts taken together suggest that the reciprocal lattice angles of the sodium-rich phases may be utilized in determining their compositions. Perpendiculars drawn from the points representing the sodium-rich phases to the curve for the high-temperature alkali feldspars give a range of compositions from about $Or_{15}Ab_{85}$ to $Or_{26}Ab_{74}$ for the specimens plotted in Fig. 2. The compositions derived in this manner show no relation to the values obtained for the sodium-rich phases of the same specimens as obtained from the spacing of the $\bar{2}01$ planes (see Table 1).

The discrepancy between the compositions of the sodium feldspar phases as determined by these two methods is rather disconcerting since it cannot yet be shown which method gives a closer approximation to the true compositions. It is known in the case of orthoclase-microperthites that the spacing of the $\bar{2}01$ planes sometimes gives impossible results for the compositions of both the sodium and potassium feldspar phases (Laves, 1952; Coombs, 1954). Even after allowing for the difference in $d_{\bar{2}01}$ for low- and high-temperature albite, impossible results may be obtained for the composition of the sodium feldspar phase of some orthoclase-microperthites. All the sanidine- and anorthoclase-cryptoperthites examined here give possible values, but it is not be be expected that the sodium feldspar phase would be almost pure albite in each case as has been found here (Table 1). Laves (1952) has suggested that the separate phases in a perthite cannot be expected to show the same lattice constants as the individually crystallized phases would exhibit and that the strain produced by unmixing is kept to a minimum by some distortion of the lattices of the separate phases. The same writer has also noted that a cryptoperthite may have a triclinic potash phase which is not microcline but potash feldspar forced to be triclinic by the influence of the triclinic soda phase which is the host material. One example of this has been found in this investigation (specimen No. 17) and will be discussed in a following section (p. 422).

Use of the spacing of the $\bar{2}01$ planes for determining the composition of alkali feldspars depends chiefly on the rather large change in the a^* parameter with change in chemical composition. From what has been noted above regarding the distortion of the lattice in the separate phases in cryptoperthites it would seem that the reciprocal lattice angles also may be unreliable for determining the composition of the sodium feldspar phase. However, from the close correspondence of the points in Fig. 2 to the curve showing the change in α^* and γ^* with chemical composition in sodium-rich feldspars, it is believed that the reciprocal lattice angles give a better approximation to the composition of the sodium feldspar phase than do the reciprocal lattice edges.

For comparison with Fig. 2, Fig. 3 shows the plot of α^* against γ^* for the sodium feldspar phases of eight orthoclase-microperthites. With the exception of specimen *E*, the positions of the points indicate that the sodium feldspar phase in the orthoclase-microperthites is a low-temperature albite or oligoclase. The case of specimen *E* has been discussed in the earlier paper (MacKenzie and Smith, 1955) from which this figure is reproduced.

A careful study of the *b*-axis *x*-ray oscillation photographs of high-temperature cryptoperthites makes it possible to deduce the probable sequence of events in the unmixing of a monoclinic feldspar. The first stage is shown by diffuse streaks associated with each of the main reflections and lying parallel to the layer lines. (It may be noted here that reflections from a pericline-twinned sodium feldspar phase in a perthite lie on the layer lines of the potassium-rich phase since the twin axis *b* coincides with the *b*-axis of the potassium feldspar phase.) This is followed by the appearance of an intensity maximum on each of the diffuse streaks and these maxima represent the untwinned sodium feldspar referred to on a preceding page. This must not be used as evidence for the existence of a monoclinic form of albite since this phase almost certainly has a considerable amount of potassium feldspar in solid solution and may represent a composition more potassium rich than $Or_{37}Ab_{63}$. The splitting up of these single reflections into a number of small well-defined spots gives the fine structure which is a common feature of the sodium-rich phase in the *x*-ray diffraction patterns of many perthites (Chao and Taylor, 1940; Laves, 1952; Ito and Sadanaga, 1952). The final stage is the development of a pericline-twinned sodium-rich phase which results from the merging of the fine structure into two sharp spots, a single spot sometimes remaining between the two pericline-twinned spots.[8]

---

[8] This discussion of the development of pericline twinning of the sodium feldspar phase would not be generally applicable to anorthoclase-cryptoperthites since twinning developed in the homogeneous feldspar would be expected to influence that in the unmixed phases.

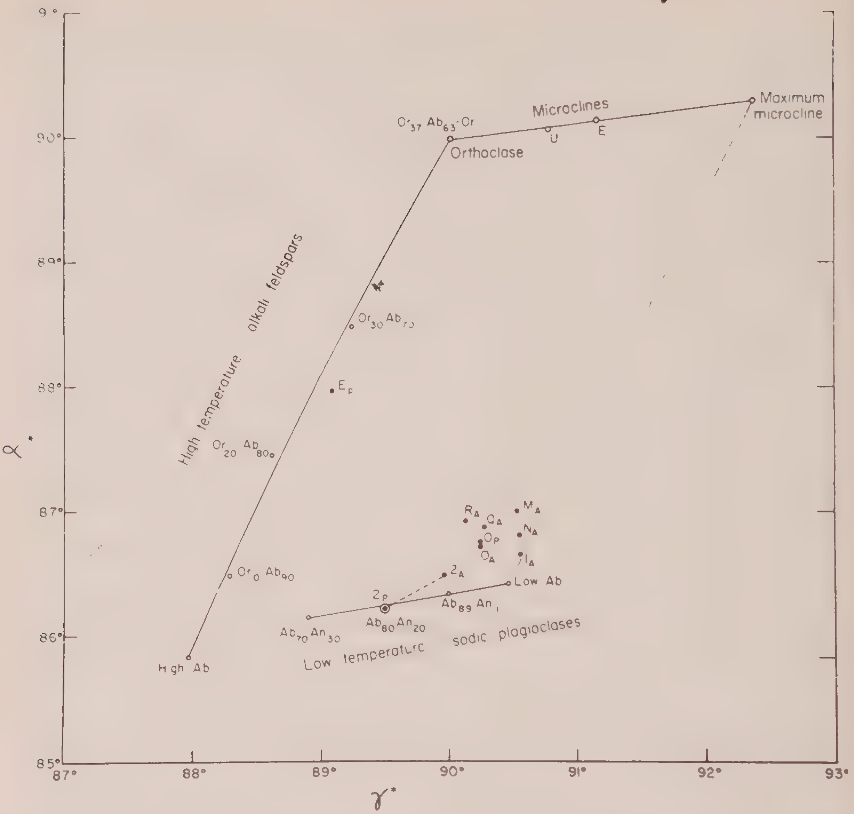

FIG. 3. This diagram is constructed in the same manner as Fig. 2. Points representing the sodium feldspar phases of eight orthoclase-microperthites are plotted and, with one exception, these have reciprocal lattice angles similar to those of low-temperature albite or oligoclase. Diagram reproduced from paper I of this series (MacKenzie and Smith 1955).

VARIATIONS IN OPTIC AXIAL ANGLE

Preliminary measurements indicated that there was frequently a considerable variation in optic angle in different crystals from a single rock specimen (Tuttle, personal communication). Since many of the specimens were known to be unmixed it was considered that this optic angle variation might be related to their inhomogeneity and so the effect of heating on the values of the optic angle was studied. The possibility that part of the variation in optic angle was the result of differences in chemical composition within individual crystals or between separate crystals was considered. The sharpness of the 201 reflection in the *x*-ray powder diffraction patterns of homogenized specimens indicated that the range of chemical composition was very slight and could be neglected.

Although variations in optic angle between different crystals were found in most of the specimens, only in one case was an appreciable variation in a single crystal fragment found. The sanidine from Mineral Creek, San Juan region, Colorado (No. 4), described by Larsen and Larsen (1938) was considered by these writers to be foreign to the latite-andesite from which it was separated. One crystal of this sanidine showed a large variation in optic angle, being zoned from a high-sanidine[9] with $2V=7.8°$ to a low-sanidine with $2V=17.5°$. No discontinuity in the zoning was observed, and an intermediate zone was uniaxial. From the broken cleavage fragment it was impossible to determine which was the rim and which the core of the crystal.

Table 3 gives the measured values of the optic angle in a number of crystals from both the unheated and heated samples. Although sufficient measurements have not been made to obtain a good estimate of the variation in both the unheated and heated samples, there are in many cases indications of a reduction in the variation resulting from the heating. Specimen 3 is distinctive because there is a marked increase in the 2V variation in the sample heated at 900° C. for 24 hours; two of the heated crystals have the optic plane parallel to (010) so that this short period of heating has been sufficient to promote the transformation to the high-sanidine form. The increase in the variation in 2V in this specimen is undoubtedly due to the inversion to the high-sanidine form having proceeded fairly rapidly in this specimen and in some crystals to a greater degree than in others.

High-temperature cryptoperthites can be readily homogenized by heating at 700° C. for a few hours, and therefore the effects of homogenization alone have not been investigated since all these samples were heated at 900° C. for approximately 24 hours. As some of the homogeneous specimens show variations in optic angle in different crystals it is unlikely that these variations are related only to unmixing.

Tuttle and Keith (1954) have attributed variations in the optic axial angle of the alkali feldspars in a single specimen of granite to transitions from sanidine-cryptoperthite to orthoclase-microperthite, the change having progressed further in some grains than in others. Coombs (1954) has noted large variations in the optic axial angle of ferriferous potassium feldspars from Madagascar and he considers these to be due to states transitional between high-sanidine and sanidine or orthoclase. The variations in optic axial angle reported here are much smaller than those considered by Tuttle and Keith or by Coombs, but they undoubtedly

---

[9] The curve showing the relation between chemical composition and optic axial angle for the high-sanidine series (Fig. 1) is considered to define this series, but it is convenient to describe as a high-sanidine any potassium-rich feldspar in which the optic plane is parallel to (010).

TABLE 3. OPTIC AXIAL ANGLE MEASUREMENTS

	Unheated									Heated at 900° C. for 24 hours									Effect on mean value of optic angle of heating at 900° C.	
	1	2	3	4	5	6	7	Variation	Mean	1	2	3	4	5	6	7	Variation	Mean	Decrease	Increase
1. Eifel*	10.4	12.7	8.0	10.9	10.0			4.7	10.4										—	
2. Kokomo	31.6	32.4	32.6	35.4	27.0			8.4	31.8	30.0	26.4	29.2	26.7	30.1			3.7	28.5	3.3	
3. Alder Creek*	25.8	22.8	24.0	21.6	25.1	21.8		4.2	23.5	15.5	11.4	21.0	25.3	19.0	(7.0‡)		13.9	18.4	5.1	
4. Mineral Creek	11.8	12.4	11.5	15.2	(17.5†–7.8‡)			3.7	12.7										—	
5. Grant Co.	32.6	30.0	31.1	31.7	30.4	31.5	31.3	2.6	31.2	28.6	30.1	30.3	29.8	29.1	29.9		1.7	29.6	1.6	
6. S. C. XX	38.0	40.3	39.4	38.3	40.2			2.3	39.2	36.2	36.0	37.2	35.6	37.0			1.6	36.4	2.8	
7. Pine Creek Mesa	36.9	37.2	34.9	33.0	36.7			4.2	35.7	29.8	31.1	33.5	31.9	30.0	28.0		5.5	30.7	5.0	
8. Nathrop	30.9	30.7	29.4	34.6	29.0	32.2		5.6	31.1	32.6	33.5	32.3	31.5	31.7	34.4		2.9	32.7		1.6
9. Sparling Gulch	40.3	38.9	42.1	39.9	47.7	45.9		8.8	42.3	48.4	48.1	47.5	48.1	48.7			1.2	48.1		5.8
10. Spring Creek	37.4	40.2	37.1	38.0	36.8	38.1		3.4	37.9	44.9	46.5	44.6	46.9	48.2	45.7		3.6	46.1		8.2
11. Mitchell Mesa	35.0	34.7	34.2	35.5	33.9	32.6	37.4	4.8	34.8	42.3	42.3	41.6	42.0	42.1			0.7	42.0		7.2
12. Old Baldy Mt.	38.4	38.7	39.2	37.3	39.8	40.2		2.9	38.9	43.9	47.1	45.9	44.4	46.4	46.8	48.1	4.2	46.1		7.2
13. Cebolla Creek	33.9	36.5	32.4	33.7	36.4			4.1	34.6	47.3	47.8	48.2	48.4	48.1			1.1	47.9		13.3
14. Grande Caldeira	46.6	47.4	46.9	46.8	45.5	46.9	46.5	1.9	46.7	47.2	47.3	46.8	47.1	46.7	46.2		1.1	46.9		0.2
15. Quatre Ribeiras	44.4	45.2	46.0	43.3	44.1	45.0		2.7	44.7	45.2	44.9	45.1	45.0	46.6			1.7	45.3		0.6
16. Mt. Franklin	53.7	57.6	56.9	54.8	54.8			3.9	55.6	56.5	53.7	54.9	56.7	56.3	55.8		2.8	55.6		0.0
17. Victoria	48.0	48.3	48.4	46.9	47.8	49.1	47.6	2.2	48.1	47.8	47.7	49.2	48.0	49.2	49.2	50.0	2.3	48.7		0.6
18. Brownhills	38.9	39.5	41.6	41.4	42.2	42.6		3.7	41.0	44.3	41.2	42.5	43.7	42.3			3.1	42.8		1.8
19. Ropp	51.9	53.1	52.9	53.7	52.1			1.8	52.7	55.1	54.7	55.3	55.6	54.7	55.2		0.6	55.1		2.4
20. Mt. Anakie	56.7	56.5	56.7	56.0	56.4	56.3		0.7	56.4	61.4	58.7	59.1	58.6				2.8	59.4		3.0

* High sanidine in nature.

† Indicates optic plane perpendicular to (010).

‡ Indicates optic plane parallel to (010).

reveal the tendency for change in optic angle in the alkali feldspars with temperature of final crystallization. The sluggish nature of this change is reflected in the differing rate of response of different crystals to change. It is believed that the variation in optic angle in each specimen might be reduced to nearly zero if the specimen were held for a sufficient time at a fixed temperature.

Effect on the Optic Angle of Heating at 900° C.

The mean values of the optic angles in the unheated and heated samples given in Table 3 are plotted in Fig. 4. The mean value of the optic angle before heating is represented by a circle and after heating by the point of an arrow head for eighteen of the specimens studied.

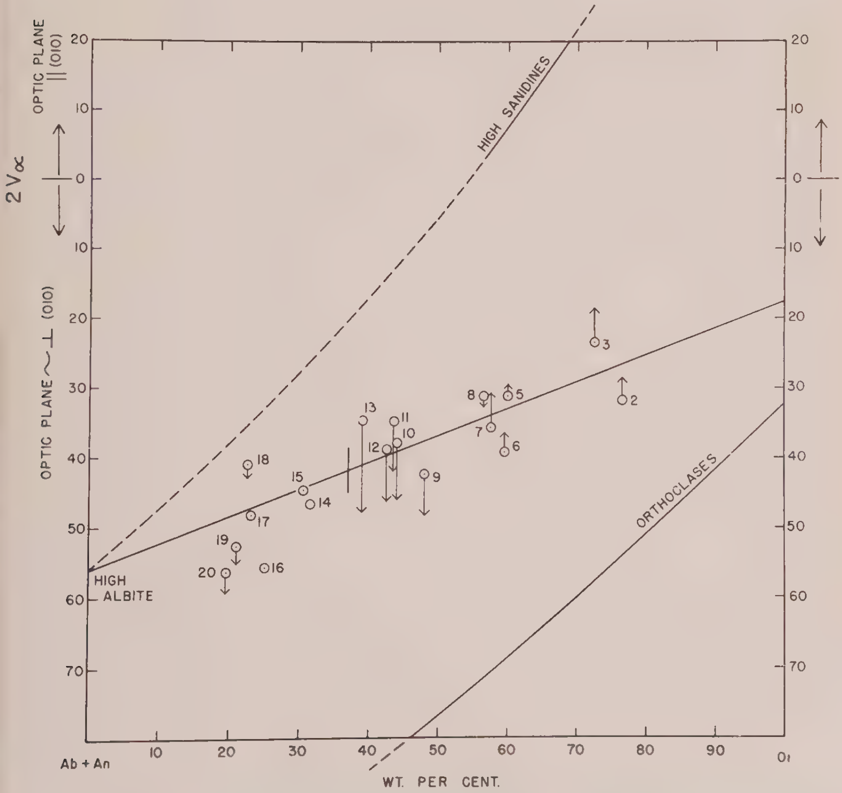

FIG. 4. Diagram showing the change in the mean value of the optic angle of high-temperature feldspars as a result of heating at 900° C. for 24 hours. The circles represent the mean value of the 2V for the unheated samples and the arrowheads the mean value of 2V for the heated samples. The numbers refer to the specimens listed in Table 1. Lines representing the variation in optic angle with chemical composition for three of the alkali feldspar series are shown.

With respect to the effect of heating at 900° C. this series of feldspars can be divided into three groups. Specimens with more than 60% potassium feldspar in their bulk composition show a slight but measurable decrease in the mean value of the optic angle. Feldspars in the compositional range $Or_{60}(Ab+An)_{40}$ to $Or_{40}(Ab+An)_{60}$ (approx.) show an increase in the mean value of the optic angle, and this increase reaches its maximum value in the most sodium-rich specimens. Alkali feldspars with less than 40% potassium feldspar show a very slight increase or no change in the mean value of the optic angle as a result of this heat treatment.

It is now fairly well established that any natural potassium-rich feldspar, if heated for a sufficiently long period at about 1050° C., is changed to the high-sanidine form by a decrease in the optic angle and rotation of the optic plane into a position parallel to the symmetry plane[10] (Spencer, 1937; Tuttle, 1952). The reduction of the optic angle in the potassium-rich specimens as a result of heating at 900° C. is the effect which would be expected since the change is in the direction of a high-sanidine, but the heat treatment has not been sufficient to convert any of the specimens completely to the high-sanidine form. The sanidine from Alder Creek, San Juan Mountains (No. 3), has a variation in optic angle in the unheated sample of 4.2° and in the heated sample it is 13.9°; it has already been noted that this is undoubtedly due to some of the crystals having been partly transformed to the high-sanidine form. Specimens 1 and 4 were transitional to the high-sanidine form in their natural state and so no optical measurements were made on the samples heated at 900° C. for 24 hours.

Specimens in the compositional range $Or_{60}(Ab+An)_{40}$ to $Or_{40}(Ab+An)_{60}$ (approx.) do not show a tendency to change to the high-sanidine form as a result of heating at 900° C. for 24 hours since the mean value of the optic angle increases. Additional evidence for a discontinuity in the effect of heat treatment at the composition $Or_{60}(Ab+An)_{40}$ is given by the results of prolonged heating at 1030° C. Heating a number of specimens at 1030° C. for seven months showed that specimens more potassium-rich than $Or_{60}(Ab+An)_{40}$ were changed to the high-sanidine form but more sodium-rich specimens were not thus changed. No systematic study has been made of the optic angle in the specimens heated at 1030° C. Slight increases in optic angle as a result of heat treatment of feldspars in this compositional range have been found by Kôzu and Suzuki (1925) and Spencer (1937). Spencer's studies indicate that such feldspars may be changed to the high-sanidine form but that the process is very much more sluggish than in the case of the potassium-rich specimens.

---

[10] Some microclines are not changed to the high-sanidine form even after heating for 6 months at 1050° C. but it is believed that longer heating will effect this change (personal communication from Dr. F. Chayes).

The increase in optic angle resulting from heating at 900° C. reaches its maximum value in a feldspar of composition near $Or_{40}(Ab+An)_{60}$ (No. 13). At this composition there is a pronounced change in the effect of heat treatment since feldspars more sodium-rich than this composition show a very slight increase or no measurable increase in the mean value of the optic angle. It is possible that this alteration in the effect of heat treatment is related to the change in symmetry in the high-temperature alkali feldspars at the composition $Or_{37}(Ab+An)_{63}$ (Donnay and Donnay, 1952), but this is rather a surprising result since the other physical properties do not show an abrupt discontinuity at this composition, the symmetry change being temperature dependent (MacKenzie, 1952; Laves, 1952).

No explanation can be advanced at the present time for the differing response of these three groups of specimens to this heat treatment. Similar studies with differing times and temperatures of heating would undoubtedly go a long way toward solving this problem.

Optically Monoclinic Anorthoclase-Cryptoperthites

It is frequently important to know the symmetry of an alkali feldspar, and petrologists have usually relied on optical methods of symmetry determination. In the absence of visible multiple twinning it may be difficult to determine the symmetry with certainty, and if the feldspar is unmixed on a sub-microscopic scale the optical symmetry may be quite misleading. Tuttle (1952) reported that some anorthoclase-cryptoperthites are optically monoclinic or have very small extinction angles in the zone [010] but that after heating to homogenize the crystals there is no doubt about their triclinic character because of the oblique extinction in the zone [010].

All sanidine-cryptoperthites investigated have optically monoclinic symmetry but anorthoclase-cryptoperthites may be either optically monoclinic or distinctly optically triclinic. Two of the anorthoclase-cryptoperthites studied here are optically monoclinic or have very small and variable extinction angles in the zone [010] before being homogenized. One of these is an anorthoclase-cryptoperthite from Victoria, Australia (No. 17), investigated by Tuttle (1952) and the other an anorthoclase-cryptoperthite from Ropp, Nigeria (No. 19), described by Joyce and Game (1952). All the Victoria anorthoclase crystals examined are untwinned, but some fragments of the Ropp anorthoclase show multiple twinning and others show straight extinction on the [010] zone. It is of interest to determine whether there is any genetic reason for this difference in the optical character of anorthoclase-cryptoperthites.

The optical symmetry of an anorthoclase-cryptoperthite may depend on the relative temperatures of the non-quenchable change from triclinic to monoclinic symmetry and the temperature at which exsolution begins. If the feldspar is monoclinic when it begins to unmix it is possible that only the sodium feldspar phase will invert to triclinic symmetry and the crystal might more readily appear optically monoclinic.[11] The temperatures of inversion to monoclinic symmetry of the two specimens here considered, viz. No. 17 ($Or_{23.3}Ab_{75.5}An_{1.2}$) and No. 19 ($Or_{23.0}Ab_{69.2}An_{7.8}$), have been determined to be 360° ± 10° C. and 540 ± 10° C., respectively (MacKenzie, 1952). From the experimentally determined alkali feldspar solvus (Bowen and Tuttle, 1950) the temperature of commencement of exsolution of a binary feldspar of composition $Or_{23}Ab_{77}$ is close to 610° C. The effect of an increase in the anorthite content of an alkali feldspar is to raise the temperature of the solvus, so that specimen 17 would be expected to unmix at a temperature slightly greater than 610° C. and specimen 19 at a much higher temperature. Both specimens should therefore begin to unmix while still monoclinic in symmetry, and this may be the reason for the optical symmetry shown by these anorthoclase-cryptoperthites. It does not follow, however, that an optically triclinic cryptoperthite must have been triclinic when unmixing began, since some of the fragments of the Ropp anorthoclase are optically triclinic.

A single-crystal *b*-axis oscillation photograph of the Victoria anorthoclase is reproduced in Fig. 5. The sodium and potassium feldspar phases are each represented by sets of paired reflections in albite twin relationship.[12] Diffuse streaks join the albite-twinned reflections of the sodium-rich phase to the corresponding reflections of the potash phase. Between each pair of reflections of the albite-twinned sodium feldspar phase are a series of very faint spots giving the effect of a diffuse line joining the two spots. One possible interpretation of this *x*-ray photograph is that the two phases unmixed from an albite-twinned, and therefore triclinic, crystal. This interpretation, however, is in disagreement with the conclusion already reached that the feldspar was still monoclinic when unmixing began.

[11] Laves (1952), in discussing ternary sodium-rich feldspars, has made a similar suggestion, but this hypothesis applies equally well to potassium-sodium feldspars with a negligible amount of calcium.

[12] This albite-twinned, and therefore triclinic, potassium feldspar phase is forced to be triclinic by the influence of the sodium feldspar phase, which is present in much greater proportion and so is the host structure (Laves, 1952). That the potassium feldspar phase is constrained to be triclinic is shown by the values of α^* and γ^* for this phase, since these fall on the curve representing the variation in α^* and γ^* for high-temperature alkali feldspars (Fig. 2) near the point $Or_{30}Ab_{70}$.

If we consider the temperature at which the monoclinic-triclinic inversion curve cuts the solvus for a binary alkali feldspar as 570° C. (MacKenzie, 1952) and neglect the small anorthite content of the Victoria anorthoclase, it is found that the temperature will have to fall only 40° C. from the beginning of unmixing until the sodium feldspar phase changing in composition along the solvus reaches the monoclinic-triclinic inversion curve and so inverts to triclinic symmetry. Thus, although unmixing may start from a monoclinic crystal, the greater proportion of the crystal will invert to triclinic symmetry after a fall in temperature of only 40° C. An interpretation of the x-ray photograph of the Victoria anorthoclase-cryptoperthite in harmony with this is that when the sodium feldspar phase became triclinic it developed albite twinning and the potassium-rich phase, under the influence of the predominant sodium-rich phase, also twinned. It is of interest to note that none of the crystals of a sample of the Victoria feldspar, heated until homogeneous, showed any twinning, either microscopic or on a sub-microscopic scale.

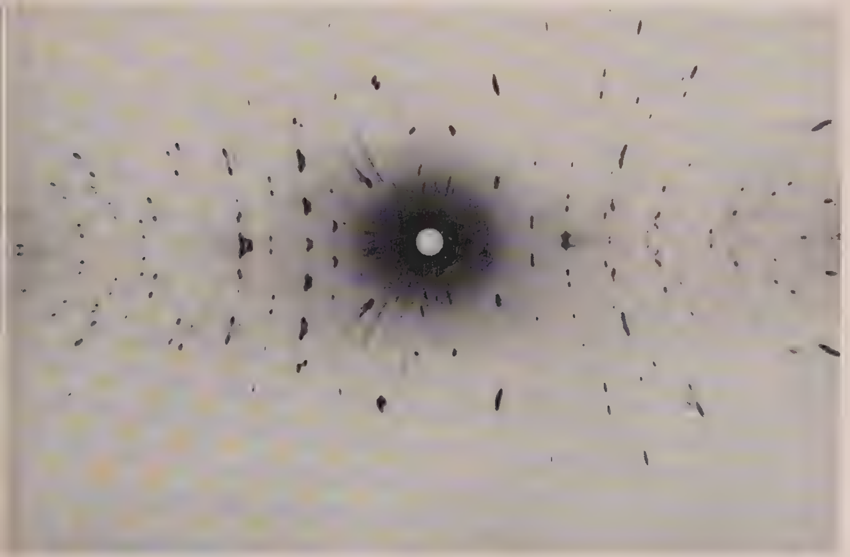

FIG. 5. A b-axis x-ray oscillation photograph of the anorthoclase-cryptoperthite from Victoria, Australia (No. 17). The (001) plane is set in the center of a 15° oscillation arc. Both the sodium and potassium feldspar phases are albite twinned (see text for further details).

SUMMARY AND CONCLUSIONS

From the curves relating optic axial angle with chemical composition in the alkali feldspars (Tuttle, 1952) eighteen of the twenty specimens described here belong to the sanidine-anorthoclase-high-temperature albite series, the remaining two specimens being transitional to the high-sanidine series. *X*-ray studies show that all the specimens in the composition range $Or_{60}Ab_{40}$-$Or_{25}Ab_{75}$ are unmixed to some extent, although in some cases the unmixing is very slight. Doubtless completely homogeneous specimens in this composition range could be found.

Those unmixed feldspars which have been classified, on the basis of the value of the optic axial angle, as belonging to the sanidine-anorthoclase-high-temperature albite series, have been found to have a *high-temperature sodium feldspar phase.* Orthoclase-microperthites, on the other hand, have, with one or two exceptions, *a low-temperature sodium feldspar phase* (MacKenzie and Smith, 1955). The importance of this difference cannot be overemphasized since this gives a useful basis for subdividing perthitic feldspars.

It is in many cases possible to decide whether a given feldspar has a high- or low-temperature sodium feldspar phase simply by comparing the *x*-ray single-crystal pattern with standard patterns; it is, of course, essential that all the photographs compared have been taken in identical orientation. From *x*-ray photographs showing albite and pericline twinning in a low-temperature sodium feldspar phase and in a high-temperature sodium feldspar phase, comparison of the separation of several sets of albite-twinned or pericline-twinned reflections in the unknown sodium-rich phase with those of the standard patterns readily indicates whether the phase is high or low temperature.

Laves (1952) has suggested that there are only two stable forms of potassium feldspar, viz. sanidine and microcline, and that "common" orthoclase is unstable. This may or may not be true, but for the purposes of petrographic description it seems advisable to retain the terms orthoclase and orthoclase-microperthite. The name orthoclase has generally been associated with the optically monoclinic feldspars of some granites and pegmatites, whereas the term sanidine has been used for the monoclinic feldspars of volcanic rocks. The curves drawn by Tuttle (1952) relating optic axial angle with chemical composition make it possible to define these terms more precisely and to remove the genetic significance attached to the names. Thus in certain granites the alkali feldspar may be a sanidine-cryptoperthite (Tuttle and Keith, 1954) instead of the more common orthoclase-microperthite or microcline and low-albite association.

The subdivision of the microperthitic and cryptoperthitic feldspars on the basis of the value of the optic axial angle is supported by the *x*-ray evidence of the difference in the nature of the sodium feldspar phase in the orthoclase-microperthite and sanidine-cryptoperthite series. The existence of specimens whose optic angle places them intermediate between these two series in no way detracts from the usefulness of this subdivision since these specimens have two sodium feldspar phases, one a low-temperature phase and the other a high-temperature phase (Tuttle and Keith, 1954). Further examination of specimens intermediate between the two series has revealed that the size of the optic angle is proportional to the relative amounts of the high-temperature and the low-temperature sodium feldspar phases. This will be discussed in more detail in a subsequent paper.

The optical and *x*-ray studies, the results of which are reported in the foregoing pages, are a part of a systematic study of alkali feldspars from different geologic environments. It is believed that the feldspars, by virtue of their apparent complexity and the sluggish nature of the changes which they undergo, will be of the greatest value in eventually unraveling the history of the rocks in which they occur.

Acknowledgments

Dr. N. L. Bowen and Professors O. F. Tuttle and C. E. Tilley kindly made available all the analyzed feldspar specimens they had on hand. Reference to the original source of the individual specimens is given in Table 2. The above-named gentlemen and Dr. W. H. Taylor offered many helpful suggestions in the course of this work and their many kindnesses are gratefully acknowledged here. The authors are indebted also to the various members of the staff of the Geophysical Laboratory who offered suggestions and constructive criticism of this manuscript.

Appendix

Notes on specimens 1, 5, 8 and 15

1. *Eifel sanidine.* The sample of the Eifel sanidine used here was that studied by Kracek and Neuvonen (1952). It was found that this specimen was transitional to the high-sanidine form, the optic plane being parallel to (010). The studies of Des Cloizeaux (1861), Kôzu (1916), Kôzu and Seto (1921) and Kôzu and Suzuki (1923) have shown that the optic axial angles of sanidines from this locality are very susceptible to temperature changes, and it is not surprising therefore to find natural samples transitional to the high-sanidine form. Some of the specimens described in the literature have the optic plane parallel to (010) and others have the optic plane perpendicular to (010).

5. *Grant County sanidine.* This sanidine occurs in a pegmatite within a rhyolite porphyry in Rabb Canyon, Grant County, New Mexico. Kelley and Branson (1947) have described the pegmatites in this rhyolite porphyry, and, noting the unusual feature of the presence of sanidine in

a pegmatite, have concluded that the pegmatites crystallized at high temperature and at shallow depth. Since the publication of their paper it has been found that the plagioclase of these pegmatites is also a high-temperature form (personal communication from Dr. Bowen). A specimen of this plagioclase has been analyzed by Mr. J. H. Scoon and its composition calculated to be $Or_{8.3}Ab_{78.8}An_{12.9}$.

8. *Nathrop sanidine.* Cross (1886) has briefly described the Nathrop rhyolite from Chaffee County, Colorado, because of the presence of topaz and spessartine in lithophyses. Although remarking on the sanidine, Cross does not mention the presence of a plagioclase. There is, however, in addition to the sanidine a high-temperature plagioclase in this rock, and a partial analysis of this plagioclase by Mr. J. H. Scoon gives a composition of $Or_{7.8}Ab_{81.2}An_{11}$.

15. *Quatre Ribeiras anorthoclase.* The sample of the anorthoclase from Quatre Ribeiras, Ile de Terceira, Azores, was part of the material originally described by Fouqué (1883) and was made available to the writers by Professor C. E. Tilley. The chemical analysis by Fouqué indicated that this mineral was almost pure albite, and Dana (1906) referred to it as an abnormal form of albite. Tuttle and Bowen (1950) suggested that Fouqué's chemical data were probably unreliable, and a new determination of the alkalies by Mr. J. H. Scoon gave the following values: $Na_2O = 7.65$ and $K_2O = 5.40$, indicating that this is anorthoclase and not albite.

References

Bowen, N. L., and Tuttle, O. F. (1950), The system $NaAlSi_3O_8$—$KAlSi_3O_8$—H_2O: *Jour. Geol.*, **58**, 489–511.

Chao, S. H., and Taylor, W. H. (1940), The lamellar structure of potash-soda feldspars: *Proc. Roy. Soc. London*, ser. A, **174**, 57–72.

Coombs, D. S. (1954), Ferriferous orthoclase from Madagascar: *Mineral. Mag.*, **30**, 409–427.

Cross, W. (1886), On the occurrence of topaz and garnet in lithophyses of rhyolite: *Proc. Colorado Sci. Soc.*, p. 61.

Dana, E. S. (1906), A System of Mineralogy. New York, John Wiley & Sons.

Des Cloizeaux, A. (1861), Note sur les modifications temporaires et sur une modification permanente que l'action de la chaleur apporte à quelques propriétés optiques du feldspath orthose: *Compt. Rend. Acad. Sci. Paris*, **53**, 64–68.

Donnay, G., and Donnay, J. D. H. (1952), The symmetry change in the high-temperature alkali-feldspar series: *Am. Jour. Sci.*, Bowen volume, 115–132.

Edwards, A. B. (1938), The Tertiary volcanic rocks of central Victoria: *Quart. Jour. Geol. Soc., London*, **94**, 243–318.

Fairbairn, H. W., and Podolsky, T. (1951), Notes on precision and accuracy of optic angle determinations with the universal stage: *Am. Mineral.*, **36**, 823–832.

Fouqué, M. (1883), Feldspath triclinique de Quatre Ribeiras (Ile de Terceira): *Bull. Soc. Min. de France,* **6**, 197–219.

Ito, T., and Sadanaga, R. (1952), The lamellar structure of certain microcline and anorthoclase: *Acta Cryst.*, **5**, 441–449.

Joyce, J. R. F., and Game, P. M. (1952), Note on anorthoclase from Nigeria: *Bull. British Mus.* (*Mineralogy*), **1**, 85–94.

Kelley, V. C., and Branson, O. T. (1947), Shallow, high-temperature pegmatites, Grant County, New Mexico: *Econ. Geol.*, **42**, 699–712.

Kôzu, S. (1916), The dispersion phenomena and the influence of temperature on the optic axial angle of sanidine from the Eifel: *Mineral. Mag.*, **17**, 237–252.

———, and Seto, K. (1921), Sanidine from the Eifel: *Sci. Rep. Tôhoku Univ.*, ser. 3, **1**, 25–32.

———, and Suzuki, M. (1923), Further studies on the influence of temperature on the optic axial angle of sanidine: *Sci. Rep. Tôhoku Univ.*, ser. 3, **1**, 233–241.

———, and ——— (1925), The influence of temperature on the optic axial angle of adularia, yellow orthoclase and moonstone: *Sci. Rep. Tôhoku Univ.*, ser. 3, **2**, 187–201.

Kracek, F. C., and Neuvonen, K. J. (1952), Thermochemistry of plagioclase and alkali feldspars: *Am. Jour. Sci.*, Bowen volume, 293–318.

Larsen, E. S., Jr., and Larsen, E. S., 3rd (1938), Petrologic results of a study of the minerals from the Tertiary volcanic rocks of the San Juan region, Colorado. 8. Orthoclase: *Am. Mineral.*, **23**, 417–429.

Laves, F. (1952), Phase relations of the alkali feldspars: *Jour. Geol.*, **60**, 436–450; 549–574.

MacKenzie, W. S. (1952), The effect of temperature on the symmetry of high-temperature soda-rich feldspars: *Am. Jour. Sci.*, Bowen volume, 319–342.

———, (1954), The orthoclase-microcline inversion: *Mineral. Mag* , **30**, 354–366

———, and Smith, J. V. (1955), The alkali feldspars. I. Orthoclase-microperthites: *Am. Mineral.*, **40**, 707–732.

Osten, J. F. (1951), Identificatie van natuurlijke alkaliveldspaten met behulp van Röntgen-poederdiagrammen: Doctorate Thesis, University of Leiden, Holland.

Smith, J. V. (1956), The powder patterns and lattice parameters of plagioclase feldspars. I. The soda-rich plagioclases: *Mineral. Mag.*, in press.

———, and MacKenzie, W. S. (1955), The alkali feldspars. II. A simple *x*-ray technique for the study of alkali feldspars: *Am. Mineral.*, **40**, 733–747.

Spencer, E. (1930), A contribution to the study of moonstone from Ceylon and other areas and of the stability-relations of the alkali-felspars: *Mineral. Mag.*, **22**, 291–367.

——— (1937), The potash-soda-felspars. I. Thermal stability: *Mineral. Mag.*, **24**, 453–494.

Tuttle, O. F. (1952), Optical studies on alkali feldspars: *Am. Jour. Sci.*, Bowen volume, 553–567.

———, and Bowen, N. L. (1950), High-temperature albite and contiguous feldspars: *Jour. Geol.*, **58**, 572–583.

———, and Keith, M. L. (1954), The granite problem: Evidence from the quartz and feldspar of a Tertiary granite: *Geol. Mag.* **91**, 61–72.

Manuscript received June 15, 1955.

PHYSICAL PROPERTIES OF END-MEMBERS OF THE GARNET GROUP*

BRIAN J. SKINNER, *Harvard University, Cambridge, Massachusetts.*†

ABSTRACT

Unit cell size (a_0), molar volume (V_m), density (ρ), refractive index (n), and the linear (d_a) and volume (d_v) coefficients of thermal expansion from 298° to 1023° K. have been determined for synthetic pure end-member garnets. The following values were found for a_0, V_m, ρ, and n at 298.16° K. (25° C.):

	a_0, Å	V_m, cc./mole.	ρ, gm./cc.	n (Na)
Grossularite	11.851	125.31	3.594	1.734
Andradite	12.048	131.69	3.859	1.887
Almandite	11.526	115.28	4.318	1.830
Spessartite	11.621	118.15	4.190	1.800
Pyrope	11.459	113.29	3.582	1.714

The linear and volume coefficients of thermal expansion have been determined as polynomial functions of temperature. The constants of the equations are given in Table 10 in the body of the paper.

INTRODUCTION

The physical properties of the end-members of the garnet group have been predicted by Ford (1915) and later revised by Fleischer (1937). The predictions were made by extrapolating the properties of natural garnet solid solutions back to the pure end-members. Since insufficient variables have been measured to completely specify the compositions, it is desirable that the predicted properties of the pure end-members be checked.

For the present study, pure synthetic end-member garnets were available. The Norton Company supplied pyrope, spessartite and andradite, grown at unstated temperatures and pressures. The garnets were synthesized from the pure component oxides. Dr. H. S. Yoder of the Geophysical Laboratory, Carnegie Institute, supplied specimens of almandite grown at 10,000 bars and 800° C., and grossularite grown at 9,000 bars and 970° C. To both of these suppliers thanks are due for their ready cooperation and help.

Table 1 compares the values of the unit cell size (a_0), of the pure end-members with the values obtained by Fleischer (1937) and Stockwell (1927). The values of a_0 determined by Fleischer and Stockwell have been corrected from the old kX units to Ångstrom units, using Bragg's (1947) recommended conversion factor. Both Fleischer and Stockwell

---

* Contribution from the Department of Mineralogy and Petrography, Harvard University, No. 360.

† Present address: Department of Geology, University of Adelaide, South Australia.

TABLE 1. VALUES OF a_0 FOR THE GARNETS AT 25° C.

	Fleischer a_0, Å	Stockwell a_0, Å	Skinner a_0, Å
Grossularite	11.864	11.864	11.851
Andradite	12.069	12.064	12.048
Almandite	11.518	11.516	11.526
Spessartite	11.613	11.600	11.621
Pyrope	11.463	11.453	11.459

obtained their values by extrapolation from garnets of mixed composition. Stockwell's values were determined from his own measurements, while Fleischer's values were derived from published data on the garnets. The agreements are reasonably good, except for andradite. Fleischer's value for andradite is 0.021 Å larger than the present author's value. It is interesting to note that the measured value of a_0 for a garnet containing ing 85% of the andradite end-member used by Fleischer in his work was 0.033 Å lower than the computed value from his extrapolated pure end-member values. For the only other high andradite garnet quoted by Fleischer, on which a_0 was determined, the agreement between measurement and prediction is exact. Considered as a group, the measurements show surprisingly good agreement with the extrapolated values.

Refractive indices were measured by matching the refractive index of the sample with that of an immersion liquid, then finding the refractive index of the liquid by the minimum deviation method. The only estimates available for the refractive indices were those of Ford (1915) who obtained them by extrapolation. They are compared with the values obtained in the present work in Table 2. The agreement between the two sets of data is excellent except for pyrope and andradite. A synthetic pyrope grown by Dr. E. C. Robertson at 950±10° C. and 20,000±1,000 bars had the same index as the sample used in the present study. It was not possible to get an independent check on the index of andradite. The discrepancy is probably due to the method of extrapolation used by Ford, since he used only two variables in a five component system.

TABLE 2. REFRACTIVE INDICES OF GARNETS IN SODIUM LIGHT AT 25° C.

	Ford	Skinner	Difference
Grossularite	1.735	1.734±0.002	−0.001
Andradite	1.895	1.887±0.002	−0.008
Almandite	1.830	1.830±0.002	0.000
Spessartite	1.800	1.800±0.002	0.000
Pyrope	1.705	1.714±0.002	+0.009

TABLE 3. DENSITIES OF GARNETS AT 25° C.

	Fleischer, measured S.G.	Skinner, calculated density, gm./cc.	Difference
Grossularite	3.530	3.594 ± 0.001	+0.064
Andradite	3.835	3.859 ± 0.001	+0.024
Almandite	4.325	4.318 ± 0.001	−0.007
Spessartite	4.180	4.190 ± 0.001	+0.010
Pyrope	3.510	3.582 ± 0.001	+0.072

Due to the fine grained nature of the samples direct measurements of the specific gravity could only be made for pyrope. The densities quoted are those determined from the volume of the unit cell, using Wichers' (1952) atomic weights. The specific gravity of pyrope was determined by selecting a 15 mg. sample of pure single crystals and weighing them in a metal basket on the Berman balance. Toluene was the immersion liquid used. The accuracy of the measurement is not good, since surface effects are large in the basket method. The measured specific gravity at 25° C. is 3.57 ± 0.03, and is perhaps fortuitously close to the value computed from the unit cell. The only good measured values available for comparison are those quoted by Fleischer (1937), and again these values were obtained by extrapolation from measurements on natural compound garnets. The big differences are difficult to explain. The measured specific gravity of pure pyrope on the Berman balance gives a much better check with the calculated density than does Fleischer's value. The big difference between the measured and calculated values of grossularite could not be checked.

The molar volumes (V_m) of the pure end-member garnets have not been previously determined. Table 4 gives the molar volumes at 298.16° K. (25° C.) and 1 atmosphere, with the unit cell sizes used to calculate them. Birge's (1944) value of $(6.02338 \pm 0.00043) \times 10^{23}$ mole^{-1} for Avogadro's number was used in the calculations. The probable accuracy of measurement for the values of a_0 is given as 0.001 Å. The precision of measurement is 0.0005 Å, but due to possible errors in the method of determina-

TABLE 4. UNIT CELL SIZE AND MOLAR VOLUMES OF THE GARNETS AT 298.16° K. AND 1 ATMOSPHERE

	a_0, A	V_m, cc./mole.
Grossularite	11.851 ± 0.001	125.31 ± 0.03
Andradite	12.048 ± 0.001	131.69 ± 0.03
Almandite	11.526 ± 0.001	115.28 ± 0.03
Spessartite	11.621 ± 0.001	118.15 ± 0.03
Pyrope	11.459 ± 0.001	113.29 ± 0.03

tion it is not felt that the accuracy can be stated any closer than 0.001 Å (Skinner, 1955).

The presence of any $(OH)_4$ replacing (SiO_4) in a garnet would probably seriously alter the physical properties, so all possible care was taken to determine whether or not any $(OH)_4$ was present. The hydrogrossularites have a much lower density and refractive index than grossularite, according to Pabst (1932, 1942). It is very probable that the $(OH)_4$ radical in the other garnet molecules would have the same effect as in grossularite, and lower the refractive index and density. Belynakin and Petrov (1941) showed that a strong endothermic reaction occurred at 650° C. when the hydrogrossularite hibschite was heated. The effect is apparently not reversible and they suggest that the transition is "from the original crystalline phase into an amorphous phase." Their heating curves also show exothermic reactions at 870° and 940° C. Natural grossularites, containing no water, do not show any of these reactions. It is very probable that the endothermic reaction at 650° C. corresponds to a breakdown of the hibschite and a loss of water. The garnets used in the present study were individually heated to 750° and 850° for varying periods of time. If the garnets contained some of the hydrogarnet molecules it was expected that the indices of refraction would be increased after the heating, corresponding to a destruction of the hydrogarnet. No such change was found. In all cases the index of refraction was the same before and after heating. It was concluded that the synthetic garnets used do not contain any $(OH)_4$ groups in their structure.

The unit cell size (a_0) and molar volume (V_m) of each garnet was determined at temperatures up to 750° C. in a special 16 cm. diameter *x*-ray powder camera (Skinner 1955). From these data the linear and volume thermal expansion coefficients were determined as a function of temperature from 298° K. to 1023° K. The coefficients (Table 10) are given in the form,

$$\alpha_a = \frac{1}{a_s}\left(\frac{\partial a}{\partial T}\right)_P = b + cT - dT^{-2}$$

and

$$\alpha_v = \frac{1}{V_{ms}}\left(\frac{\partial V_m}{\partial T}\right)_P = b_1 + c_1T - d_1T^{-2}$$

where

α_a and α_v are the linear and volume thermal expansion coefficients respectively.
a_0 and a_s are the unit cell sizes at T° K. and 298.16° K. respectively.
V_m and V_{ms} are the molar volumes at T° K. and 298.16° K. respectively.
b, c, d and b_1, c_1, d_1 are constants of the equations.
P is a constant pressure of 1 atmosphere.
T is the temperature in degrees Kelvin.

TABLE 5. GROSSULARITE: MEASURED VALUES OF a_0 AND CALCULATED VALUES OF V_m AT DIFFERENT TEMPERATURES

Temperature, °C.	a_0, Å	V_m, cc./mole
19.0	11.8503	125.297
21.4	11.8504	125.301
25.0	11.8507	125.309
57.2	11.8529	125.380
94.1	11.8556	125.466
108.8	11.8566	125.497
185.5	11.8626	125.686
277.7	11.8705	125.938
387.9	11.8805	126.257
389.9	11.8807	126.265
480.1	11.8893	126.537
589.3	11.8996	126.866
707.7	11.9123	127.272

Since it is frequently desired to determine the unit cell size or the molar volume at a particular temperature the constants of integration for the above equations are also given. When the equations above are integrated, functions of the form below are obtained.

$$\frac{\Delta V_m}{V_{ms}} = I + b_1 T + \tfrac{1}{2} c_1 T^2 + d_1 T^{-1}$$

where

ΔV_m is the total difference in molar volume from 298.16° K. to T° K.
I is the constant of integration.
T is the temperature in degrees Kelvin.

TABLE 6. ANDRADITE: MEASURED VALUES OF a_0 AND CALCULATED VALUES OF V_m AT DIFFERENT TEMPERATURES

Temperature, ° C.	a_0, Å	V_m, cc./mole
21.4	12.0481	131.676
25.0	12.0484	131.686
59.0	12.0513	131.781
109.1	12.0558	131.928
149.3	12.0593	132.043
208.9	12.0648	132.224
304.2	12.0740	132.527
349.0	12.0783	132.669
427.1	12.0861	132.926
501.8	12.0937	133.176
589.2	12.1032	133.491
629.9	12.1082	133.656
690.0	12.1144	133.862

Table 7. ALMANDITE: Measured Values of a_0 and Calculated Values of V_m at Different Temperatures

Temperature, ° C.	a_0, Å	V_m, cc./mole
21.5	11.5256	115.276
25.0	11.5258	115.283
50.5	11.5274	115.330
108.6	11.5314	115.451
146.9	11.5342	115.535
205.4	11.5388	115.673
243.8	11.5421	115.782
321.0	11.5490	115.980
361.6	11.5528	116.095
401.0	11.5565	116.206
455.5	11.5616	116.360
489.2	11.5653	116.472
543.2	11.5703	116.623
581.3	11.5740	116.735
644.0	11.5813	116.956
709.3	11.5885	117.174
771.0	11.5955	117.387

The details of measurement and method of determining the various parameters in the above equations are described by Skinner (1955).

Tables 5, 6, 7, 8, and 9 show the measured values of a_0 and the computed values of V at different temperatures. All measurements were made with both rising and lowering temperatures to detect any irreversible changes.

Table 8. SPESSARTITE: Measured Values of a_0 and Calculated Values of V_m at Different Temperatures

Temperature, ° C.	a_0, Å	V_m, cc./mole
18.7	11.6200	118.132
19.3	11.6203	118.141
25.0	11.6207	118.154
68.5	11.6242	118.260
129.7	11.6292	118.413
232.5	11.6390	118.713
299.3	11.6465	118.942
394.2	11.6555	119.218
443.5	11.6600	119.356
501.0	11.6675	119.587
557.5	11.6745	119.802
623.0	11.6825	120.049
702.0	11.6915	120.314

Table 9. PYROPE: Measured Values of a_0 and Calculated Values of V_m at Different Temperatures

Temperature, ° C.	a_0, Å	V_m, cc./mole
11.0	11.4578	113.254
25.0	11.4590	113.290
27.7	11.4592	113.296
56.0	11.4612	113.358
89.6	11.4642	113.444
122.3	11.4670	113.527
153.9	11.4697	113.608
195.5	11.4736	113.723
247.1	11.4780	113.854
270.5	11.4805	113.929
289.0	11.4822	113.979
328.1	11.4859	114.089
395.9	11.4924	114.283
441.0	11.4973	114.430
524.2	11.5050	114.660
597.1	11.5138	114.923
629.5	11.5163	114.997
698.5	11.5240	115.228
758.0	11.5305	115.422

The volume thermal expansions of the garnet group are shown in Fig. 1. Pyrope, grossularite and andradite are close to each other. Spessartite, though having a larger expansion than pyrope, grossularite or andradite, is essentially similar in behaviour in that the curves are roughly parallel above 200° C. Almandite is anomalous and the curve does not flatten out as with the other garnets. The effect is completely reversible and cannot be ascribed to strains in the structure being released as the temperature rises or to oxidation effects.

Insufficient data are available on the specific heats of the garnets to determine the characteristic temperatures. The compressibilities of almandite and grossularite have been determined by Adams and Gibson (1929), and of pyrope and andradite by Bridgman (1928). The only data on the elastic constants of the garnets are those by Ramachandra Rao (1945) who determined s_{11}, s_{12}, s_{44} for seven natural iron-bearing garnets.

Using Rao's data for a garnet containing 80% of the almandite end-member, and the molecular weight of pure almandite, a characteristic temperature of 350° K. was obtained for almandite. Since the compressibility alone is insufficient for determining the characteristic temperature, and other data on the elastic constants of the pure end-member garnets are not available, an assumption is necessary to calculate the characteristic temperature. The assumption used was that the ratio of the velocity

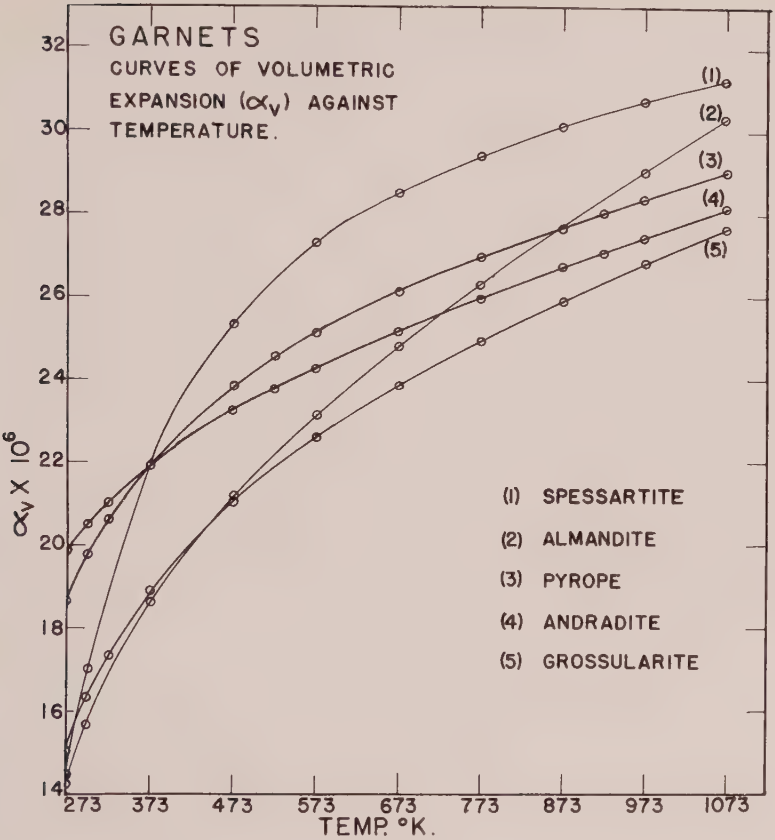

Fig. 1

Table 10. Parameters of Functions Giving the Linear and Volume Coefficients of Thermal Expansion

Substance	Function	Parameters				Accuracy	Temp. range
		b	c	d	I		
		$\times 10^{-5}$	$\times 10^{-9}$		$\times 10^{-3}$		298° K. to
Grossularite	α_a	0.6502	2.697	0.1658	−2.6137	0.3%	973° K.
	α_v	1.951	8.089	0.4972	−7.8406	0.5%	973° K.
Andradite	α_a	0.7010	2.280	0.07468	−2.4407	0.2%	973° K.
	α_v	2.103	6.839	0.2245	−7.3238	0.5%	973° K.
Almandite	α_a	0.5922	4.046	0.1690	−2.5115	0.3%	1023° K.
	α_v	1.776	12.14	0.5071	−7.5347	0.6%	1023° K.
Spessartite	α_a	0.9758	0.9087	0.3856	−4.2422	0.3%	973° K.
	α_v	2.927	2.726	1.156	−12.723	0.6%	973° K.
Byrope	α_a	0.7703	1.985	0.1513	−2.8912	0.3%	1023° K.
	α_v	2.311	5.956	0.4538	−8.6736	0.4%	1023° K.

of the dilational waves (V_p) to the velocity of the rotational waves (V_s) is 1.7 (Birch, 1952, p. 250). With this assumption and the compressibilities of Adams and Gibson (1929) and Bridgman (1928), the characteristic temperatures of andradite, grossularite and pyrope were determined as 270°, 300° and 320° K. respectively. The thermal expansion curves of the garnets (Fig. 1) suggest that these values are too low and that characteristic temperatures between 400° and 550° K. are more reasonable.

REFERENCES

ADAMS, L. H., AND GIBSON, R. E. (1929), The elastic properties of certain basic rocks and minerals: *Proc. Nat. Acad. Sci.*, **15,** 713–724.

BELYANKIN, D. S., AND PETROV, V. P. (1941), The grossularoid group (hibschite, plazolite): *Am. Mineral.*, **26,** 450–453.

BIRCH, F. (1952), Elasticity and constitution of the earth's interior: *Jour. of Geophysics Research*, **57,** 227–286.

BIRGE, B. T. (1945), The 1944 values of certain atomic constants with particular reference to the electronic charge: *Am. Jour. Phys.*, **13,** 63–75.

BRAGG, W. L. (1947), Letter to the editor. *Am. Mineral.*, **32,** 592.

BRIDGMAN, P. W. (1928), The linear compressibility of thirteen natural crystals: *Am. Jour. Sci.*, **15,** 287–296.

FLEISCHER, M. H. (1937), The relation between chemical composition and physical properties in the garnet group: *Am. Mineral.*, **22,** 751–759.

FORD, W. E. (1915), A study of the relations existing between the chemical, optical and other properties of the garnet group: *Am. Jour. Sci.*, **40,** 33–49.

PABST, A. (1937), The crystal structure of plazolite: *Am. Mineral.*, **22,** 861–868.

——— (1942), Re-examination of hibschite: *Am. Mineral.*, **27,** 783–792.

RAMACHANDRA RAO, B. (1945), Elastic constants of garnets: *Proc. Indian Acad. Sci.*, **22,** 194–198.

SKINNER, B. J. (1955), A new *x*-ray heating camera and the thermal expansions of thoria, periclase and diamond: In press.

STOCKWELL, C. H. (1927), An *x*-ray study of the garnet group: *Am. Mineral*, **12,** 327–344.

WICHERS, E. (1952), Report of the committee on atomic weights of the American Chemical Society: *Jour. Am. Chem. Soc.*, **74,** 2447–2450.

Manuscript received May 25, 1955.

THE ABSORPTION AND REFRACTION CORRECTIONS AND THE LATTICE CONSTANT OF CHROMIUM*

M. E. Straumanis and C. C. Weng, *University of Missouri School of Mines and Metallurgy, Department of Metallurgy, Rolla, Missouri.*

Abstract

It has been shown by using x-radiations from a Cu and a Cr target that the absorption correction can be neglected at Bragg angles larger than 76°, if the powder mounts are thin enough (0.12 to 0.2 mm. in diameter), using a Lindemann glass hair as a core. However, refraction corrections are necessary to balance the constants obtained with x-radiations of different wavelengths. Adequate correction equations were derived by Ewald, and by A. J. C. Wilson.

The lattice constants of high purity electrolytic chromium and of chromium obtained by the decomposition of chromium iodide were determined with chromium radiation (see Table 3). A refraction correction of +0.00015 kX was added to the results. In contrast to the results obtained with Cu-radiation, no breaks could be detected in the expansivity curves between +10 and 50° C. because of the lower precision of determination (1:40,000 to 1:60,000 with Cr radiation. (Precision with Cu-radiation: about 1:400,000, taking the probable errors in consideration). The average expansion coefficients of the samples agreed with those obtained by Hidnert.

Introduction

It was shown previously that *no* absorption correction is necessary for lattice constants computed from the last strong line of Debye-Scherrer patterns, if thin Lindemann glass hairs of a diameter 0.08 to 0.1 mm., covered with the powder under study, are used as powder samples.[1,2] It also was shown that the application of the refraction correction *is necessary* in order to balance the lattice constants of the same substance obtained with different x-radiations.[3] However, the introduction of the refraction correction in the case of precision lattice constant determinations from powder patterns has been questioned again recently.[4] Therefore, it seemed advisable to check experimentally once more the question of refraction correction and simultaneously that of the absorption correction.

---

* Extract from a thesis submitted by C. C. Weng in partial fulfillment of the requirements for the Master's degree at the University of Missouri, School of Mines and Metallurgy, Rolla, Mo.

[1] Straumanis, M., and Ievinš, A., Die Präzisionsbestimmung von Gitterkonstanten nach der asymmetrischen Methode, J. Springer Berlin 1940, p. 36; reprinted by Edwards Brothers, Inc., Ann Arbor, Michigan (1948). See also *J. Appl. Phys.*, **20**, 726, 728 (1949).

[2] Klug, H. P., and Alexander, L. E., X-Ray Diffraction Procedures, J. Wiley, New York (1954), pp. 455 and 98.

[3] Straumanis, M., Ievinš, A., and Karlsons, K., *Z. physik. Chemie,* **B42,** 143 (1939).

[4] Barrett, C. S., Structure of Metals, McGraw-Hill, New York (1952) p. 150.

A good opportunity was afforded by the determination of the lattice parameters of four high purity chromium samples, using the radiations obtained from a copper and from a chromium target. The starting material was a sintered electrolytic chromium sample (see Table 1), which produced with Cu-radiation very sharp lines even in the highest back reflection region, so that the last line No. 14 (indices 321)[5] at a Bragg angle of 87.36° (at 30° C.) could be measured very well.[6] The line 321, as shown on Fig. 1, has the appearance of a small circle. The difference in diameter of the circle could be clearly seen with the naked eye when the temperature of the sample was changed by 10° C. Fig. 1 shows the diffraction rings at greater temperature differences.

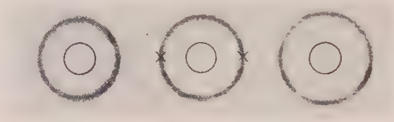

FIG. 1. Back reflection $321\alpha_1$ line ($\theta = 87.474°$ to $87.106°$) of chromium produced by copper radiation. Temperatures of the sample: 10°, 30° and 60° C. (from left to right). The hole for the collimator is 2 mm. wide. The crosses indicate the points of measurement of the lines. Magnification: 2×

Because of the large back reflection angle and the sharpness of the line the reproducibility of the lattice constant measurements was very high, better than 1:400,000 (considering the probable error), so that a slight break in the expansivity curve of chromium at 32.5° C. could be detected.[6] This point could not be found by other *x*-ray methods because of their lower precision.[7]

The result of the direct measurement of the *a* constant of the chromium sample (see below) with copper radiation was

$$2.879123 \pm 0.000007 \text{kX at } 20.0° \text{ C.}$$

not corrected for refraction. As the diameter of the sample was around 0.12 mm. and the reflection angle was above 87°, no absorption correction was applied, because for such a sample at such high angles the absorption correction vanishes. So, the constant above was regarded as a correct one within the given error limits and was used as a standard for comparison with lattice parameters obtained with the same and similar samples but with chromium radiation, yielding the last line No. 6 at a comparatively low Bragg angle of 76.4°. The question of shifting the lines due to absorption by very thin samples (0.1 to 0.2 mm. in diameter) was then attacked by: (1) construction of an a-θ (Bragg angle) diagram, and (2) by comparing the lattice parameters as obtained by chromium and copper radiations.

---

[5] Straumanis, M. E., *Am. Mineral.*, **37,** 48 (1952).

[6] Straumanis, M. E., and Weng, C. C., *Acta Crystallogr.*, **8,** 367 (1955).

[7] Fine, M. E., Greiner, E. S., and Ellis, W. C., *J. Metals*, **3,** 56, 189 (1951).

I. The Chromium Used and the Experimental Procedure

Four high purity chromium samples were used, two of them produced by electrolytic methods and the other two by the iodide method.[8] The two latter samples (from the Battelle Memorial Institute) consisted of shiny crystals and were of two different compositions: one sample being low in metallic admixtures, and the other low in non-metallics, such as hydrogen, nitrogen, carbon and sulfur.[8] The chemical analyses of the three samples, as given by the manufacturers, differ somewhat and are listed in Table 1. The purity of the fourth sample, an electrolytic, degassed chromium (from C. Hardy Inc.) was probably of the same grade as that of the sintered sample (it was treated in hydrogen at an elevated temperature) because of the close agreement of the lattice constants of the two samples (see Table 3).

Table 1. Composition of 3 High Purity Chromium Samples

Impurity	Sintered electrol. Cr. in % by weight	Iodide Cr. (low in metalics) in % b.w.	Iodide Cr. (low in nonmetallics) in % b.w.
H	0.0001	0.0009	0.0001
O	0.0088	0.014	0.001
N	0.019	0.013	0.001
C	0.005		0.001
S			0.003
Sb	0.01		
Si		<0.001	0.001
Fe		<0.001	0.005–0.1
Cu		<0.001	<0.001
Mn		<0.001	0.001–0.01
Mg		<0.001	<0.001
Co		<0.001	—
Ni		—	<0.005
Ca		<0.001	<0.001
Re		<0.001	0.0001–0.001
W		<0.1*	0.001–0.01

* Tungsten probably not present but standard used was only this sensitive.

---

[8] Goodwin, H. B., Gilbert, R. A., Schwartz, C. M., and Greenidge, C. T., *J. Electrochem. Soc.*, **100,** 152 (1953). Metallurgical evaluation of iodide chromium; see Maykuth, D. J., Klopp, W. D., Jaffee, R. J., and Goodwin, H. B., *ibidem* **102,** 316 (1955).

Small quantitites of each of the samples were ground in agate mortars. Because of plastic deformation, the metal, after being ground for several hours, was in the form of fine leaflets. The powder was then carefully sieved through a 325 mesh screen. Only the fine powder that passed the sieve was placed in a silica glass bulb, which was evacuated while being heated, then sealed off. Next, the bulb was heated at 850° C. for $2\frac{1}{2}$ hours to expel the remainder of the dissolved gasses in the chromium powder, and to recrystallize the highly deformed metal leaflets. A longer time for heating or a higher temperature could not be applied, because otherwise the grain size would become so coarse that spots would be formed on the *x*-ray powder diagrams.

The exact values of the lattice constants of the 4 chromium samples were calculated from powder diagrams obtained in precision cameras of 64 mm. diameter, the sample and the camera having a constant temperature. The constancy of the temperature was maintained within limits of $\pm 0.05°$ C. by placing the camera in a special thermostat for a few hours previous to the exposure. The temperature was controlled by circulating water of a thermostatic bath, as previously described.[1,9,10] The exposures were made at ten-degree intervals between 10 and 50° C. For measuring the films, which were 18 cm. in length, a comparator accurate to 0.001 mm. was used. The bare films were inserted into the camera in the asymmetric position so that no correction for film shrinkage nor comparison with a standard substance was necessary. The values of the lattice constants were computed directly from the Bragg angles obtained from the measurement of the films[10] without application of any analytical or graphical extrapolation method. The powder mount was as thin as possible, 0.12 to 0.2 mm. in diameter,[1,9,10] and was rotated during the exposure. In contrast with copper radiation, chromium radiation could be used without complications; the films were clear and the lines sharp and uniform, even without scanning the sample.[11] The collimator bore was 0.8 mm. However the low Bragg angle of 76.4°, of the last doublet No. 6 (211 α_1 and α_2 of Cr radiation) appreciably decreased the precision of the calculated lattice constants. The doublet was clearly resolved, though only α_1 could be used for the lattice constant calculations because the constants calculated from α_2 lines were too low. Evidently the readings of the α_2 lines (according to Bradley and Jay) were influenced by the strong lines which were in close proximity.[12] The wavelength of $CrK\alpha_1$ used was 2.28503kX, and the exposure time was one hour.

---

[9] Straumanis, M. E., and Aka, E. Z., *J. Appl. Phys.*, **23**, 330 (1952).

[10] Straumanis, M. E., *Analyt. Chem.*, **25**, 700 (1953).

[11] Straumanis, M. E., and Aka, E. Z., *Rev. Scient. Instr.*, **22**, 843 (1951).

[12] Bradley, A. J., and Jay, A. H., *Proc. Physic. Soc.*, **44**, 563, 574 (1932).

II. The Absorption Correction

For the construction of the θ-a curve the four strongest interferences in the powder patterns of chromium (chromium radiation) were used: 110β, 110α, 200α and $211\alpha_1$. However the respective Bragg angles, as determined from only *one* film would very seldom give the true a-θ curve, because of the great fluctuation of the constants calculated from lines at lower angles, due to the presence of $\sin\theta$ in the Bragg equation. The only possibility of obtaining the true average statistical curve is to measure the mentioned lines on several films and then to plot the average results.

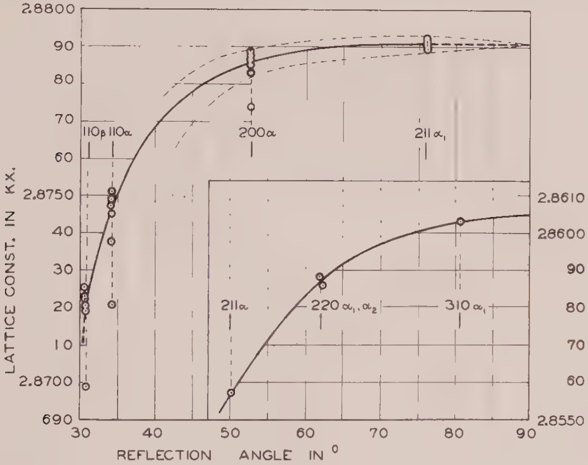

FIG. 2. Lattice constant of Cr (powder mount 0.12 to 0.2 mm. in diameter) versus θ (Cr radiation); 64 mm. camera; 30.0° C. Inset: Lattice constant of Armco Fe (the powder mount was thicker) versus θ (Co radiation) according to Bradley and Jay; 90 mm. camera.

Six films were used for this purpose, these were of electrolytic chromium at a sample temperature of 30.0° C.

As the lattice constants of both electrolytic chromium and the sintered sample (Table 1) agreed closely (Fig. 3), three powder patterns of each sample were used. From the four mentioned lines the lattice parameters were computed and plotted against the Bragg angle θ. Of course, the scattering of the computed lattice parameter values (because of $\sin\theta$) increased with a decreasing angle of reflection. To show the a-θ relation the Kettmann extrapolation curve[13] was drawn through the estimated peaks of the accumulations of the computed points and a smooth curve (Fig. 2) which seemed to terminate in a line parallel to the abscissa, was obtained. This may mean that the average constant as computed from $211\alpha_1$ ($\theta=76.4$) is the final value and *does not have to be corrected* for absorption, providing powder mounts as previously described are used.[1,9,10] The downwards tendency of the curve at lower angles is the result of the increased absorption (and refraction) effect at these angles. In the inset of Fig. 2 a curve, obtained from the data compiled by Bradley and Jay,[14] is shown. Here a correction of the constant calculated from the highest reflection angle is necessary. The thin broken lines on Fig. 2 indicate the increase of the accidental error in the lattice constant measurement with decreasing angle θ. To be sure that the position of the last 211 lines is not affected by absorption within the error limits, the a-constant calculated from this line was compared with that obtained with copper radiation, being free of any influence, as mentioned in the introduction. For this purpose the precise value of the a-constant of sintered electrolytic chromium, determined with chromium radiation, and the linear expansion coefficient to reduce the obtained values to 20° C., was necessary.

---

[13] Kettmann, G., *Z. f. Physik.*, **53**, 198 (1929).

The exposures were made at three different sample temperatures, the $211\alpha_1$ lines were measured and the constants were calculated. From the latter the expansion coefficient was determined, and then the constants were reduced to 20.0° C., as previously shown[1,2,9,10] The results are summarized in Table 2. As the precision of the determinations when compared with the measurements made with copper radiation, was lower (probable error ±0.00005 kX), the break in the a–t curve could not be detected and a straight line was drawn through the middle of the experimental points (Fig. 3). Nevertheless, the average linear expansion coefficient of $\alpha=5.73\times10^{-6}$ was close to the value of 5.93×10^{-6}, the mean obtained with copper radiation. Hence, the two lattice constants of the

TABLE 2. LATTICE CONSTANT OF SINTERED ELECTROLYTIC CHROMIUM COMPUTED FROM THE 211 α_1 LINE (CrK α_1 RADIATION). AVERAGE VALUES OF TWO FILMS AT EACH TEMPERATURE

t in ° C.	Lattice constant in kX		Expans. coeff. in deg.$^{-1}$
	a_t	a_{20}	
10.0	2.87885	2.87902	
30.0	2.87905	2.87889	5.73×10^{-6}
50.0	2.87951	2.87902	
	Average	2.87898±0.00005 kX	

---

[14] Bradley, A. J., and Jay, A. H., *Proc. Physik. Soc.*, **44**, 563, 574 (1932).

sintered sample, obtained with the two different radiations and reduced to 20° can now be compared:

$CuK\alpha_1$; $\theta = 87.420°$ $a_{20} = 2.87912$ kX (rounded off)
$CrK\alpha_1$; $\theta = 76.429°$ $a_{20} = 2.87898$ kX

The considerable difference of 0.00014 kX between these two values, which is completely outside of the experimental error limits given above, indicates that a correction is still necessary. As there is no plausible reason for another correction, *except the refraction correction* to balance out the results obtained with various wavelength radiations, this was applied.

III. The Refraction Correction

The correction for refraction was introduced by the use of the equation as derived by Ewald:[15]

$$a_{corr.} = a_n\left(1 + \frac{5.4a^2d}{h^2}10^{-6}\right) \tag{1}$$

a_n being the constant calculated from the angle θ, λ, and *hkl*; d is the density of the substance, and Σh^2 the sum of the squares of x-ray indices. This equation was derived from

$$a = a_n\left(1 + \frac{\delta}{\sin^2\theta}\right) \tag{2}$$

δ being 1-μ, where μ is the refraction index. The equations are valid only for the case of symmetrical reflection from the plane *hkl*, and the correction increases with increasing density and with decreasing *hkl*. Consequently, constants determined with soft radiations (Cr, Fe) will need larger corrections than those obtained with short waves (Cu, Mo).

The fact that the application of a refraction correction to the measurements of x-ray wave lengths, as calculated from different orders of reflection of the rays from a plane of a single crystal, is necessary, was shown by Stenström, Hjalmar and Larsson in Siegbahn's laboratory.[16] The same correction was also applied in the case of the determination of precise lattice parameters using a single crystal plane, for example by DuMond and Bollman,[17] and recently by Ericsson.[17a]

There is no agreement as to whether the refraction correction should be applied to lattice parameters calculated from powder patterns. Many authors used,[18] and still are using it in the form as indicated by eq. (1) or a similar one,[19] but some authors recommend neglecting this correction.[4]

---

[15] See e.g. Lindh, A. E., in Wien-Harms, Handb. d. Experimentalphysik, XXIV/2, pp. 94, 116, Akad. Verlagsges., Leipzig (1930).

[16] Siegbahn, M., Spektroskopie der Röntgenstrahlen, 2nd ed., p. 21, Berlin, J. Springer (1931).

[17] DuMond, J. W. M., and Bollman, V. L., *Phys. Rev.*, **50,** 524 (1936).

[17a] Ericsson, G., *Ark. Fysik*, **7,** 415, 420 (1954); See also Brogren, G., *ibidem*, **7,** 47, 53 (1953).

The reason for this uncertainty is, without doubt, the difficulty of making the decision by direct measurements because of the minuteness of the correction and because of the somewhat lower accuracy of the powder method as compared with the spectroscopic method. The uncertainty still remains even if the very last lines were used for computation but no precautions concerning constancy of the temperature of the sample, which frequently happens, were made.[1,9,10] However the precision of the method used in this work is high enough[1,6,10] to establish the difference in lattice constants obtained with various x-radiations.

The theoretical considerations of Wilson showed that the refraction correction also has to be applied to lattice spacings calculated from *powder patterns* to obtain the true lattice spacing. In the case of a cubic crystal the extrapolated lattice spacing has simply to be increased by a fraction (1-μ) of itself.[20] According to Klug and Alexander this conclusion of Wilson can be written in a form:[2]

$$a_{corr.} = a_{obs} \times (1 + \delta) \tag{3}$$

where $\delta = 1 - \mu$, and can be calculated for a certain substance from the dispersion equation,[2,15,21] which gives values close to the experimentally determined indexed of refraction.[15,16] In comparing equation (2) with (3) it is easily seen that the latter can be derived from the former if θ approaches $\pi/2$.[22] Hence, using equations (1) or (3), nearly the same corrections should be obtained for constants computed from high Bragg angles.

Consequently for the refraction correction of chromium ($d = 7.2$) with copper and chromium radiations, values 6.1×10^{-5}, and 13.6×10^{-5} kX respectively were obtained with the simple Wilson formula (3). These corrections agree very well with those calculated by eq. (1). The final value of the corrected lattice constant of sintered electrolytic chromium at 20° C., obtained with Cu$K\alpha_1$ and Cr$K\alpha_1$ radiations, is then as follows:

Cu$K\alpha_1$:	2.87912	Cr$K\alpha_1$: 2.87898 kX
Refr. corr (eq. 1):	0.000064 (Wilson 0.000061)	0.00015 (Wilson 0.000136)
a_{20}=	2.87918 ± 0.00001 kX or 2.88500 Å	2.87913 ± 0.00005 kX

---

[18] Miller, P. H., Jr., and DuMond, J. W. M., *Phys. Rev.*, **57,** 198, 203 (1940).

[19] Jette, E. R., and Foote, F., *J. Chem. Phys.*, **3,** 605, 611 (1935).

[20] Wilson, A. J. C., *Proc. Cambr. Phil. Soc.*, **36,** 485 (1940).

[21] See also v. Laue, M., Röntgenstrahl-Interferenzen, Akad. Verlagsges. Leipzig (1948), p. 294, equat. (27.4).

[22] Straumanis, M. E., *Acta Crystallogr.*, **8,** 654 (1955).

As the two results agree now within the error limits (probable error ±0.00005 kX) of the less precise determination, there might be, or might not be at all, any difference in the two determinations. Some doubt in discarding the absorption correction in the case of chromium radiation may arise, because the constant was calculated from $211\alpha_1$, at a relatively low angle of only 76.4°, and because the extrapolation operation used might be too rough (it also could terminate in a line not quite parallel to the abscissa). So the absorption correction was computed,[23] and found to be +0.00003 kX for an opaque sample. As this value is smaller than the precision of determination ±0.00005 kX, it is quite unimportant. However, the absorption correction can definitely be omitted at angles of reflection around and above 80°, because the correction decreases with increasing angle of reflection, and because of the nearly transparent sample used.[1,2,10] In any case, this example with chromium shows that the absorption correction is *negligible*, while the *refraction correction is necessary* because the latter diminishes the differences in the lattice constant values as obtained by the *x*-radiations of different wavelenghts.

IV. LATTICE CONSTANTS AND EXPANSION COEFFICIENTS OF FOUR HIGH PURITY CHROMIUM SAMPLES

Finally, lattice constant and expansion coefficient determinations of 3 more chromium samples of high purity (see Table 1) were made for purposes of comparison. Chromium radiation was used because these 3 samples did not produce the last interference with a sufficient sharpness with copper radiation.

As before, no breaks in the expansivity curves could be found with these samples, because of the lower precision of measurements. All of the constants at 20° and corrected for refraction are summarized in Table 3.

TABLE 3. LATTICE CONSTANTS (CORRECTED FOR REFRACTION) AND EXPANSION COEFFICIENTS OF FOUR KINDS OF CHROMIUM AT 20.0° C.

Chromium	Radiation	Lattice constant in		Aver. exp. coeff. in deg.$^{-1}$ betw. 10 and 50° C.
		kX	Å	
Sintered Electrol.	Cu	2.87918±0.00001	2.88500	5.93×10^{-6}
Sintered Electrol.	Cr	2.87913±0.00005	2.88495	5.73
Electrolytic	Cr	2.87915±0.00004	2.88497	5.56
Iodide (low metallic)	Cr	2.87909±0.00006	2.88491	4.92
Iodide (low nonmetallic)	Cr	2.87907±0.00007	2.88489	6.14

---

[23] Eq. 18A, p. 404, of M. J. Buerger's X-ray Crystallography, J. Wiley, New York (1942).

The error limits given in the Table are (the rounded off) probable errors, and they do not include the systematic errors.

The variation of the lattice parameter of the four chromium samples with temperature is shown in Fig. 3.

Table 3 shows finally that the lattice parameter of the two electrolytic chromium samples agrees within the error limits with that obtained with copper radiation, while the parameter of the two high purity chromium samples obtained by the thermal decomposition of chromium iodide is only slightly smaller, if the error limits given are considered. The expansion coefficients of all four samples are similar.

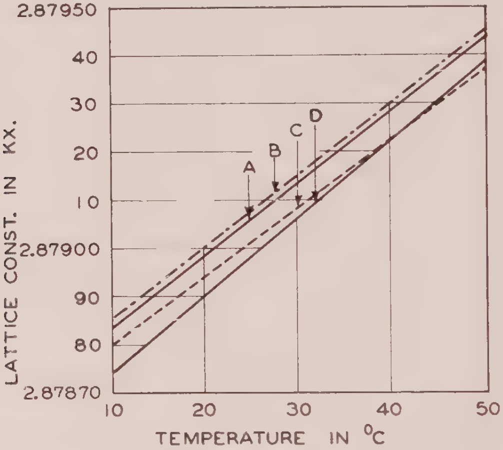

Fig. 3. Lattice parameter of Cr (Cr radiation) versus temperature. The constants are not corrected for refraction. A—sintered electrolytic Cr. B—electrolytic Cr. C—iodide Cr low in metallics. D—iodide Cr low in nonmetallics.

V. Discussion and Conclusions

It follows from theoretical consideration and from the measurements that a smooth θ-a curve can only be obtained if several (at least 4 or 6) precision films are measured and the computation results are plotted. Hence, the probability that a good curve, as shown on Fig. 2, will be obtained from the measurement of only one film is low. Consequently, the analytical and graphical extrapolation methods, using for the extrapolation the lines above 60° from only one film, may give a much larger mistake than anticipated even when the sample was kept at constant temperatures. Correct results will be obtained by determining the angles of reflection from several films, and then using the average values of all or of the closest results for each line for the further operations. In this respect the methods using a larger number of interferences on one film starting for instance from 30°, are more reliable.[24] In all cases the largest weight should be and is given to the last back reflection line,[25] because the constant calculated from this line is affected by the smallest random error. In the present article it is shown again that the lattice parameter of cubic substances can be calculated with high precision from one single last line, and, if the powder mount is thin enough (0.1–0.2 mm. in diameter), without application of the absorption correction. Thus the time-consuming extrapolation procedures can be avoided. Nevertheless, the precision of the method (with the film in the asymmetric position to exclude film shrinkage) is higher than that of the extrapolation methods, as demonstrated with Table 3. Even with chromium radiation producing the last line at a comparatively low Bragg angle, the precision concerning accidental errors is 1 part in 40,000 to 60,000, but in the case of copper radiation it is 1 part in about 400,000 and better.

The films used for lattice constant determination (Table 2) also make it possible to calculate the expansion coefficient. Although only one last line on each film was utilized, the agreement with the measurements of others, working with extrapolation methods, is within the error limits found by them. Constants between 2.8784 to 2.8790 kX at temperatures 18 to 20° have been reported in recent years,[7,26,27] which agree very well with our values: 2.8792 and 2.8791 kX at 20° C. The slightly larger constants obtained in our work may be due to the high purity of the chromium used.

From the agreement of these measurements with the best results of other authors it follows that working with a thin powder mount, with a film in the asymmetric position, and with a precise camera, any correction can be neglected for constants computed from lines above 77°, except the refraction correction which has to be added to the constant directly calculated from the Bragg angle of the respective line.

For the calculation of the refraction correction, equations (1) and (3), giving nearly identical results, can be used. However, for constants obtained from lines at a reflection angle below 80°, equation (1) is preferred. There are no sufficient reasons for omitting this correction;[22]

---

[24] Taylor, A., and Sinclair, H., *Proc. Phys. Soc.* (London), **57,** 126 (1945); Nelson, J. B., and Riley, D. P., *Proc. Phys. Soc.* (London) **57,** 160 (1945).

[25] Hess, J. B., *Acta. Cryst.*, **4,** 209 (1951).

[26] Taylor, A., and Floyd, R. W., *J. Inst. Metals*, **80,** 577 (1952).

[27] Pearsons, W. B., and Hume-Rothery, W., *J. Inst. Metals,* **81,** 311 (1953).

moreover, it has been shown that the correction helps in balancing out the constants calculated from films obtained with different wavelengths radiations.

The average expansion coefficients (Table 3) of 4.92 to 6.14×10^{-6} deg.$^{-1}$ of chromium between 10 and 50° C. agree fairly well with those established by Hidnert[28] (5.7 to 6.6 or 7.5×10^{-6} up to 100° C.).

ACKNOWLEDGMENTS

The authors wish to express their appreciation to the Research Corporation for the Frederick Gardner Cottrell Grant which supported the present investigation. The authors are also grateful to Dr. R. A. Gilbert of the Battelle Memorial Institute for the iodide chromium samples and their analyses, and to Dr. A. W. Schlechten, Chairman of the Metallurgy Department of the School, for assisting with the manuscript.

[28] Hidnert, P., *J. Res. Nat. B. St.*, **26**, 81 (1941); *Phys. Rev.*, **39**, 186 (1932).

Manuscript received June 17, 1955.

AN INTERPRETATION OF THE LAW OF DONNAY AND HARKER

P. HARTMAN AND W. G. PERDOK, *Kristallografisch Instituut der Rijksuniversiteit, Melkweg 1, Groningen, Netherlands.*

ABSTRACT

A physical interpretation of the law of Donnay and Harker is given in terms of bonds between building units in a crystal structure. The following conclusions could be drawn:

(*a*) The law of Donnay and Harker is well obeyed, when the crystal structure is complicated, i.e. when the building units are uniformly distributed throughout the unit cell and occupy several general positions.

When the structure is relatively simple, three conditions must be fulfilled:

(1) The centers of the building units must lie in a general position or in such special positions which do not introduce extra extinctions;
(2) Only one general or special position must be occupied;
(3) The bond energy must decrease with increasing bond length, the latter term being defined as the distance between centers of building units.

(*b*) When these conditions are not fulfilled, a pseudo-lattice may sometimes be found to express the observed morphology better than does the structural lattice. This pseudo-lattice is always determined by the bonds in the structure.

(*c*) It may occur that no lattice or pseudo-lattice can be found to give a sequence of forms in agreement with the observed morphology. This can be traced back to the influence of one or more of the following structural features:

(1) Building units of one kind in special positions;
(2) Like building units in different positions;
(3) Different kinds of building units;
(4) Different kinds of bonds (e.g. strong repulsive energies in ionic structures);
(5) Particularly non-spherical shape of molecules.

(*d*) The relations between morphology and structure are of a more fundamental nature than the relations between morphology and space group. The presented physical interpretation of the law of Donnay and Harker accounts not only for the validity of this law, but also for its exceptions.

INTRODUCTION

The law of Donnay and Harker, which is a generalization of the law of Bravais, states (Donnay and Harker, 1937):

> "The morphological importance of a crystal face is inversely proportional to its reticular area S if the lattice is of the hexahedral mode (no centering) and the space group is devoid of screw axes and glide planes. The effect of lattice centering, screw axes and glide planes is corrected for if the face indices are replaced, in the S formula, by the "multiple indices" of the lowest order of x-ray reflection compatible with the space group symmetry."

This law has been presented as a law of observation; Donnay and Harker gave examples in which the law is obeyed, but showed also that sometimes anomalies do occur, which in some cases can be removed by referring the morphology to a pseudo-lattice.

The present authors have shown (Hartman and Perdok, 1955*a*, *b*) that the consideration of bond energies in the structure gives a better agreement with the observed morphological aspect than do the reticular areas of the lattice. Nevertheless there are many cases of striking agreement between the Donnay-Harker reticular densities and the observed morphological importance, and we have to explain why the geometrical parameters (space group and cell dimensions) of the lattice can rule a physical process like crystal growth to such an extent. We will give here a physical interpretation of the Donnay-Harker law, and show:

(*a*) In which cases we may expect a good agreement,
(*b*) Under which conditions a pseudo-lattice will be found,
(*c*) Why sometimes the Donnay-Harker law is not obeyed at all.

EXTERNAL AND INTERNAL FACTORS

The morphology of a crystal is determined by external and internal factors. External factors are e.g. the influences of solvent and cosolutes. The contribution of these factors may be reduced, when statistical methods are applied which derive one "genotype" from a large number of "phaenotypes" as observed e.g. on a widely spread mineral (Niggli, 1941, p. 450) or on laboratory products under different conditions. Internal factors deal with the structure: its geometry (cell dimensions, symmetry, atomic coordinates) and its physics (type and strength of bonds). The fact that the geometrical law of Donnay and Harker is often obeyed indicates that the factors which rule the morphology converge, so to say, into the lattice. This creates the impression that the lattice rules the morphology and that its influence outweighs the influence of other factors.

PHYSICAL INTERPRETATION OF THE LAW

It follows from the statement of the law that the morphological extinctions correspond with the x-ray extinctions for atoms in the general position. For a physical interpretation we have to consider "building units" rather than atoms. These building units are particles that exist already in the disordered phase and therefore they may be ions and molecules as well as atoms. The geometrical position of an ion or molecule is then taken as the center of gravity of the positions of the constituent atoms and it will be referred to as the "center" of the building unit.

Imagine a structure with building units occupying only the equivalent sites of one general position. Suppose further that the energies of the bonds between the building units decrease with increasing bond lengths. According to our theory that face will be the more important one, for which the attachment energy is smaller. The attachment energy is the bond energy released when one building unit is attached to the surface of a crystal face. We consider the F-faces only. The whole structure can be divided into slices parallel to these F-faces. Only the bonds between two neighboring slices contribute to the attachment energy. Evidently the attachment energy is small when:

(*a*) The bonds are weak,
(*b*) There is only one bond per building unit (see Fig. 1).

In case (*b*) the bond is in general nearly perpendicular to the slice, because the chance that the building unit is attached to the slice with a second bond increases when the first bond deviates more and more from the direction of the normal to the slice.

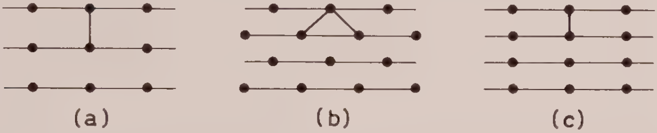

Fig. 1. The effect of bond length and number of bonds per building unit on the distance between slices. Dots represent centers of building units. Only bonds going from one building unit of the upper slice to the next slice are shown. (*a*) One relatively long bond is (nearly) perpendicular to the slices. (*b*) One building unit is attached with two bonds to a lower slice. (*c*) One building unit is attached with one shorter bond to a lower slice.

The attachment energy can increase in two ways:

(1) The bonds become stronger,
(2) There are more bonds per building unit.

In both cases the distance between the slices decreases (Fig. 1). In case (1) because a stronger bond corresponds to a shorter bond length and in case (2) because the bonds can no longer be perpendicular to the slice.

Hence it can be concluded that a face is the more important, the larger the distance between the slices (as this corresponds to a lower attachment energy) and therefore the greater $d_{(hkl)}$.

It may be emphasized that this statement holds for any space group, because we consider the real reticular areas of a structure with building units in the general position. The S-formula used by Donnay and Harker gives reticular areas in a primitive lattice. The procedure of multiplying the indices in the S-formula is essentially to find real reticular areas, by taking into account the effect of lattice centerings and of symmetry operations that have a translation component.

For a physical interpretation of the law the following conditions must be fulfilled:

(1) The centers of the building units must lie in a general position or in such special positions which do not introduce extra extinctions;
(2) Only one general or special position must be occupied;
(3) The bond energy must decrease with increasing bond length, the latter term being defined as the distance between centers of building units.

We may expect that under these conditions the law of Donnay and Harker will hold. In the following lines we shall discuss cases where these conditions are not fulfilled.

EXAMPLES OF EXCEPTIONS TO THE LAW

(1) The first condition is not fulfilled when building units are situated in special positions that introduce extra extinctions in addition to those of the general position.

An example is provided by the *naphthalene* structure, first discussed by Wells (1946). In the morphological setting the space group symbol is $P2_1/a$ (with the b-axis along the twofold axis). The dimensions of the cell are: $a = 8.23$ Å, $b = 6.00$ Å, $c = 8.66$ Å, and $\beta = 122°55'$. The crystals are plates {001}, bounded by {110} and {201}. The latter two forms are of about equal importance; sometimes {111} appears. The law of Donnay and Harker gives the sequence:

$$\{001\}, \{\bar{1}11\}, \{011\}, \{110\}, \{20\bar{1}\}, \cdots$$

In this case the law is not well obeyed: in the third place it gives {011}, a form never observed. Now the centers of the molecules lie in (000), which special position introduces in the space group $P2_1/a$ the condition that $h+k=2n$ for (hkl). Therefore (011) should be (022), so that it does no longer appear among the most important forms. The extinction condition $h+k=2n$ for (hkl) indicates a pseudo-centering of (001); consequently the structure should have a pseudo-lattice $C2/m$. This is indeed the case. The forms {110} and {201} do not, however, appear in the second and third rank.

Still worse is the agreement in the case of *p-benzoquinone* (Wells, 1946), which substance exhibits the same morphology as naphthalene. The cell dimensions are: $a = 7.03$ Å, $b = 6.79$ Å, $c = 5.77$ Å and $\beta = 101.0°$. Here the Donnay-Harker sequence (referred to the pseudo-lattice $C2/m$) is:

$$\{001\}, \{110\}, \{\bar{1}11\}, \{111\}, \{200\}, \{020\}, \{20\bar{1}\}, \cdots$$

Here {201} ranks 7th instead of 3rd. Attention may be called to the fact that only the coordinates of the *centers* of the molecules are considered and not those of the atoms, because only complete molecules are the building units of the structure. In this connection, it may be remarked that (contrary to the views of Wells (1946) a physical interpretation of the law does not require coplanarity of atoms.

The morphology of naphthalene can be related to its structure by applying the concept of periodic bond chains.* A schematic picture of the naphthalene type of structure is drawn in Figs. 2 and 3.† The bonds between the molecules are of the Van der Waals type. Because the bond energy decreases rapidly with increasing distance, only nearest neighbor interaction has to be considered. Four bonds can be found and because of the special positions of the molecules, every P.B.C. vector corresponds with only one bond (Table 1).

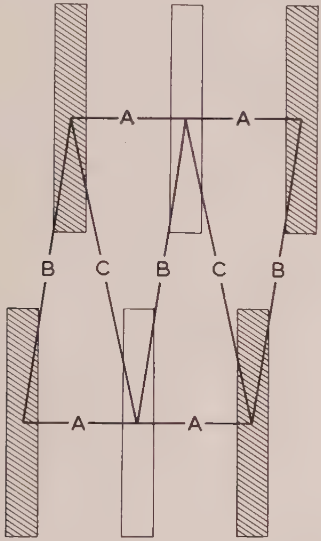

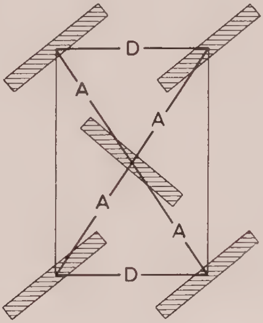

FIG. 2. Schematic picture of the naphthalene type of structure projected on (010). Molecules are represented by rectangles, the centers of the shaded ones being at heights 0 and 1, the others at height $\frac{1}{2}$. The heavy lines indicated by letters represent *P.B.C.* vectors. Note that there is no *P.B.C.* vector in the direction $[\frac{1}{2}\frac{1}{2}1]$.

FIG. 3. Schematic picture of the naphthalene type of structure projected parallel to [001]. For significance of rectangles, lines and letters see Fig. 2.

The four P.B.C. vectors define the *F*-forms:‡ {001}, {110}, $\{20\bar{1}\}$, $\{\bar{1}11\}$ and {100}. The relative importance of these *F*-forms is deter-

---

* The treatment in Hartman, 1953, does not consider the attachment energy.

† In order to show the bonds more clearly, the molecules in Figs. 2, 3, and 5 are not drawn on the same scale, nor do the dimensions of the unit cell refer to any particular substance.

‡ An *F*-form has faces containing at least two P.B.C. vectors.

Table 1. P.B.C. Vectors in the Structure of Naphthalene

P.B.C. vector	Between molecules the centers of which lie in:	Energy
A $[\frac{1}{2}\frac{1}{2}0]$	$(000)-(\frac{1}{2}\frac{1}{2}0)$	a
B $[001]$	$(000)-(001)$	b
C $[\frac{1}{2}\frac{1}{2}1]$	$(000)-(\frac{1}{2}\frac{1}{2}1)$	c
D $[010]$	$(000)-(010)$	d

mined by the attachment energies. A Van der Waals bond between two molecules is the stronger, the more numerous are the places of contact. From the structure it follows that these places of contact between two molecules forming bond a and d are more numerous than those between the molecules forming bond b and c. Therefore the former bonds are the stronger ones. Table 2 gives the attachment energies. If we assume that $a=d$ and $b=c$, then the most important form is $\{001\}$. Next come $\{110\}$ and $\{20\bar{1}\}$, which are about equally important, and then $\{\bar{1}11\}$ and $\{100\}$ follow. This result is in good agreement with the observed morphology, mentioned at the beginning of this section. The same morphology can be deduced for substances having a similar structure (e.g., anthracene, diphenyl, p-benzoquinone, pyrene, durene; cf. Hartman, 1953).

(2) There are two cases in which the second condition is not fulfilled.

(*a*) The building units are all alike, but they occupy more than one position.

An example can be found in the structure of *dibiphenylene-ethylene* (Fenimore, 1948). The space group is *Pcan* and the dimensions of the unit cell are: $a=17.22$ Å, $b=36.9$ Å and $c=8.23$ Å. The molecules are nearly planar; they are parallel to the a-axis and make an angle of about $35\frac{1}{2}°$ with the face (001). The centers of the molecules lie in (000) and in $(\frac{1}{2}, \frac{1}{6}, 0.434)$, so that there are twelve molecules per unit cell. In the direction of the c-axis, the molecules lie close together with their planes approximately parallel. Hence the Van der Waals bond in the direction of the c-axis is very much stronger than in other directions, so that the

Table 2. Attachment Energies of the *F*-forms of Naphthalene

F-form	Attachment energy
$\{001\}$	$b + 2c$
$\{110\}$	$a + c + d$
$\{20\bar{1}\}$	$2a + b$
$\{\bar{1}11\}$	$a + b + c + d$
$\{100\}$	$2a + 2c$

substance must crystallize in needles parallel to the *c*-axis, which was in fact observed by Fenimore. The needles were bounded by {130} dominant and {100} small. Figure 4 gives a projection of the structure on (001). Each pile of molecules in the direction of the *c*-axis is represented by a small circle. It can be seen from this projection that the strongest periodic bond chains run in the directions ⟨310⟩ and ⟨010⟩, which fact accounts for the development of the forms {130} and {100}.

The sequence of the law of Donnay and Harker is:

{020}, {110}, {130}, {200}, {111}, {121}, · · ·

Donnay and Fenimore (1948) pointed out that the structure consists of (001)-centered pseudo-cells with a *b*-axis equal to one third of the structural period. For this pseudo-cell the order given by the law of Donnay and Harker is:

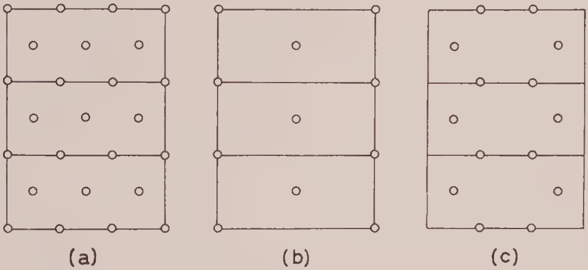

FIG. 4. Projection of the structure of dibiphenylene ethylene on (001). Only the centers of the molecules are shown. Each figure represents three unit cells. (*a*) complete structure; (*b*) molecules in special position; (*c*) molecules in general position.

{130}, {200}, · · ·

Thus we see that the acceptance of a pseudo-cell is necessary in order to have the law of Donnay and Harker obeyed, just because of the interaction of two crystallographically different kinds of molecules. *It may be emphasized that the shape of the pseudo-cell is determined by the bonds between the molecules.*

(*b*) There is more than one kind of building units.

A beautiful example of the difficulties which can arise here, has been discussed by Wells (1946), namely *cuprite* Cu_2O. The Cu atoms form an *F*-lattice, the O atoms an *I*-lattice, while the space group is *Pn*3*m*.

The sequences considered by Wells (1946) are:

space group *Pn*3*m*:	{011}, {111}, {001}, {112}, {122}, · · ·
Cu atoms only	{111}, {001}, {011}, {113}, {133}, · · ·
O atoms only	{011}, {001}, {112}, {013}, {111}, · · ·

The most important form is the octahedron (Kleber & Schroeder, 1935); the theoretical order derived from attachment energies (Hartman & Perdok, 1955*d*): {111}, {011}, {001}, correctly expresses this fact.

Another example is *chalcopyrite*, discussed by Garrido (1949). The S atoms are situated in position (d) $(x, \frac{1}{4}, \frac{1}{8})$ with $x=\frac{1}{4}$. This special position introduces additional extinctions, namely: $h+k+l=2n$ and $2k+l=4n$ for (hkl); $k=2n$ and $l=2n$ for $(0kl)$; $h=2n$ and $k=2n$ for $(hk0)$. The sequence obtained when only S atoms are considered is even somewhat better than the sequence given by the pseudosymmetry $F\bar{4}3m$ (Table 3).

TABLE 3. ORDER OF IMPORTANCE OF FORMS OF CHALCOPYRITE ACCORDING TO THE LAW OF DONNAY AND HARKER AND ACCORDING TO TWO MODIFICATIONS. THE COEFFICIENTS INDICATING THE IMPORTANCE HAVE BEEN TAKEN FROM GARRIDO (1949)

Space group $I\bar{4}3d$		Pseudosymmetry $F\bar{4}3m$		Considering S atoms only	
order	imp.	order	imp.	order	imp.
{011}	6	{112}	7	{112}	7
{112}	7	{010}	4	{010}	4
{013}	4	{001}	6	{001}	6
{010}	4	{110}	5	{011}	6
{001}	6	{012}	5	{110}	5
{121}		{132}		{012}	5
{123}		{116}	3	{132}	
{015}		{332}		{116}	3
{110}	5	{136}		{013}	4
{012}	5	{120}			
		{011}	6		

The cause of this peculiarity can be found when the periodic bond chains are considered. The strongest bonds in chalcopyrite are those between the S atoms and the nearest metal atoms. There are two kinds of periodic bond chains, namely in the directions ⟨110⟩ and ⟨201⟩, consequently the dominant form is {112}. In these chains a sulfur atom is bound to a nearest sulfur atom through a metal atom, so that the structure can be considered to consist of sulfur-sulfur "pseudo-bonds." The law of Donnay and Harker is therefore best obeyed when only S atoms are considered.

(3) (*a*) In ionic structures a smaller distance does not always correspond to a stronger bond.

An example can be found in the development of the zone [001] of *barite* (Hartman & Perdok, 1955*c*).

The observed order of importance is:

(210), (200), (020), (220), (410), · · ·

The law of Donnay and Harker gives the sequence:

(200), (210), (020), (220), (410), · · ·

The anomaly of the first two forms can be understood when the periodic bond chains are considered. In the direction [120] lies a chain the period of which is $[\frac{1}{2}10]$; the chain in the direction of the *b*-axis has the shorter period [010]. The potential energy of an ion in the former chain is higher than that in the latter chain, although its period is longer. This is caused by the fact that the chain in the direction [120] is relatively straight, whereas the other chain is of the zigzag type, so that the repulsion between ions of like charges is greater.

(*b*) The third condition can also be violated when the shape of the molecules differs considerably from that of a sphere. An example is *p-diphenylbenzene*, which has a structure similar to that of naphthalene. The cell dimensions are: $a = 8.08$ Å, $b = 5.60$ Å, $c = 13.59$ Å and $\beta = 91°55'$. This compound crystallizes in tablets {001}, {110}, on which the form {201} has sometimes been observed. In contradistinction to the morphology of naphthalene, the form $\{20\bar{1}\}$ never appears. This is caused by the fact that the longest dimension of the molecules lies in the acute angle β (Fig. 5), while in naphthalene it is found in the obtuse angle β.

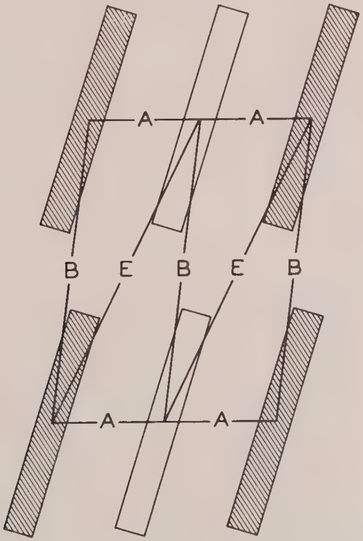

FIG. 5. Schematic picture of the p-diphenylbenzene type of structure, in which the molecules slope backward in the acute angle β. Projection on (010). For significance of rectangles, lines and letters see Fig. 2. Note that in this case there is a *P.B.C.* vector $E[\bar{\frac{1}{2}}\frac{1}{2}1]$ instead of $C[\frac{1}{2}\frac{1}{2}1]$.

The result is that $[\frac{1}{2}\frac{1}{2}1]$ becomes a *P.B.C.* vector instead of $[\frac{1}{2}\frac{1}{2}1]$, although it is the longer of the two. Hence the form $\{201\}$ is an *F*-form, whereas the form $\{20\bar{1}\}$ is an *S*-form and therefore unimportant. The sequence given by the law of Donnay and Harker is:

$$(001), (011), (110), (\bar{1}11), (111), (012), (200), (20\bar{1}), (\bar{1}12), (201), (112), \cdots$$

The rank of the observed form $\{201\}$ is 10; it should be 3.

COMPLICATED STRUCTURES

The crystals that do not obey the law of Donnay and Harker usually have relatively simple structures. For crystals with complicated structures, one may expect the law of Donnay and Harker to be generally followed, although this seems to be in contradiction with the second condition. In such crystal structures several general positions are occupied by building units and if the structure is not fibrous or micaceous, the building units are about "uniformly" distributed in the unit cell. All building units are surrounded by a number of shorter and longer bonds. The longer bonds will, on the average, point more or less into the directions of the normals to the planes with the larger lattice spacings d_{hkl}. The shorter bonds are, on the average, more or less parallel to these planes. Because in general the bond strength is a decreasing function of the bond length, the longer bonds will be at the same time the weaker bonds, so that the attachment energies will be smaller for planes with greater d_{hkl} values, which are therefore the more important ones.

SPACE GROUP DETERMINATIONS

Donnay and collaborators have used the morphological extinctions for space group determinations (Donnay, 1946). It may be inferred from the above considerations that often a lattice can be found in agreement with the law. This lattice, however, is not necessarily identical with the structural lattice. In the case of naphthalene the morphological aspect leads to the space group $C2/m$, which in reality is the symmetry of the pseudo-lattice inherent in the structure. The symmetry of the structural lattice is obscured by the special position of the molecules. For a pseudo-lattice to be detected by suitable application of the law, coplanarity of atoms or centers of building units is not required (see dibiphenylene-ethylene). Morphological extinctions do not entirely correspond with x-ray extinctions. This is an advantage for the application of the law of Donnay and Harker in the first stages of a structure determination (Donnay and Fenimore, 1948), but at the same time it puts a limitation on the method. An advantage, because it can give information as to whether the structure possesses a pseudo-lattice. A limitation, because one is never certain whether a certain morphological extinction is caused by a symmetry element or by a building unit in a special position, until the morphological results are compared with the x-ray results.

CONCLUSIONS

It has been shown (Hartman and Perdok, 1955*a*) that for each structure a set of periodic bond chains gives the clue to the morphology. When this set of periodic bond chains is the same as the set that can be derived from a hypothetical structure with building units in the sites of one general position in the same unit cell, then the law of Donnay and Harker correctly expresses the morphology.

When a pseudo-lattice expresses the law better than does the structural lattice, this pseudo-lattice is determined by the set of periodic bond chains. These chains run in the directions of the axes of the pseudocell (P-lattice), or the face diagonals (A-, B-, C- or F-lattices), or the body diagonals (I-lattice).

ACKNOWLEDGMENT

The authors are very much indebted to Professor P. Terpstra, head of the Crystallographic Institute, for his continuous interest and criticism. Professor J. D. H. Donnay kindly agreed to go over the English of the manuscript.

REFERENCES

DONNAY, J. D. H., AND HARKER, D. (1937), A new law of crystal morphology, extending the law of Bravais: *Am. Mineral.*, **22**, 446–467.

DONNAY, J. D. H. (1946), La détermination du groupe spatial par les données morphologiques: *Bull. Soc. Franç. Minér.*, **69**, 151–155.

DONNAY, J. D. H., AND FENIMORE, C. P. (1948), Groping stages in some organic crystal structure determinations: *Am. Mineral.*, **33**, 755.

FENIMORE, C. P. (1948), The crystal structure of dibiphenylene ethylene: *Acta Cryst.*, **1**, 295–303.

GARRIDO, J. (1949), Sur la morphologie de quelques cristaux à structure pseudosymétrique: *Acta Cryst.*, **2**, 197–201.

HARTMAN, P. (1953), Relations between structure and morphology of crystals: *Thesis*, Groningen.

HARTMAN, P., AND PERDOK, W. G. (1955*a*), On the relations between structure and morphology of crystals, Part 1: *Acta Cryst.*, **8**, 49–52.

HARTMAN, P., AND PERDOK, W. G. (1955*b*), On the relations between structure and morphology of crystals, Part 2: *Acta Cryst.*, **8**, 521–524.

HARTMAN, P., AND PERDOK, W. G. (1955*c*), On the relations between structure and morphology of crystals, Part 3: *Acta Cryst.*, **8**, 525–529.

HARTMAN, P., AND PERDOK, W. G. (1955*d*), Ueber die Beziehungen zwischen Morphologie und Struktur des Cuprit: *N. Jahrb. für Min.*, *Monatsh.*, 97–105.

KLEBER, W., AND SCHROEDER, R. (1935), Ueber die morphologischen und strukturellen Verhältnisse Kuprit: *N. Jahrb. für Min., Geol. und Pal., Beil. Bd.*, *A* **69**, 364–387.

NIGGLI, P. (1941), Lehrbuch der Mineralogie und Kristallchemie. 3. Aufl. Teil 1. Borntraeger, Berlin.

WELLS, A. F. (1946), Crystal habit and internal structure II: *Phil. Mag.*, (7), **37**, 217–236.

Manuscript received May 27, 1955.

ON THE COMPOSITION OF SOME INDIAN CHROMITES*

P. D. Malhotra and G. H. S. V. Prasada Rao,
Geological Survey of India, Calcutta 13, India.

Abstract

Chemical analyses and a study of the composition of some Indian chromites are presented for the first time. Complete analyses of nine samples of separated chromite and partial analyses of 29 samples of chrome ore are given. The samples have been collected from the States of Andhra, Bihar, Madras, Mysore and Orissa. One of the samples completely analyzed is from Baluchistan in Pakistan. On plotting the unit cell compositions of the nine samples of chromite on the triangular diagram, they are all found within the field of aluminian chromites. The Orissa deposits are mostly of metallurgical grade with Cr:Fe ratio exceeding 3:1. In the chromite from Singhbhum, Bihar, there is an appreciable amount of normative magnetite. In the case of the Kondapalle deposit, Andhra, there is a little normative magnetite in the chromite of the reef ore, which is absent in the chromite of detrital ore. The spinel content also is less in the detrital ore. This may be due to leaching of iron, some magnesia and alumina during weathering. In the Mysore chromite normative magnetite is high. The samples from Sittampundi, Madras, show high aluminum and total iron with low chromium.

Introduction

The aim of the present investigation was to study the chemical composition of some Indian chromites, as thus far no complete analyses of pure Indian chromites have been published. The materials are representative of some of the Indian chromite deposits in Andhra, Bihar, Orissa, Mysore and Madras, and include one specimen from Baluchistan in Pakistan. The location of the main chromite deposits of India is indicated on the accompanying sketch map.

Uses of Chromite

Chromite is used for various purposes which can be classed as metallurgical, refractory and chemical. For metallurgical purposes chrome ore is first converted into ferrochrome containing 60 70 pei cent chromium. Ore suitable for this purpose should have at least 48 per cent chromic oxide, with a chromium:iron ratio of not less than 3:1. Silica should be low and combined alumina and magnesia should be less than 25 per cent.

Chromite as a refractory has a high resistance to corrosion and thermal changes and has a neutral character towards slags. Refractory grade chromite should have over 57 per cent of total chromic and aluminum oxides and not more than 5 per cent silica and 10 per cent iron.

For chemical purposes chromite is converted into alkali chromates or bichromates, some of which are used for (i) tanning leather, (ii) manufac-

---

* Published by permission of the Director, Geological Survey of India.

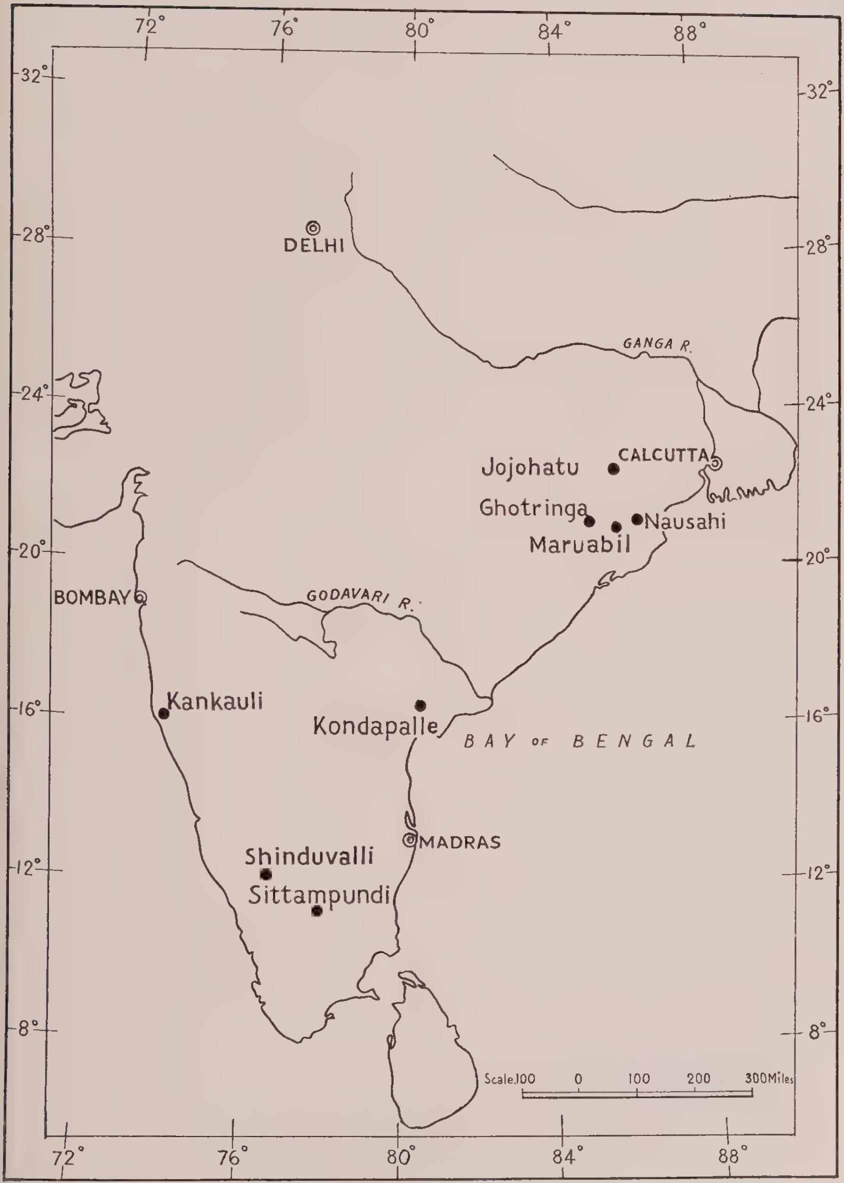

del. M. D.

FIG. 1. Map showing major chromite deposits of India.

ture of pigments, (iii) for dyeing and (iv) for the surface treatment of metals. Chemical grade chromite should have a minimum of 45 per cent chromic oxide with a chromium: iron ratio of about 1.6:1. Silica should generally not exceed 8 per cent while the iron content may be high.

GEOLOGY OF CHROMITE DEPOSITS

Chromite deposits have been classified by Sampson (1942) into the following types: (1) Evenly scattered (or disseminated), (2) Schlieren-banded, (3) Stratified (with a bedded appearance), (4) Sack-form (or pockety) and (5) Fissure form (or vein-like). The deposits in India fall into these types. A brief description is given of the localities where the chromites studied in this paper have been taken.

Shinduvalli, Mysore. Here the chromite occurs as lenses and veins in a narrow band of peridotite running N–S for a couple of miles. The deposits are of the fissure-filling type or locally sack-form. Some of the lenses extend to a depth of 560 feet after which they fray out.

Kondapalle, Andhra. The chromite is found segregated into numerous small lenses and pockets in partly serpentinized ultrabasic charnockites consisting largely of enstatite and hypersthene. Much disseminated ore is also seen.

Sittampundi, Salem District, Madras. Here the chromite occurs in amphibolized pyroxenite rocks which occur as layered sheets with anorthosite. The ultrabasics are intrusive into biotite-gneisses. The chromite forms veins, lenses and disseminated bodies.

Singhbhum, Bihar. About 10 miles W.S.W. of Chaibasa, Singhbhum District, there are three laccolithic bodies of ultrabasics consisting of serpentinized peridotite, saxonite, dunite and pyroxenite, which are intrusive into shales. Chromite occurs as bands and segregations at or near the junction of the different types of rocks. The sides of the laccoliths are nearly vertical and faulted while the central portions are flat dipping.

Keonjhar, Orissa. The chromite deposits are situated on the south-eastern fringe of Boula State forest, where the strike of the iron-ore series suddenly changes from N.E.-S.W. to W.N.W.-E.S.E. Into this disturbed zone of iron-ore series are intruded a group of rocks consisting of gabbro, peridotites and dunites associated with chromite, and anorthosite with vanadifrerous and titaniferous magnetite. The chromite forms schlieren bands, massive lenses and dissemminations in serpentine.

Cuttack and Dhenkanal, Orissa. The deposits here are found in a shear zone 30 miles long with a E.N.E.–W.S.W. strike in the eastern part (Sukinda area) and a N.W.–S.E. strike in the western part (Dhenkanal), the strike changing south of Maruabil (Dhenkanal). The shear zone is roughly parallel to the major shear between the Eastern Ghat facies (khondalite-charnockite-granulite) and the iron-ore series. The chromite was intruded along the junction between quartzite and ultrabasics (south of Kaliapani, Sukinda), into the shear zone of peridotite (south of Maruabil) and along the marginal shears in quartzite (at the junction with granophyric granite?) near Ghotringa.

The deposits at *Hindubagh in Baluchistan, Pakistan*, are found as veins and irregular segregations in saxonite and dunite.

Geochemistry of Chromium

According to Goldschmidt (1937) the crystallization and separation of minerals are influenced greatly by the size of the ions of the principal metallic constituents. The smaller ions form a tighter bond and would be concentrated in the early crystals of an isomorphous series. The ions Al''' (ionic radius 0.57 Ångstrom), Cr''' (0.64 Å), Fe''' (0.67 Å), and Ti''' (0.69 Å) have similar ionic radii and consequently form isomorphous series, at least to a limited extent. Since these elements have relatively small ionic radii, they are differentated early during the crystallization of a magma. With the exception of iron, these elements are lithophilic and remain in the silicate magma even if a sulfide phase separates out early. Although iron is siderophile or thiophile, due to its abundance over sulfur in a normal magma, most of it must remain in the silicate-oxide phase.

As the ionic radii of Al''' and Cr''' are smaller than those of Fe''' and Ti''', it should be expected that they are more abundant in the early formed crystals, while iron and titanium will become concentrated in the later crystals of an isomorphous series. The divalent cations in chromite are MgO and FeO. Since Mg'' (0.78 Å) has a smaller radius than Fe'' (0.83 Å), it will be concentrated in comparison with iron in the early formed crystals. Thus, early formed chromite should be expected to be rich in aluminum, chromium and magnesium, while the later segregations should be progressively enriched in ferrous and ferric iron and titanium. Due to low iron in the early formed chromites, these are expected to have a high chromium:iron ratio. The end member ferrochromite, $FeO \cdot Cr_2O_3$ (32 per cent FeO and 68 per cent Cr_2O_3) cannot occur as a magmatic mineral because a natural magma always contains an abundance of aluminum and magnesium.

Separation of Chromite From the Gangue Minerals

When the chromite was ground to pass 100 mesh and separated by the use of heavy liquids, it was found that it still contained 3–4 per cent of closely adhering impurities or inclusions. A finer grinding to minus 200 mesh was adopted therefore, so as to reduce the impurities to about 1 per cent. An electric centrifuge was used for the separations. The material was examined under the microscope to ensure that it was clean for the purpose of chemical analysis.

GENERAL PLAN OF ANALYSIS

A number of methods are available for the decomposition of chromite. Fusion with a mixture of sodium carbonate and potassium nitrate (10:1 mixture) was used in the initial stages of the work. This method involves not only repeated fusions for the complete decomposition of the mineral but there is also an appreciable attack on the platinum crucible used. Fusion with sodium carbonate only in an oxygen atmosphere (Malhotra, 1954) was found to completely decompose the mineral in a single fusion in about 2 hours, without any notable attack on the platinum crucible. A stream of oxygen from a cylinder was directed on the surface of the melt by means of a bent platinum tube. Completion of the reaction was indicated by the cessation of the rise of gas bubbles in the melt. Silica, alumina, ferric oxide, titania, chromic oxide, manganous oxide, lime and magnesia were determined by the scheme of analysis shown below. Ferrous oxide was determined by the method of Gilbert (1943).

(1) Fuse 0.5 gm. chromite with 5 gm. sodium carbonate, completing the fusion by the supply of oxygen on the melt. Extract with water, add a few drops of alcohol and filter. Wash with 0.1 per cent sodium carbonate solution.

(2) Filtrate contains sodium chromate, sodium aluminate and sodium silicate. Add excess of sulfuric acid, oxidize with persulfate and neutralize with ammonium hydroxide. Redissolve and reprecipitate.

- (a) Combined filtrate contains sodium chromate. Titrate with potassium permanganate after acidifying with sulfuric acid, adding excess of ferrous sulfate, using o-phenanthroline ferrous complex as indicator.
- (b) Precipitate from (2) contains hydroxides of Al and Si. Fume with sulfuric acid, separate and estimate silica. Neutralize filtrate with ammonium hydroxide, filter, ignite and weigh as Al_2O_3 (1).

(3) Residue from (1) contains Fe, Ti, Al, Mn, Ca, Mg and silica. Dissolve in dilute HCl, bake to dehydrate silica. Dissolve in dilute HCl, filter off silica, ignite and hydrofluorize.

(4) Neutralize filtrate from (3) with ammonium hydroxide. Redissolve, reprecipitate and filter. Ignite the precipitate and weigh as $Fe_2O_3+Al_2O_3+TiO_2$. Estimate Fe_2O_3 and TiO_2, getting Al_2O_3 by difference. Add this to Al_2O_3 (1).

(5) Filtrate from (4) contains chlorides of Mn, Ca and Mg. Precipitate and weigh as pyrophosphates after ignition. Separate Ca as $CaSO_4$ with alcohol and estimate Mn colorimetrically,* obtaining Mg by difference.

---

* It is better to reprecipitate Mn and Mg as phosphates in the alcoholic solution after separating $CaSO_4$. If this solution is evaporated to drive off alcohol, an explosive mixture is formed. Mn, Mg phosphates are then dissolved in sulfuric acid for the colorimetric determination of Mn.

The exact locality of the samples analyzed is given below:

(1) Surface lode sample of chromite deposits near Maruabil (21° 03′:85° 43′), Dhenkanal district, Orissa. Collected by M. N. Deekshitulu and P. Perraju.

(2) Chrome ore produced by the Baluchistan Chrome Company, Hindu Bagh, Baluchistan.

(3) Chrome ore from Jojohatu (22° 31′:85° 38′), Singhbhum district, Bihar.

(4) Detrital chrome ore derived from disseminated ore in serpentinized pyroxenite; from deposit on hill 2 miles NW. of Kondapalle (16° 37′:80° 32½′), Kistna district, Andhra. Collected by M. S. Krishnan.

(5) Chrome ore from vein in pyroxenite. Locality near No. 4. Collected by M. S. Krishnan.

(6) Chrome ore produced by the Mysore Chromites Ltd., from Shinduvalli, Mysore.

(7) Chrome ore from Kolhan Government Estate, Singhbhum district, Bihar. Collected by H. C. Jones.

(8) Roro line of Badchambera chromite mine, Chaibasa, Bihar.

(9) Chromite from Nausahi (21° 17′:86° 20′), Keonjhar district, Orissa.

TABLE NO. 1. COMPLETE ANALYSES OF INDIAN CHROMITES

Locality	1 Maruabil	2 Hindu Bagh	3 Jojohatu	4 Kondapalle	5 Kondapalle	6 Shinduvalli	7 Holhan govt. estate	8 Chaibasa	9 Keonjhar
Cr_2O_3 %	61.44	56.46	49.38	55.17	49.98	51.52	52.77	57.38	55.93
Al_2O_3	10.66	12.35	13.80	15.17	15.86	11.56	13.36	10.63	12.19
Fe_2O_3	1.67	3.35	5.83	—	3.99	7.67	2.87	2.62	0.96
TiO_2	0.15	0.23	0.61	0.18	0.33	0.22	0.69	0.43	0.88
FeO	9.86	11.05	16.91	19.29	17.78	12.11	19.20	16.33	18.30
CaO	trace	trace	0.19	0.36	0.25	0.34	0.28	0.25	0.21
MnO	trace	trace	0.17	0.25	0.15	0.17	0.20	0.22	0.41
MgO	15.90	15.38	12.25	9.77	11.86	15.21	10.31	11.77	10.30
SiO_2	0.65	1.34	0.84	0.26	—	0.66	—	0.14	0.16
H_2O	trace	—	0.08	—	—	0.18	—	—	0.12
Total	100.33	100.16	100.01	100.45	100.20	99.64	99.68	99.77	99.46
RO/R_2O_3	0.95	1.00	1.04	1.01	1.07	1.09	1.05	1.04	1.00
Cr	42.06	38.66	33.78	37.74	34.22	35.27	36.13	39.28	38.29
Fe	8.83	10.93	17.20	14.99	16.61	14.78	16.93	17.13	14.89
Cr/Fe	4.76	3.54	1.96	2.52	2.06	2.39	2.13	2.29	2.57
% Cr_2O_3 in ore	56.0	52.30	47.0	52.53	39.40	49.00	38.20	50.60	38.42
% chromite in ore*	91.20	93.76	95.0	95.02	78.80	95.15	72.36	88.16	68.60
Impurity	Talc	Talc	Talc	Talc	—	Talc	—	Talc	Talc

Chromite separations and analysis by P. D. Malhotra.

* This has been obtained by dividing the chromium content of the ore by that of the purified mineral.

The following are the partial analyses of some run of mine Indian chrome ores:

TABLE 2

No.	SiO_2	Al_2O_3	Cr_2O_3	Total iron as FeO	MgO	Cr:Fe
1	25.08		37.18	14.12		2.3:1
2	20.40		43.86	15.21		2.5:1
3	12.08		51.08	15.67		2.9:1
4	16.92		50.31	12.41	3.6	3.6:1
5	16.60		48.50	17.06		2.6:1
6	15.12		45.92	16.44		2.5:1
7	16.80		49.79	13.81		3.2:1
8	16.76		47.98	13.03		3.2:1
9	7.18		50.47	12.99		3.4:1
10	7.62		49.96	13.38		3.3:1
11	8.74		48.94	12.80		3.4:1
12	6.40		51.23	13.57		3.3:1
13	11.66		46.38	11.82		3.5:1
14	12.50		43.20	13.08		2.9:1
15	6.18	5.24	52.12	18.12	15.38	2.6:1
16	7.84	1.53	56.64	16.67	16.09	3.3:1
17			54.21	12.48		3.8:1
18			55.98	12.42		4.0:1
19	0.68	17.90	46.16	23.06	9.2	1.8:1
20	6.32	17.35	38.89	22.75	10.21	1.5:1
21	4.60	17.80	45.80	20.80	9.2	1.9:1
22	0.90	19.80	48.30	21.80	8.5	2.0:1
23	3.32	16.32	49.90	20.36	10.0	2.2:1
24	6.18	24.04	24.44	34.50		0.6:1
25	13.32	41.31	21.73	22.53		0.9:1
26	14.36	29.98	28.20	22.38		1.1:1
27	0.25	25.62	32.98	27.96	5.41	1.0:1
28	1.54	27.76	36.08	30.21	10.02	1.1:1
29	1.56	13.29	50.63	18.51	14.65	2.4.1

Nos. 1 to 14: Surface lode samples of Boula chromite deposit, Keonjhar district, Orissa. Collected by P. K. Ghosh, G. H. S. V. Prasada Rao and S. V. P. Iyengar. Analyzed by P. D. Malhotra.

Nos. 15 & 16: Hand dressed ore from Boula chromite deposits Keonjhar district, Orissa. Collected by G. H. S. V. Prasada Rao. Analyzed by P. D. Malhotra.

Nos. 17 & 18: Surface lode samples of chromite deposits near Maruabil, Dhenkanal district. Collected by M. N. Deekshitulu and P. Perraju. Analyzed by P. D. Malhotra.

Nos. 19 & 20: Chrome ore near Kondapalle, Kistna district. Collected by M. S. Krishnan. Analyzed by Geological Survey of India.

Nos. 21 & 22: Chrome ore near Kondapalle, Kistna district, Andhra. Collected and analyzed by N. Venkatappayya.

No. 23: Chrome ore concentrate from Kondapalle, Kistna district, Andhra. Beneficiated by tabling by Mr. P. I. A. Narayanan.

Nos. 24 to 26: Chrome ore from Sittampundi, Salem district, Madras. Collected by N. K. N. Aiyengar and A. P. Subramaniam. Analyses by Geological Survey of India.

Nos. 27 & 28: Chrome ore concentrate from Sittampundi, Salem district, Madras. Collected by N. K. N. Aiyengar and A. P. Subramaniam. Analyzed by P. T. Ramacharlu.

No. 29: Chrome ore from Shinduvalli, Mysore, B. Rama Rao, (1945).

Composition of Chromite

Chromite is a member of the spinel group of minerals and has the general formula $RO''.\ R_2'''O_3$, where R'' stands for a bivalent metal (mainly ferrous iron and magnesium) and R''' represents trivalent chromium, aluminum, iron and titanium. The formula may be written as $(Fe, Mg)O \cdot (Cr, Al, Fe)_2O_3$. The analyses in Table 1 show that Fe_2O_3 is a minor constitutent in all the specimens excepting the detrital specimen from Kondapalle. Following the method of Thayer, the composition may be expressed in terms of molecular ratio of RO and R_2O_3 constituents. The formulae for the nine complete analyses are as follows:

No. 1	$(Mg_{78}\ Fe_{22})$	$(Cr_{78}\ Al_{20}\ Fe_2)$
No. 2	$(Mg_{71}\ Fe_{29})$	$(Cr_{72}\ Al_{24}\ Fe_4)$
No. 3	$(Mg_{57}\ Fe_{43})$	$(Cr_{66}\ Al_{27}\ Fe_7)$
No. 4	$(Mg_{49}\ Fe_{51})$	$(Cr_{71}\ Al_{29})$
No. 5	$(Mg_{58}\ Fe_{42})$	$(Cr_{63}\ Al_{30}\ Fe_7)$
No. 6	$(Mg_{71}\ Fe_{29})$	$(Cr_{66}\ Al_{22}\ Fe_{12})$
No. 7	$(Mg_{50}\ Fe_{50})$	$(Cr_{70}\ Al_{26}\ Fe_4)$
No. 8	$(Mg_{57}\ Fe_{43})$	$(Cr_{76}\ Al_{21}\ Fe_3)$
No. 9	$(Mg_{51}\ Fe_{49})$	$(Cr_{75}\ Al_{24}\ Fe_1)$

It is thus seen that except for the detrital chromite from Kondapalle (No. 4) and the chromite from Singhbhum (No. 7), the rest of the chromites show a high molecular percentage of magnesium.

Ionic content of chromite unit cells

Following Bragg and Stevens, the unit cells of spinel structure are assumed to contain 8 $(R''O \cdot R''_2O_3)$. Taking this as the unit cell content, the number of atoms of each metal present in the unit cell was calculated from the complete analyses in Table 1.

The method of calculation is as follows: Molecular ratios of oxides were first obtained by dividing the percentage of each oxide by molecular weights. After deducting the calculated amounts of silicate and ilmenite impurities the ratio of (RO) to (R_2O_3) was calculated. In all the analyses except No. 5 and No. 6 the ratio of RO to R_2O_3 was equal to 1, within experimental error (.95 to 1.05). But the values of ratios in No. 5 and No. 6 were 1.07 and 1.09, respectively. The Fe atoms in these analyses were adjusted between FeO and Fe_2O_3 so as to give the ratio of RO to R_2O_3 exactly equal to 1. The molecular ratios are then recalculated to atoms per unit cell, assuming 8 bivalent and 16 trivalent atoms in each unit cell.

The calculations for analysis No. 1 is given below as an example:

ANALYSIS NO. 1

	Per cent	Mol wt.	Molecular ratio	Atoms per unit cell	
Cr_2O_3	61.44	152.02	0.40415	Cr	12.454
Al_2O_3	10.66	101.94	0.10457	Al	3.224
Fe_2O_3	1.67	159.68	0.01046	Fe'''	0.322
			0.51918		16.000
FeO	9.86	71.84	0.10904–.00188[a] =0.10716	Fe''	1.732
MgO	15.90	40.32	0.39437	Mg	6.268
MnO	trace	70.93	—		—
CaO	trace	56.08	—		—
			0.50341–.0100[b] = .49341		8.000
TiO_2	0.15	79.90	.00188		
SiO_2	0.65	60.06	.00182		

$$RO/R_2O_3 = \frac{.49341}{.51918} = 0.95037$$

(*a*) Subtracting .00188 for ilmenite.
(*b*) Subtracting .00188 for ilmenite and .00812 for talc.

The number of trivalent and bivalent metallic ions per unit cell of the chromites are given in the table below:

No.	Cr.	Al	Fe'''	Fe''	Mg
1	12.46	3.22	0.32	1.73	6.27
2	11.57	3.78	0.65	2.30	5.70
3	10.46	4.36	1.18	3.46	4.54
4	11.35	4.65	—	4.12	3.88
5	10.10	4.78	1.12	3.38	4.62
6	10.54	3.53	1.93	2.29	5.71
7	11.19	4.23	0.58	4.03	3.97
8	12.12	3.35	0.53	3.45	4.55
9	11.93	3.88	0.19	3.92	4.08

The spinel triangular prism of composition: Variations in the chemical composition of chromite can be studied by plotting the unit cell compositions in the triangular prism devised by W. D. Johnston Jr. and described by R. E. Stevens. The six corners of the prism are occupied by

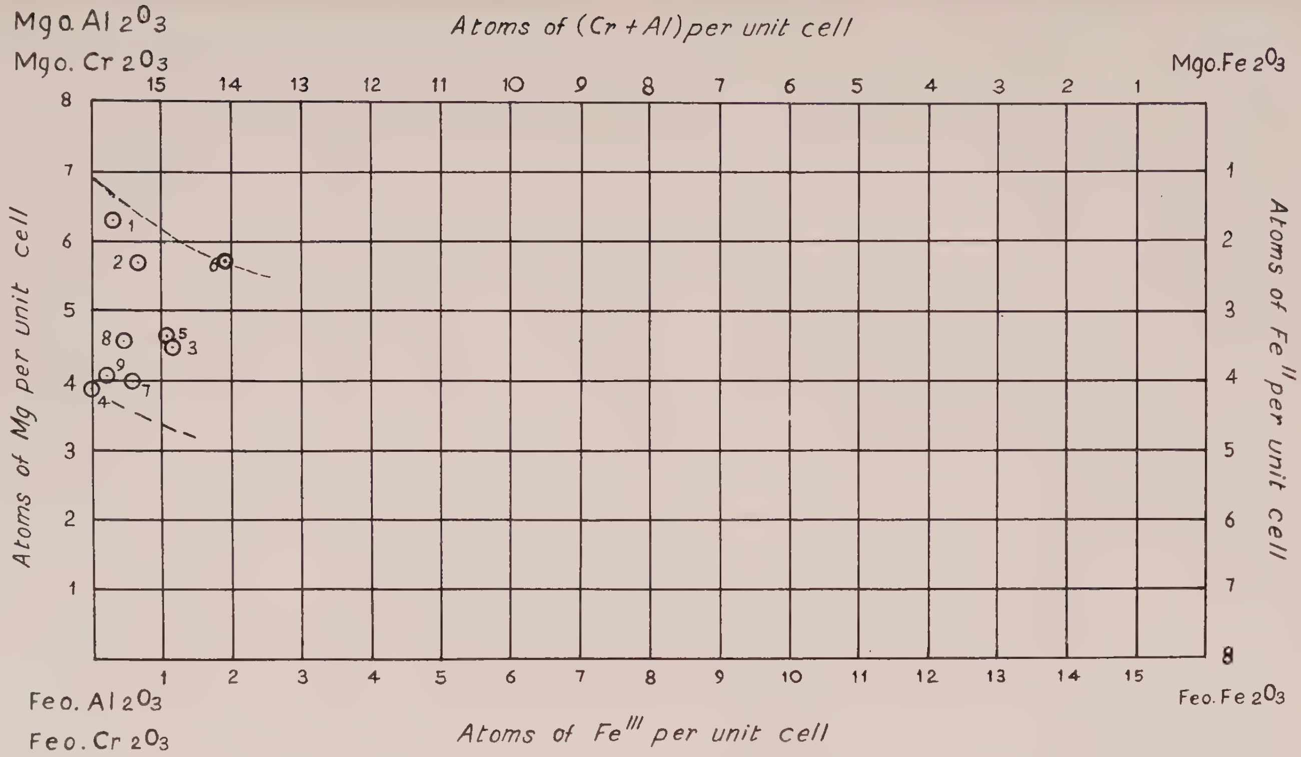

FIG. 2. Graph showing view of spinel triangular prism of composition along line of sight parallel to lines of equal ferric oxide content, showing zone of isomorphism.

$FeO \cdot Cr_2O_3$ (ferro-chromite), $FeO \cdot Al_2O_3$ (hercynite), and $FeO \cdot Fe_2O_3$ (magnetite) at the base of the prism and by $MgO \cdot Cr_2O_3$ (magnesiochromite), $MgO \cdot Al_2O_3$ (spinel), and $MgO \cdot Fe_2O_3$ (magnesio-ferrite) at the top. Thus as the top of the prism is approached the magnesium content increases. The zone of isomorphism obtained by plotting the values can be seen in Fig. 2.

Triangular diagram: The triangular diagram (after R. E. Stevens) is divided into six fields by joining the apices of the triangle with the centers of opposite sides. The apices of the triangle are occupied by $(Mg \cdot Fe)O \cdot Cr_2O_3$, $(Mg \cdot Fe)O \cdot Al_2O_3$, and $FeO \cdot Fe_2O_3$. Compositions falling in the upper two segments in which Cr_2O_3 is the major constituent in R_2O_3 radical, are classified as *chromites*. Those falling in the pair at lower left may be classed *spinels* and those falling in the pair on the right as *magnetites*. Plotting of the Indian chromites in this diagram shows that all of them are within the field of aluminian chromite (Fig. 3).

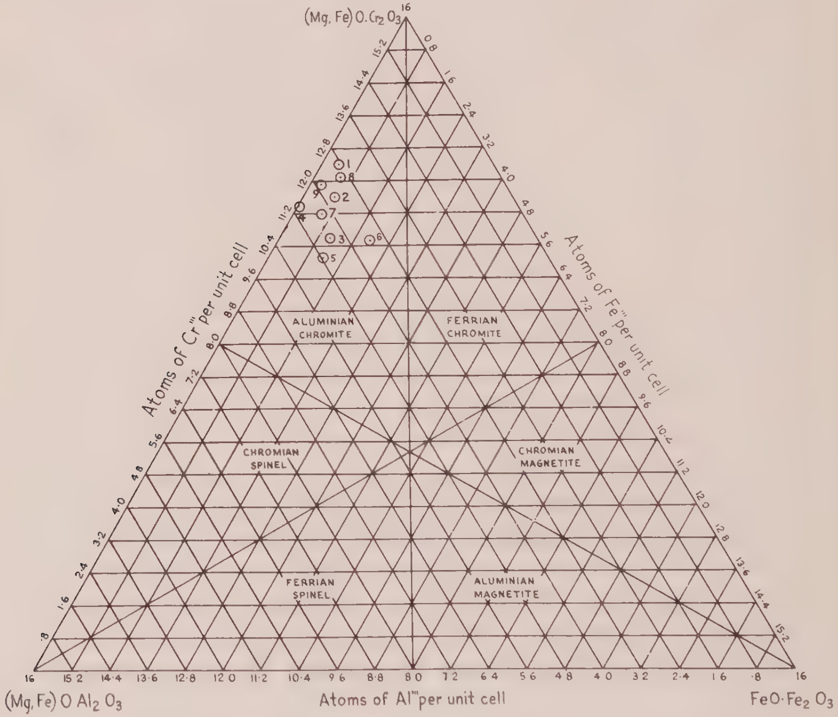

FIG. 3. Triangular diagram showing composition of Indian chromites.

Expression of analyses in terms of end members: The end member system devised by Stevens, suited to express the chemical composition of Indian chromites is spinel-magnesiochromite-ferrochromite-magnetite.

The assignment of particular ions to particular end-member in this method is an arbitrary one adopted for comparing composition. The end member formulae per unit cell are obtained by the following equations:

$$\text{Spinel} = \text{Al}/2$$
$$\text{Magnesio-chromite} = \text{Mg} - \text{Al}/2$$
$$\text{Ferro-chromite} = (\text{Cr} + \text{Al})/2 - \text{Mg}$$

where each element is given in atoms per unit cell. Magnetite can be obtained by subtracting the other end members from the eight formula weights taken as a unit cell.

TABLE 3

End member percentages

	1	2	3	4	5
	Formula percentage				
Analyses Nos. (Table 1)					
Spinel	20.2	23.6	27.2	29.1	30
Magnesio-chromite	58.2	47.6	29.5	19.4	28
Ferro-chromite	19.6	24.8	35.9	51.5	35
Magnetite	2.0	4.0	7.4	—	7
	Weight percentage				
Spinel	15.1	27.3	20.1	21.3	22.2
Magnesio-chromite	59.2	42.6	29.4	19.2	28.0
Ferro-chromite	22.3	25.8	41.6	59.5	41.3
Magnetite	2.4	4.3	8.9	—	8.5
	Formula percentage				
	6	7	8	9	
Spinel	22.1	26.5	21.0	24.2	
Magnesio-chromite	49.3	23.1	35.9	26.8	
Ferro-chromite	16.6	46.8	39.8	47.9	
Magnetite	12.0	3.6	3.3	1.1	
	Weight percentage				
Spinel	16.4	19.3	15.3	17.6	
Magnesio-chromite	49.6	22.8	35.3	26.3	
Ferro-chromite	19.5	53.6	45.6	54.7	
Magnetite	14.5	4.3	3.8	1.4	

Formula percentages are obtained by multiplying the formulae per unit cell by 100 and dividing by 8. The weight percentages of the end members are obtained by multiplying the formulae per unit cell by molecular weight and recalculating them to a total of 100. Table 3 shows formula percentages and weight percentages of the end members for the Indian chromites.

SUMMARY

The chromites from the Keonjhar deposits show high chromium content and high Cr:Fe ratio. For Keonjhar one complete analysis, 14 partial analyses of lode samples and two analyses of dressed ore are presented. Most of them show a Cr:Fe ratio of more than 3:1, reaching 3.6:1 in one case. When the analysis is expressed in terms of end members, the ferrochromite content is higher than magnesio-chromite. But together with normative spinel, magnesium exceeds iron.

One complete analysis of chromite and two partial analyses of the samples from Dhenkanal are given. The Cr:Fe ratio is higher than 3.8:1 reaching 4.76:1 in the pure mineral. Here magnesio-chromite content exceeds ferro-chromite. On geochemical grounds, the chromite of Dhenkanal area appears to be an earlier differentiate than that of other areas.

The Singhbhum deposits are associated with peridotites, dunites and pyroxenites which are free from feldspar. Three complete analyses are presented with Cr:Fe ratio ranging from 1.96:1 to 2.29:1. The molecular composition varies from $(Mg_{57}\ Fe''_{43})\ (Cr_{66}Al_{27}Fe'''_{7})$ to $(Mg_{57}\text{-}Fe''_{43})\ (Cr_{76}\ Al_{21}\ Fe'''_{3})$. In the end member composition, ferro-chromite is more than magnesio-chromite. There is appreciable magnetite content, but the total magnesium, together with the metal represented in normative spinel, is more than iron.

The Kondapalle deposits are found in pyroxenite and norite which are associated with acid to intermediate charnockites. From these, two complete analyses (one reef and one detrital sample) and four partial analyses are presented. The Cr:Fe ratio in the reef ore ranges from 1.5:1 to 2.06:1. In the end members, the composition of ferro-chromite is more than magnesio-chromite. Spinel is particularly high, this showing magnesium far in excess of iron. In the detrital ore the Cr:Fe ratio is 2.52:1. A little normative magnetite present in the reef sample is absent, while spinel is less than in the reef sample. This may possibly be interpreted as due to the leaching of iron, some magnesia and alumina during weathering, though one cannot be sure to what extent leaching does take place.

The Shinduvalli deposits occur in peridotites associated with dunites. One complete analysis and one partial analysis are given. The Cr:Fe ratio is 2.4:1. In the end members, the content of magnesio-chromite is in excess of ferro-chromite. Normative magnetite is appreciably high.

The Sittampundi chromite is in (aluminan) pyroxenite bands which are closely interbanded with anorthosites. They are represented by three partial analyses, with very high aluminum and total iron and low chromium. Cr:Fe ratio varies from 0.6:1 to 1.1:1.

ACKNOWLEDGMENTS

We are greatly indebted to Dr. M. S. Krishnan for initiating this investigation and to him and Mr. V. P. Sondhi for their keen interest and encouragement throughout this work. We express our thanks to Dr. R. K. Dutta Roy for his valuable advice and to Dr. A. P. Subramaniam for his helpful suggestions in the preparation of this paper. Thanks are also due to Dr. R. E. Stevens for his critical reading of the paper.

REFERENCES

1. AIYENGAR, N. K. N., Chromite deposits in the Tiruchengodu and Namakkal Taluks, Salem district: *Ind. Minerals*, **III** (4), 201–204 (1949).
2. AIYENGAR, N. K. N., AND SUBRAMANIAM, A. P., Chromite deposits in the Salem district (unpublished report, 1945).
3. AIYENGAR, N. K. N., AND SUBRAMANIAN, A. P., A note on the petrology of the corundum and chromite-bearing rocks of the Sithampundi-Ramadevam area, Namakkal Taluk, Salem District, Madras: *Curr. Sci.*, **17,** 211–212 (1948).
4. DEEKSHITULU, M. N., On the emplacement of chromite in quartzite near Ghotringa, Dhenkanal district: *Proc. Ind. Sci. Cong.*, **1955.**
5. DEEKSHITULU, M. N., AND PERRAJU, P., Chromite deposits of Maruabil, Dhenkanal, district, Orissa: *Proc. Ind. Sci. Congr.*, session 1955.
6. GHOSH, A. M. N., AND PRASADA RAO, G. H. S. V., Some observations on the chromite occurrences of Nausahi, Keonjhar district, Orissa: *Rec. Geol. Surv. India*, **LXXXII** pt. 2, 281–299 (1952).
7. GILBERT, E. S., Estimation of ferrous iron in difficultly soluble materials: *Ind. Eng. Chem.* (Anal. Ed.), **15,** 189 (1943).
8. GOLDSCHMIDT, V. M., The principles of distribution of chemical elements in minerals and rocks: *J. Chem. Soc.*, 655–673 (1937).
9. KRISHNAN, M. S., Chromite in Kondapalle hills, Kistna district, Madras: *Madras Govt. Dev. Dept. G.O.* No. 1419 *Fort. St. Geor. Gazette* (18th April 1944).
10. KRISHNAN, M. S., Chromite: *Bull. Geol. Surv. India*, Ser. A. No. **7** (1953).
11. MALHOTRA, P. D., A modified method for the decomposition of chromite: *Analyst*, **79,** 785–786 (1954).
12. PRASADA RAO, G. H. S. V., Progress report for the field season 1951–1952 (unpublished).
13. PRASADA RAO, G. H. S. V., A note on visit to the chromite deposits of Sirhikadan area, Singhbhum district, Bihar (unpublished, 1951).
14. RAMA RAO, B., Chromite: *Jour. Sci. Ind. Res.*, **IV**(1), 35–47 (1946).

15, 16. RIDGWAY, R. H., AND SAMPSON, E., *U. S. Bureau of Mines*, Mineral Yearbook 1949. Chromite Deposits. In "Ore deposits as related to Structural Features," Princeton University Press, Princeton, New Jersey (1942).

17. STEVENS, R. E., Composition of some chromites of the Western Hemisphere: *Am. Mineral.*, **29,** 1–34 (1944).
18. THAYER, T. P., Preliminary chemical correlation of chromite with the containing rocks: *Econ. Geol.*, **41,** 202–217 (1946).
19. VENKATAPPAYYA, N., Origin of chromite in the Kondapalle area (Krishna district). Thesis submitted to Andrha University for M.Sc. degree (unpublished, 1947).
20. WILSON, H. D. B., Geology and geochemistry of base metal deposits: *Econ. Geol.*, **48,** 370–407 (1953).

Manuscript received July 6, 1955

OCCURRENCE AND AGE OF CHEVKINITE FROM THE DEVIL'S SLIDE FAYALITE-QUARTZ SYENITE NEAR STARK, NEW HAMPSHIRE*

HOWARD W. JAFFE, HOWARD T. EVANS, JR., AND RANDOLPH W. CHAPMAN,
U. S. Geological Survey, Washington 25, D. C.

ABSTRACT

Chevkinite, a titano-silicate of the cerium earths, occurs as a well-crystallized accessory mineral in fayalite-quartz syenite of the Devil's Slide ring dike near Stark, New Hampshire. The mineral is monoclinic; space group $C2/m$, $C2$, or Cm; $a=13.56$ Å., $b=5.82$, $c=11.21$, $\beta=100°45'$. Crystals are black and prismatic, of splendent luster, irregular fracture, and are metamict. Cores of crystals are birefringent with strong pleochroism, n minimum $=1.97$ (brown), n maximum $=2.05$ (black), 2V variable from medium to large $(-)$; rims of crystals are metamict, isotropic, and brown with n variable from 1.93–1.96. Density is variable, averaging 4.53. The x-ray powder diffraction pattern agrees with that for chevkinite from Bedford County, Va., and Mohave County, Ariz., but differs from that for chevkinite from Kobe-mura, Japan, and perrierite from Nettuno, Italy. The crystal symmetry and cell volume indicate a cell content of 48 oxygen atoms, but mutual substitution of ions such as Si, Ti, Al, Fe^{3+}, Y, Th, Nb, Ca, Fe^{2+}, Mg, Mn, and H is so extensive and complex that a structural formula cannot be established with certainty.

An age determination of the mineral by the lead-alpha activity method gave 207 million years compared with a maximum uncorrected age of 208 million years from total Pb, U, and Th analyses. The age of zircon from the same rock is 227 million years. Geologically the rock belongs to the White Mountain plutonic volcanic series (Mississippian ?).

INTRODUCTION

Chevkinite, a titano-silicate of the cerium earths, occurs as a well-crystallized accessory mineral in fayalite-quartz syenite of the Devil's Slide ring dike just northwest of the village of Stark, New Hampshsire. This is the third occurrence of chevkinite in this country; it has previously been reported by Eakins (1891) and Price (1888) from Bedford and Nelson Counties, Virginia, and by Kauffman and Jaffe (1946) from the Aquarius Mountains, Mohave County, Arizona. The most recent occurrence of chevkinite has been described by Takubo and Nishimura (1953) where it occurs at Kobe-mura, Japan, in its typical geological environment, pegmatite. Other foreign localities include the Ural Mountains, Russia (Rose, 1844; Hermann, 1866; Alimarin, 1935; and Boldireff, 1924, 1925); the Torendrika-Ifasina region of Madagascar (Lacroix, 1915, and Ungemach, 1916); the Kogendo region of Korea (Hata, 1940); Sabaragamuwa Province in Ceylon (Tschernik, 1913, 1914, and 1915), and the Salem district of Southern India (Damour, 1861). A mineral of similar composition found in the sands of Nettuno, Italy, has been described as a new mineral, perrierite, by Bonatti and Gottardi (1950 and 1954).

---

* Publication authorized by the Director, U. S. Geological Survey.

Very little information on the field occurrence of chevkinite is given in the literature. Where the field data are reported, the only previously confirmed occurrences of chevkinite, other than as float, are in pegmatite. Lacroix (1915) suggests that in Madagascar the mineral originated in a pegmatitic phase of an alkalic aegirine granite. The New Hampshire occurrence in fayalite-quartz syenite represents the first time that chevkinite has been recognized as an accessory mineral in an igneous rock other than pegmatite.

PETROGRAPHY

The chevkinite described here occurs in the Devil's Slide syenite, one of the major rock components of the Devil's Slide ring dike which lies just northwest of the village of Stark, New Hampshire. Typically, the Devil's Slide syenite is rather coarse-grained and low in quartz, but the specimen from which the chevkinite comes is a medium-grained fayalite-quartz syenite with 12 to 15 per cent quartz. The following description applies to this specimen.

TABLE 1. MODE OF THE DEVIL'S SLIDE QUARTZ SYENITE NEAR STARK, N. H.

Mineral	Volume per cent*
Microperthite	77.3
Plagioclase	2.7
Quartz	13.9
Hedenbergite	1.8
Hornblende	0.5
Fayalite	3.1
Chevkinite	0.2
Biotite	0.2
Apatite	0.1
Zircon	0.1
Magnetite, pyrite	0.1
Total	100.0

* Average of point count modes of 2 thin sections, determined by R. W. Chapman and H. W. Jaffe.

The quartz syenite is a tough, even-grained, subporphyritic rock composed essentially of greenish feldspar, quartz, and ferromagnesian minerals. The feldspar crystals are equidimensional to lathlike, with lengths ranging from 3 to 5 mm., and with widths of about 1 mm. The ferromagnesian minerals are smaller and more irregular. Carlsbad twins are common in the feldspar. Where fresh, the quartz syenite is greenish gray or bluish gray, but on weathered surfaces it is white with brownish stains.

Microscopically the quartz syenite is hypidiomorphic granular and even-grained. An interdented texture is common. Microperthite, quartz, hornblende, and fayalite ($\alpha=1.815$, $\beta=1.851$, $\gamma=1.862$; $2V$ (calc.) $=57°$, negative) are the principal minerals; and hedenbergite, plagioclase, chevkinite, biotite, apatite, zircon, magnetite, and pyrite are the accessories. Secondary minerals include yellow chlorite, sericite, epidote, and "leucoxene." A mode of the quartz syenite, in volume per cent, is shown in Table 1.

MINERALOGY

Separation and purification

A 25-pound sample of the quartz syenite was crushed and screened to pass a 20-mesh sieve. The $-60+200$ mesh fraction was used for concentration of the chevkinite, at which size the mineral was free of attached impurities. Preliminary separations were made in bromoform to remove the quartz and feldspar which constituted most of the sample. Magnetite was removed with an Alnico hand magnet held above the grains. When the sample was brushed with the magnet, some of the fayalite was magnetic enough to be picked up. The magnetite-free fraction was then further concentrated in methylene iodide and the heavy fraction passed through the Frantz isodynamic magnetic separator at a pitch and tilt of 10° each. Most of the fayalite concentrated at an intensity of 0.1 ampere and all of it at 0.2 ampere. The magnetic concentrate at 0.3 ampere was almost pure chevkinite. Numerous repeated passes at 0.3 and 0.35 ampere finally yielded a 500-mg. concentrate of chevkinite of 99+% purity. Under the binocular microscope, the mineral is black, with a splendent luster, not unlike that of ilmenite, and breaks with an irregular fracture. The concentrate yielded several well-developed prismatic crystals which were hand-picked for crystallographic study. These crystals were also used to determine the density of the mineral by means of the Berman balance. The results were found to vary considerably from sample to sample: 5.6 mg. sample, $d=4.48$; 10.8 mg. sample, $d=4.55$; 12.33 mg. sample, $d=4.63$. The average value of these measurements was $d=4.53$.

Optical properties

Chevkinite from New Hampshire is partly a metamict mineral; while it may form well-developed crystals, optical studies show that these are not all homogeneous. Within a single crystal, two phases, a fresh and a metamict zone, can be recognized. Commonly the cores of the small crystals are fresh and strongly pleochroic from brown to black, whereas the outer metamict zones of the crystals are a light brown and isotropic with a lower index of refraction. Intermediate stages may also be present. The freshest material has a minimum index of refraction of 1.97 and a maximum of 2.05, Z∧elongation is 6°–9°, 2V is variable from medium to large, and the optic sign is negative. The isotropic metamict phase has an index of refraction ranging from 1.93 to 1.96. The presence of a metamict phase and the difficulties encountered in attempting to calculate a neutral formula for this and other occurrences of chevkinite suggest that the metamict phase may be amorphous and variable in composition, whereas the composition of the fresh mineral is not yet proved. This will be discussed further in the section on the chemistry of chevkinite.

CRYSTALLOGRAPHY

Single crystals about 0.3 mm. in size were mounted for *x*-ray crystallographic study by the Buerger precession method. The (*hk*0)-lattice photograph showed clearly the twinning on the (001) plane. Microscopic examination indicates that almost all crystals exhibit contact twinning on (001) in a manner strongly reminiscent of epidote. Upper level photographs indicate a centered cell and the space group is $C2$, Cm, or $C2/m$, most likely the last (C_{2h}^3). The dimensions, accurate to 0.5 per cent, are given in Table 2. It was noted that the precession patterns, made from untreated crystals, were somewhat diffuse, presumably because of their partly metamict character.

TABLE 2. UNIT CELL DATA FOR CHEVKINITE

	N. H. (unheated) (1)	N. H. (heated) (2)	Italy (3)	Russia (4)
a	13.56 Å	13.44	13.59	13.9
b	5.82	5.72	5.61	5.7
c	11.21	11.10	11.61	11.1
β	100°45′	100°20′	113°28′	100°08′

1. Measured by Buerger precession method.
2. Measured by least squares fit to powder diffraction data.
3. Measured by Weissenberg method on crystals of perrierite from Nettuno, Italy, by Bonatti and Gottardi (1950).
4. Inferred from morphological study on crystals from Mount Ilmen, Urals, by Boldireff (1924), with value for *b* assumed.

The crystals gave morphological measurements of poor quality, but the measurements were sufficiently accurate to identify the forms with certainty. Among those observed are the following:

c	001	*e*	021	*p*	112
b	010	*M*	101	*n*	111
a	100	*t*	201	*Q*	$\bar{1}12$
m	110	*r*	$\bar{1}01$	*o*	$\bar{1}11$
d	012	*κ*	$\bar{2}01$		

The crystals are commonly elongated parallel to the *b* axis, flattened on *a*, and twinned on *c*, as shown in Fig. 1*a*. Figure 1*b* is redrawn from Boldireff (1924) to show the similarity of habit between the crystals from New Hampshire and from the Urals. The predominance of the forms observed decreases in the order: *a*, *o*, *m*, *n*, *Q*, *t*, *M*, which is in accord with the *c* centered mode of the monoclinic lattice. The crystallographic elements, derived from the *x*-ray measurements, are as follows:

$$a:b:c = 2.329:1:1.926$$
$$\beta = 100°45'$$
$$x_0' = 0.190$$
$$p_0' = 0.842$$
$$q_0' = 1.926$$

The similarity of crystals from the American and Russian localities is fully evident from the extensive crystallographic description given by Boldireff (1924) for the latter material. His morphological measurements give axial ratios which may be compared as follows:

$a:b:c = 2.426:1:1.955$, $\beta = 100°45'$ (Russia)
$a:b:c = 2.329:1:1.926$, $\beta = 100°45'$ (New Hampshire).

Although no *x*-ray study has been made of the Russian mineral, tentative cell constants are given in Table 2 based on Boldireff's axial ratio and an assumed value of *b*.

The comparison of the single-crystal data with those given for perrierite by Bonatti and Gottardi (1950) is not so clear. They claim the unit cell constants given in Table 2, as determined from sharp Weissenberg photographs. We have not been able to reconcile this unit cell with the morphological data as they are presented by these authors, in the form of stereograms and a limited number of interfacial angles. On the other hand, their arguments showing the close relationship between perrierite, Boldireff's chevkinite, and allanite (orthite) are convincing. In fact, especially in view of the chemical parallelism which will be shown later, there is a possibility that perrierite and chevkinite are the same mineral.

It is particularly apparent from the powder data that is available for chevkinite from several localities, that the unit cell of this mineral is capable of variation in size and shape of perhaps as much as 5 per cent, reflecting the great range of chemical substitution which it apparently can tolerate. This much variation in cell dimensions would readily account

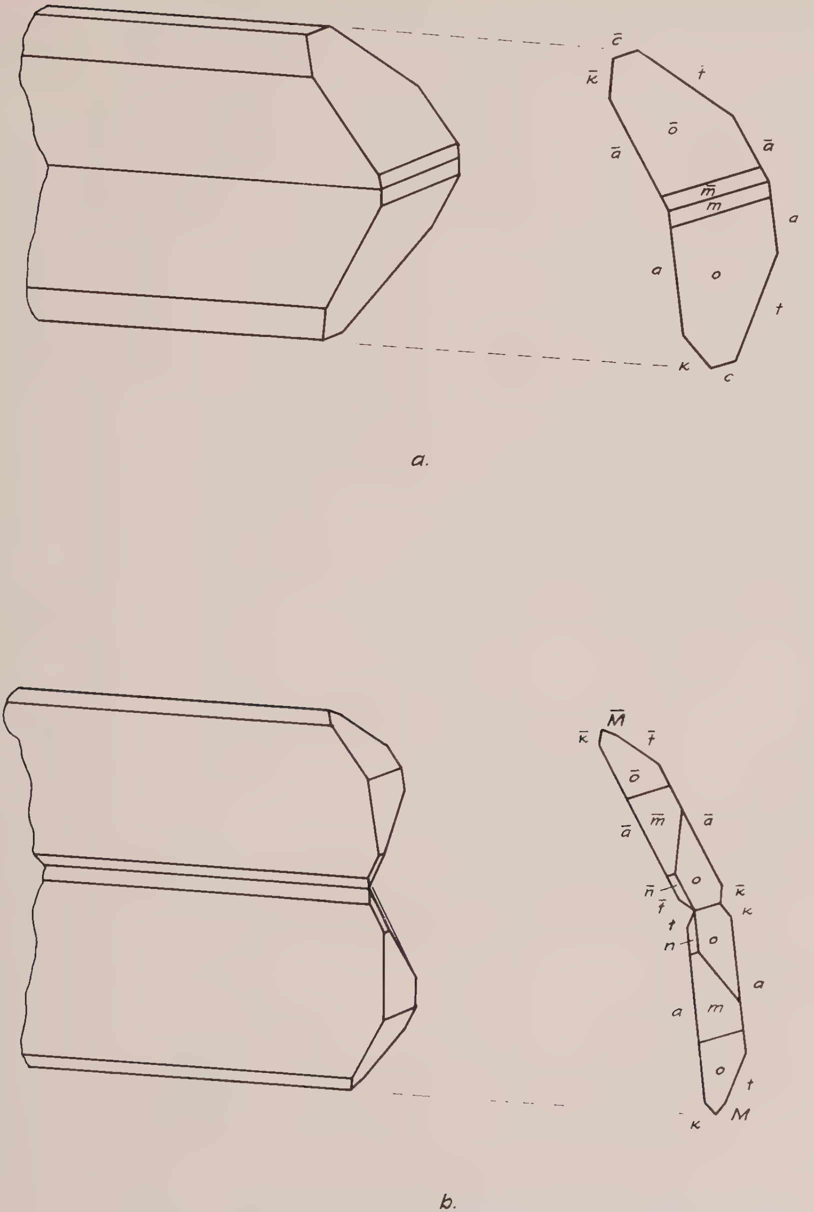

FIG. 1. Crystal habits of chevkinite from (*a*) Stark, N. H., and (*b*) Ilmen Mt., Russia, (redrawn from Boldireff, 1924). Crystals are twinned on *c*(001), and show the forms: *c*{001}, *a*{100}, *m*{110}, *M*{101}, *t*{201}, κ\{$\bar{2}$01\}, *n*{111}, *o*{$\bar{1}$11}.

for the dissimilarity of powder data obtained by us for New Hampshire chevkinite, by Takubo and Nishimura (1953) for Japanese chevkinite, and by Bonatti and Gottardi (1950) for the Italian perrierite. These data are given Table 3, together with expected *d* spacings as calculated from the unit cell constants for unheated chevkinite from New Hampshire given in Table 2. An attempt was made to index the *x*-ray pattern of the Italian material using the corresponding unit cell of Bonatti and Gottardi but without conclusive results. No attempt was made to index the Japanese pattern.

Chevkinite generally gives rather poor powder diffraction patterns because of its partial or nearly metamict character. Heating the mineral in air over a Bunsen burner for an hour was found to be effective in annealing the metamict mineral so that it gave greatly improved powder patterns. Except for sharpness, the patterns for heated and unheated material appear identical, but careful measurement indicates a slight shrinkage of the unit cell of about 1 per cent. The new cell, given in Table 2, was arrived at by a least squares refinement of the unheated cell to give the best fit to the sharpened powder data. The measurements of powder data for heat-treated samples from three American localities are given in Table 4, together with the calculated *d* spacings.

CHEMISTRY

A visual spectroscopic analysis (by H. W. Jaffe) of chevkinite from Stark, New Hampshire, gave the following results:

Major constituents (5%): Ti, Si, Ce, La, Fe
Minor constituents (0.5–5%): Ca, Nd, Al
Trace constituents (0.5%): Nb, Mg, F, Pb, Mn, Na, Y, Th.

A complete chemical analysis of the mineral is given in Table 5 and compared with selected published analyses of chevkinite from other localities. Additional analyses are tabulated by Kauffman and Jaffe (1946).

The analyses listed in Table 5 and others given in the literature do not readily yield a reasonable common formula for chevkinite, as determined by mol ratios. Several have been proposed; for example, $R^{2+}R_2^{3+}(Si, Ti)_3O_{10}$ (Boldireff, 1924), and $R_2^{3+}Ti_2Si_2O_{11}$ (Bonatti and Gottardi, 1954). None of these hypotheses is supported by any convincing evidence, nor do any of them have general applicability. The situation is certainly confused by complex substitutions of ions of different charges in particular crystal structure sites, but the chemistry is made even more uncertain by the presence of pronounced zoning in the single crystals and a widely varying density, as pointed out earlier.

The best approach to the problem of the constitution of chevkinite is

TABLE 3. POWDER DATA FOR UNTREATED CHEVKINITES

hkl	*d* (calc), Å.	N. H. (1)		Japan (2)		Italy (3)	
		d, Å.	*I*	*d*, Å.	*I*	*d*, Å.	*I*
001	11.014			5.399	2	3.85	43
200	6.656			5.195	3	3.50	37
$\bar{2}01$	6.235			4.834	1	2.92	100
002	5.506	5.50	W	4.104	2	2.81	46
110	5.332			3.566	4	2.67	40
201	5.277			3.462	4	2.50	41
$\bar{1}11$	4.947	4.92	MW	3.405	4	2.21	37
$\bar{2}02$	4.695			3.217	2	2.15	55
111	4.665	4.67	M	3.045	5	1.94	78
$\bar{1}12$	3.982			2.983	10	1.81	41
202	3.901			2.956	10	1.78	40
112	3.695			2.841	7	1.73	40
003	3.671	3.67	W	2.699	6	1.65	55
310	3.529			2.579	2	1.59	43
$\bar{3}10$	3.515	3.51	MW	2.513	3	1.45	43
$\bar{2}03$	3.497			2.458	4	1.40	51
$\bar{4}01$	3.364			2.247	2	1.34	55
400	3.328			2.231	2	1.24	47
311	3.224			2.176	5		
$\bar{3}12$	3.194	3.20	Sb	2.158	4		
$\bar{1}13$	3.135			2.108	2		
$\bar{4}02$	3.117	3.11	M	1.952	3		
411	3.033			1.723	2		
203	2.988	2.98	W	1.659	3		
113	2.924			1.612	3		
020	2.905	2.90	M	1.597	2		
021	2.813						
312	2.789	2.79	MW				
$\bar{3}13$	2.757						
004	2.754	2.74	VS				
$\bar{4}03$	2.732						
$\bar{2}04$	2.731						
220	2.666						
402	2.639						
$\bar{2}21$	2.637						
022	2.573	2.60	W				
221	2.548						
$\bar{1}14$	2.525						
		2.19	W				
		1.99	MW				

Intensity (*I*) symbols: VS = Very strong; S = Strong; M = Medium; MW = Medium weak; W = Weak; F = Faint; VF = Very faint; b = Broad.

(1) Measurements by Mary E. Mrose, +0.2%; rad. used, CuKα.

(2) From Takubo and Mishimura (1953).

(3) From Bonatti and Gottardi (1954).

Table 4. Powder Data for Heat-treated Chevkinites, *d* in Å. ±0.2% Measured by Daphne D. Riska; CuKα Radiation

hkl	*d*(calc)	N. H.		Ariz.		Va.		N. H.		Ariz.		Va.	
		d	*I*	*d*	*I*	*d*	*I*	*d*	*I*	*d*	*I*	*d*	*I*
001	10,920	11.1	F	11.1	F	11.1	F	2.24	VF	2.24	VF	2.24	F
200	6.611							2.17	M	2.17	M	2.16	M
$\bar{2}01$	6.167							2.08	VFb	2.08	VFb	2.08	VFb
002	5.460	5.44	F	5.47	F	5.44	F	2.00	VF	2.00	VF	2.00	VF
201	5.254							1.97	Mb	1.97	Mb	1.96	M
110	5.250											1.94	VF
$\bar{1}11$	4.869	4.86	W	4.85	W	4.86	W	1.82	VF	1.83	VF		
$\bar{2}02$	4.638							1.79	VF	1.79	F	1.79	F
111	4.606	4.60	W	4.60	W	4.60	W	1.74	VFb	1.74	F	1.74	Fb
$\bar{1}12$	3.927							1.70	VF	1.71	F	1.70	F
202	3.882			3.85	VF	3.84	VF	1.67	VFb	1.67	Fb	1.67	Fb
112	3.657							1.63	VFb	1.63	F	1.62	Fb
003	3.640	3.63	VF	3.65	VF	3.64	F					1.53	VF
310	3.491											1.50	VF
$\bar{3}11$	3.472	3.47	F	3.47	W	3.47	W					1.44	VF
$\bar{2}03$	3.462							1.43	VFb			1.43	VF
$\bar{4}01$	3.334	3.35	VF	3.35	F	3.34	VF	1.41	VFb			1.41	VF
400	3.306											1.37	VF
311	3.196	3.20	S	3.21	S	3.18	Sb					1.36	VF
$\bar{3}12$	3.152	3.15	S	3.15	S			1.34	VF			1.34	VF
$\bar{1}13$	3.096	3.08	W	3.10	W	3.09	W	1.29	VFb			1.29	VFb
$\bar{4}02$	3.083							1.27	VFb			1.26	VFb
401	3.017	3.00	F	3.01	W	3.00	W					1.20	VF
203	2.971											1.18	VF
113	2.896												
020	2.860	2.86	M	2.86	M	2.87	M						
312	2.768												
021	2.767	2.76	F	2.75	W	2.77	W						
004	2.730												
$\bar{3}13$	2.720												
403	2.700	2.71	S	2.71	S	2.71	S						
$\bar{2}04$	2.700												
402	2.626												
220	2.625	2.61	VF	2.61	F	2.61	F						
$\bar{2}21$	2.595												
022	2.534	2.53	F	2.52	F	2.53	F						
221	2.512												
$\bar{1}14$	2.496												
$\bar{2}22$	2.435	2.44	VF	2.44	VF	2.44	VF						
511	2.429												
510	2.400												
204	2.378												
313	2.358												
114	2.355												
$\bar{5}12$	2.342												
$\bar{4}04$	2.319	2.32	VFb	2.32	VFb	2.32	VFb						
$\bar{3}14$	2.316												
222	2.303												

Symbols as for Table 3.

TABLE 5. CHEMICAL ANALYSES OF CHEVKINITE AND PERRIERITE

	1	2	3	4	5	6	7
SiO_2	20.15	12.04	20.21	17.66	19.35	19.31	19.22
TiO_2	17.81	17.08	18.78	17.93	19.06	23.24	17.22
Al_2O_3	2.08	0.93	3.60	0.23	6.13	0.67	3.86
Fe_2O_3	1.22	9.56	1.88	8.81	1.33	1.26	4.56
Nb_2O_5	0.05	—	0.08	0.63	0.23	—	—
FeO	11.11	7.76	6.91	9.95	6.19	4.05	7.24
MgO	0.35	0.74	0.55	0.31	0.20	0.81	—
MnO	0.28	0.50	—	tr.	0.70	—	1.34
CaO	3.20	3.35	4.05	2.12	4.71	4.11	3.34
Ce_2O_3	20.74	25.29	20.05	14.21	19.02	31.80	18.58
La_2O_3	11.6						
Pr_2O_3	1.6						
Nd_2O_3	5.8	18.35	19.72	24.09	18.51	6.83	22.70
Sm_2O_3	0.7						
Gd_2O_3	0.5						
Y_2O_3	0.5	1.50	1.82	2.45	3.49	1.51	1.25
ThO_2	1.0	0.82	0.85	0.67	0.59	4.05	0.80
P_2O_5	—	0.38	—	—	—	—	
$(Na, K)_2O$	—	—	0.06	—	—	1.05	0.37+0.42
SnO_2	—	—	—	0.25	0.09	—	
H_2O	0.90	1.50	0.94	—	0.46	0.61	0.67
Total	99.59	99.80	99.50	99.31	100.06	99.30	101.57

1. Stark, N. H., Glen Edgington, Analyst.
2. Mohave County, Arizona (Kauffman and Jaffe, 1946).
3. Bedford County, Virginia (Eakins, 1891).
4. Kōgendō, Korea (Hata, 1940).
5. Kobe-mura, Kyoto Pref., Japan (Takubo and Nishimura, 1953).
6. Nettuno, Italy, perrierite (Bonatti and Gottardi, 1954).
7. Ilmen Mt., Urals (Kauffman, 1924).

Notes:

a. La, Nd, Pr, Sm, Gd, T, and Th were determined spectrographically in analysis 1 by H. J. Rose, Jr., on the rare-earth precipitate separated from chevkinite.

b. U=0.0186 in analysis 1, determined fluorimetrically by A. M. Sherwood.

c. Pb=0.0098 in analysis 1, determined spectrographically by C. L. Waring.

through a study of the limitations imposed by the size and symmetry of the unit cell as determined by the *x*-ray measurements. It is well known that most of the volume of a crystal unit cell of an oxide structure will be accounted for by the oxygen atoms alone. Neglecting all other atoms, the specific volume of oxygen in the related mineral epidote (whose structure has been established in detail by Ito, Morimoto, and Sadanaga, 1954) is 18.1 $Å^3$. Two rare-earth minerals may be cited also to show that the moderate-sized rare-earth cations still do not influence the specific volume of oxygen appreciably: in bastnaesite it is 17.6 Å^3, and in monazite it is 18.6 Å^3. Taking the value of the oxygen volume as 18.1 Å^3, as in epidote, the calculated number of oxygen atoms in chevkinite (unit cell volume 873 Å^3) is 48.2. Since the space group $C2/m$ allows atoms in groups of 2, 4, 8 or 16, we may expect to find 48 oxygen atoms in the unit cell. On this assumption we can now count the average number of all the other atoms in the cell for each chemical analysis. The atom counts corresponding to 48 oxygen atoms for the seven analyses of Table 5 are given in Table 6, each from a different locality.

TABLE 6. UNIT CELL CONTENTS FOR CHEVKINITE FROM VARIOUS LOCALITIES

Atom	New Hampshire (1)		Arizona (2)		Virginia (3)		Korea (4)		Japan (5)		Italy (6)		Russia (7)	
Ti	5.7	5.7	5.9	5.9	5.9	5.9	6.1	6.1	5.7	5.7	7.6	7.6	5.5	5.5
Si	8.6		5.5		8.4		7.9		7.6		8.3		8.1	
Al	1.1	10.1	.5	9.3	1.8	10.8	.1	11.0	2.9	10.9	.3	9.0	1.9	11.5
Fe^{3+}	.4		3.3		.6		3.0		.4		.4		1.5	
Ce	3.4		4.3		3.1		2.3		2.8		3.0		2.9	
R.E.	3.3	6.9	3.1	7.9	3.0	6.6	4.0	7.0	2.7	6.3	1.1	6.8	3.5	6.9
Y	.1		.4		.4		.6		.7		.3		.3	
Th	.1		.1		.1		.1		.1		.4		.2	
Fe^{2+}	4.0		3.0		2.4		3.7		2.1		1.5		2.6	
Ca	1.5	5.8	1.7	5.4	1.8	4.4	1.0	4.9	2.0	4.4	1.9	3.9	1.5	4.6
Mn	.1	28.5	.2	29.5	—	27.7		29.0	.2	27.3	—	27.3	.5	28.5
Mg	.2		.5		.2		.2		.1		.5		—	
H	2.6		4.6		2.6		—		1.22		1.8		1.9	
O	48.0		48.0		48.0		48.0		48.0		48.0		48.0	
d(calc.)	4.94		5.24		4.76		—		—		4.86		—	
d(obs.)	4.53(ave.)		4.67		—		—		4.38		4.53		4.45	

Note: For analysis references, see Table 5.

The data contained in Table 6 still do not lead to an unambiguous formula for the mineral, but certain consistent patterns do appear. The number of titanium atoms in the unit cell does not vary far from 6 (average 6.05). Two kinds of titanium are implied, therefore, with one kind on a symmetry center, which is consistent with the probable octahedral coordination for this atom. Such a site is not possible for the tetrahedrally coordinated silicon, and thus there are most likely 8 of these atoms in the cell, since all of the 2-fold sites in the space group $C2/m$ correspond to symmetry centers. One possible formula could be written as follows: $R_3^{2+}R_3^{3+}AlSi_4Ti_3O_{22}(OH)_2$. However, Table 6 shows considerable variation from this ideal formula, suggesting a complex system of substitutions of the various cations for one another among the various cation sites (e.g., Al^{3+} and Fe^{3+} for Si^{4+} or Ti^{4+}, Ce^{3+} for Fe^{2+}, O^{2-} for OH^-, etc.). Also, it should be remembered that, in view of the chemical disturbances resulting from the metamict state, an uncertainty of one atom more or less per group is to be expected. Consequently, it is impossible to predict of what type these sites will be in the actual structure.

When the number of atoms in the unit cell, and also the unit cell volume, are known, the density can be calculated, and these data where available are given in Table 6. The calculated densities are always considerably higher than the measured values, but this result is typical of a metamict mineral. For example, fresh zircon has a density of about 4.7, but densities of metamict zircon have been measured as low as 4.0.

Bonatti and Gottardi (1954) have described in detail the crystallographic and structural relations between chevkinite, allanite, and epidote. It seems likely that Ito's determination of the structure of epidote should aid in the solution of the chevkinite structure. The final answer to the question of the constitution of chevkinite must wait until the time when its structure is known, but until then, the above treatment probably provides the best understanding of the problem.

AGE DETERMINATION

The Devil's Slide fayalite-quartz syenite from which the chevkinite was obtained is one of the major components of the Devil's Slide ring dike near the village of Stark in the Percy Quadrangle, New Hampshire. The ring dike has been assigned by Chapman (1948) to the White Mountain plutonic volcanic series (Mississippian?). An age determination was recently made by the lead-alpha activity method (Larsen, Keevil, and Harrison, 1952) on zircon from the same rock containing the chevkinite. The zircon gave an age of 227 M.Y. confirming the age assigned by Chapman to the Devil's Slide syenite. Chevkinite from the same rock specimen was also determined and gave an age of 208 M.Y. using the approximate, uncorrected age formula of Keevil (1939) according to which

$$T = \frac{7.23 \text{ Pb}}{\text{U} + 0.322 \text{ Th}} \times 10^9$$

where Pb, U, and Th represent concentrations in percent.

The age formula of Larsen, Keevil, and Harrison (1952) is

$$T = \frac{c}{\alpha} \text{Pb}$$

where Pb is the lead concentration in parts per million, α is the alpha count per milligram per hour, and c is a constant. c is taken equal to 2613 if all of the alpha activity is due to uranium and 1988 if all of the alpha activity is due to thorium. For zircon, c is assumed to be 2400 because previous analyses of the mineral have shown that the activity is due equally to uranium and thorium. For chevkinite, the value for c is approximately 2100 based upon determinations of uranium and thorium in the mineral. The lead, uranium, thorium, alpha activities, and age calculations for zircon and chevkinite are given in Table 7.

If the chevkinite contained a large amount of original lead of crystallization, its age would not be expected to show any agreement with the zircon age. The reasonably good agreement between both ages and the geology suggests that chevkinite may have potential value as an age mineral where it occurs as an accessory constituent of igneous rocks from other localities.

TABLE 7. AGE DETERMINATIONS OF MINERALS FROM THE DEVIL'S SLIDE SYENITE, STARK, N. H.*

Mineral	U (%)	Th (%)	Alpha Count (α/mg/hr.)		Pb (ppm)	Age (M.Y.)
			Calc.	Meas.		
Zircon	—	—	—	465	44	227
Chevkinite	0.0186	1.0	953	995	98	207

* Determinations by H. W. Jaffe.

ACKNOWLEDGMENTS

The authors are indebted to their many colleagues in the U. S. Geological Survey for assistance, particularly to Glenn Edgington, A. M. Sherwood, and C. L. Waring for analytical determinations; to D. D. Riska and M. E. Mrose for powder diffraction work; and to W. L. Smith for assistance in mineral separation of chevkinite.

REFERENCES

ALIMARIN, I. P. (1935), The chemical composition of chevkinite: *Compt. rend. acad. sci. U.S.S.R.*, **1**, 648–651.

BOLDIREFF, A. (1924), Crystallographic study of chevkinite: *Bull. acad. Sci. russie*, **18**, 257–288.

——— (1925), Étude cristallographique de la tscheffkinite de l'Oural: *Bull. soc. franc. de minéral*, **48**, 120.

BONATTI, S., AND GOTTARDI, G. (1950), Perrierite, nuovo minerale ritrovato nella sabbia di Nettuno (Roma): *Acc. Naz. Lincei. Rend. Sc. Fis. Mat. e Nat.*, ser 8, **9**, 361.

——— (1954), Nuovi dati sulla perrierite: *Rendiconte della Soc. Mineralogica Italiana, Anno* **X**, 208–225.

CHAPMAN, R. W. (1948), Petrology and structure of the Percy quadrangle, New Hampshire: *Geol. Soc. Am., Bull.* **59**, 1059–1100.

DAMOUR, A. (1861), Note sur la tscheffkinite de le cote du Coromandel: *Bull. soc. géol. de France,* **19,** 2d Ser., 550–551.

EAKINS, L. G. (1891), New analyses of astrophyllite and tscheffkinite: *Am. Jour. Sci.*, 3rd ser., **6,** 34.

HATA, S. (1940), Chevkinite from Korea: *Bull. Inst. Phys. Chem. Res.* (*Tokyo*), **19,** 1321–1324.

HERMANN, R. (1866), Über die Zusammensetzung des Tschewkinits: *Bull. soc. Moscou* (Soc. Imp. des Naturalists), **39,** (1), 57–64.

ITO, T., MORIMOTO, N., AND SADANAGA, R. (1954), On the crystal structure of epiodote: *Acta Cryst.*, **7,** 53–61.

KAUFFMAN, L. E. (1924), Chemical composition of chevkinite: *Bull. acad. sci. Russie,* **18,** 315–320.

KAUFFMAN, A. J., JR., AND JAFFE, H. W. (1946), Chevkinite (tscheffkinite) from Arizona: *Am. Mineral.*, **31,** 582–588.

KEEVIL, N. B. (1939), The calculation of geological age: *Am. Jour. Sci.*, **237,** 203.

LACROIX, M. A. (1915), La bastnaesite et la tscheffkinite de Madagascar: *Bull. soc. franc. de Minéral.*, **38,** 106.

LARSEN, E. S., JR., KEEVIL, N. B., AND HARRISON, H. D. (1952), Method for determining the age of igneous rocks from accessory minerals: *Geol. Soc. Am., Bull.* **63,** 1045–1052.

PRICE, R. C. (1888), Analyses of chevkinite from Nelson County, Va.; *Am. Chem. Jour.*, **10,** 38.

ROSE, H. (1844), *Pogg. Ann.*, **62,** 591.

TAKUBO, AND NISHIMURA (1953), Chevkinite, Kobe-mura, Kyoto Pref., Japan: *Mem. Coll. Sci. Univ. Kyoto, Ser B,* **20,** 323–328.

TSCHERNIK, G. (1913), Chemische Untersuchung einiger Mineralien aus Ceylonische Kies: *Bull. acad. sci. St. Petersburg,* **174,** 365–376; 1029–1041.

——— (1914), Analysis of some minerals of Ceylon: *Bull. acad. sci. St. Petersburg,* **175,** 41–51.

——— (1915), *Neues Jahrb. f. Mineral.*, **1,** 36–40.

UNGEMACH, M. H. (1916), Contribution a la minéralogie de Madagascar: *Bull. soc. franc. de minéral.*, **39,** 5–38.

Manuscript received Aug. 10, 1955

JADEITE-BEARING METAGRAYWACKES IN CALIFORNIA

T. W. Bloxam, *Department of Geology, Princeton, New Jersey.*

Abstract

At several localities in California jadeite-bearing rocks have developed from the metamorphism of Franciscan graywackes. In the field the jadeite-bearing rocks are almost indistinguishable from somewhat sheared graywackes. Preservation of clastic structures and relict minerals in the jadeite-bearing rocks suggests metamorphism at low temperature. The presence of glaucophane and lawsonite in the jadeite-bearing rocks shows that these minerals are stable in the same environment that favors crystallization of jadeite.

The jadeite-bearing rocks occur in areas regionally occupied by unmetamorphosed rocks, so that metamorphic conditions must have been subject to marked fluctuations within short distances. As in many of the associated glaucophane schists, albite is typically absent in the rocks containing quartz and jadeite. It is concluded that jadeite is a product of the reaction: albite = jadeite + quartz.

Pressure, locally augmented by deformation, is a possible factor in their formation, while the composition of the original graywacke may also play a part. It is most likely that rocks of this nature may occur in other parts of California but have hitherto escaped notice because of their resemblance to unmetamorphosed graywacke.

Introduction

Occurrences of jadeite in California have previously been confined to small exposures in the form of lenses in serpentinite (Yoder and Chesterman, 1951); masses or veins in loose boulders of uncertain relationships (Wolfe, 1955); and as a constituent of certain rare varieties of glaucophane schist. Associated with the glaucophane schists are eclogites, the pyroxene of which is diopside-jadeite, not approaching the composition of pure jadeite (Switzer, 1945).

Recent mapping and mineralogical studies in various parts of California by the writer have revealed the presence of jadeite in metamorphosed sandstones or graywackes of the Franciscan formation. Rocks of this type were first discovered by Maddock (1955) in the Mt. Hamilton Range, Stanislaws County, and independently by the present writer at numerous other localities in California. Throughout this paper such rocks will be termed "quartz-jadeite rock" or "metagraywacke."

Field Relationships

Eastern El Cerrito, Berkeley Hills: In this area quartz-jadeite rocks with some cherts form a prominent ridge lying a few hundred yards to the west of the Hayward fault and associated serpentinite and glaucophane schist. They are terminated to the north by a mass of felsite, but relationships to the south are obscure. The locality is the same as that indicated by Brothers (1954, pp. 615, 619) for his specimens numbered 19 and 22.

North of Valley Ford, Sonoma County: The locality is on the north side of a small creek, immediately to the west of the point where it is crossed by a small farm road, 2½ miles north 17° east of Valley Ford. The farm road is accessible from the main highway from Valley Ford to Freestone. Outcrops of quartz-jadeite rock trend E.–W. with almost vertical foliation, and are in fault contact with a large area of unaltered Franciscan to the west. Lenses of unaltered Franciscan graywacke and tuffaceous material also occur within the quartz-jadeite rocks. There are no exposures of serpentinite at this locality.

Angel Island: On the shore mid-way between Point Ione and a mass of "fourchite," steeply dipping Franciscan graywackes are locally jadeitized (Ransome, 1894, p. 154). Specimens of "altered sandstone" collected by Ransome from Angel Island, at present in the collection of the Department of Geology, University of California, Berkeley, are jadeite-bearing. The jadeite in these was mistaken for zoisite.

Panoche Valley, San Benito County: The locality lies on the west side of Panoche Valley, opposite the "Glaucophane Ridge." The precise area is defined by the map references; T14S, R10E, 32, 33; Panoche Valley Quadrangle. Tightly folded beds of jadeite-bearing metagraywacke, glaucophane schist and interfolded sills or phacolithic bodies of antigoritized and actinolitized serpentinite, plunge steeply to the northwest. Here it is evident that the metamorphism giving rise to the metagraywackes and associated glaucophane schists post-dates the intrusion of the ultrabasic rocks.

It is concluded that jadeite-bearing rocks of this type occur widely in California, their close resemblance to unaltered sedimentary rocks resulting in their passing unnoticed for so long.

TEXTURE AND MINERALOGY OF THE QUARTZ-JADEITE ROCKS

The textural and mineralogical characters of the quartz-jadeite rocks collected from widely separated localities are extremely constant. In the field they are almost indistinguishable from unaltered Franciscan sandstones and graywackes, except that they nearly always appear somewhat sheared. The average density of the jadeite-bearing rocks is higher however, being 2.82; while that of the graywacke is 2.67 (average of 6 determinations each). When fresh they are gray in color, becoming buff-colored in weathered outcrops. Most have a rather crude shear-foliation parallel to the bedding, but occasionally they are unfoliated (302/144).* Their clastic granular texture is always obvious and original bedding clearly visible. Flakey carbonaceous material, characteristic of many unaltered Franciscan graywackes, can be seen on bedding surfaces (cf. Taliaferro, 1943, p. 132). Similarity in texture to unaltered graywacke is also evident in thin sections (Plates 1 and 2). Relict detrital fragments of basic rock, chert and angular quartz grains that have escaped recrystallization are common (302/*EC*3), while the crude foliation, like the bedding in the graywackes, is defined by streaks of sericite, chlorite and opaque carbonaecous material.

---

* Numbers refer to specimens in the Department of Geology, University of California, Berkeley.

Jadeite occurs as evenly distributed crystals or clusters with rounded or sub-radiate form; colorless in thin sections but frequently very turbid in appearance owing to minute inclusions of material too fine in grain for optical determination, but by *x*-ray study found to be quartz. In some cases the jadeite is present as closely sutured aggregates of small, variously orientated granules, producing a characteristic appearance under crossed nicols. Occasionally albite occurs with the jadeite and is in the process of replacement by the latter. The optical properties of the jadeite are rather variable, and because of very strong dispersion, are difficult to determine. Values of $2V_z$ and $Z:c$ in Table 1; 1 are averages of determinations made on a universal stage in sodium light. Optical data previously recorded for jadeite from Clear Creek and Cloverdale are included in Table 1; 2 and 3.

TABLE 1

	1	2	3
X=Y=Z	Colorless	Colorless	Colorless
α	1.659	1.654	1.640
β	1.663 ±0.003	1.657	1.645 ±0.003
γ	1.670	1.666	1.652
$\gamma-\alpha$	0.012	0.012	0.012
$2V_z$	86°±	70°±	67°
$Z:c$	53°±($Y=b$)	34°	40°($Y=b$)
Disp.	Very strong	—	None
S.G.	3.27(±0.03)	3.43(±0.01)	3.245

1. Jadeite from metagraywacke, Valley Ford, California.
2. Jadeite, Clear Creek, California (Coleman, 1954, p. 1241).
3. Jadeite, Cloverdale, California (Wolfe, 1955, p. 258).

In addition to clastic fragments and angular individuals, quartz occurs as a fine-grained recrystallized mosaic, frequently forming bands parallel to the foliation. Glaucophane is not uncommon in the rocks, although occasionally it is absent or insignificant (302/138*b*, 302/30). The mineral occurs as small prisms or in sub-radiating acicular sheaves, generally confined to the darker (chloritic) parts of the rock. In a few cases it forms intergrowths (replacements?) with jadeite. Glaucophane is particularly abundant in one rock with a marked blue color and better developed foliation (302/33). Probably this rock was more argillaceous

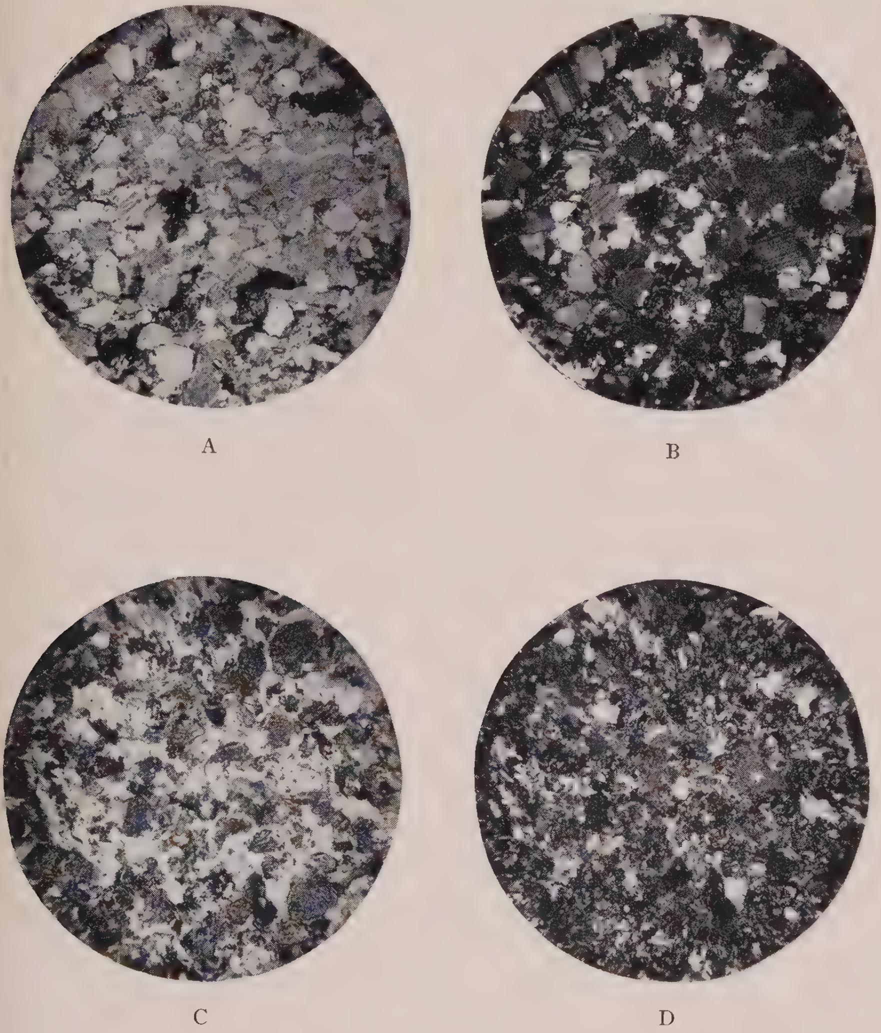

PLATE 1

A. Graywacke, Valley Ford. The lighter-colored constituents are angular grains of clastic quartz, plagioclase (albite/oligoclase) and finely crystalline chert fragments, together with sericite. Darker minerals are mainly chlorite, ilmenite/leucoxene and shaley or carbonaceous material. Ordinary light ×7.5.

B. As *A*, nicols crossed.

C. Quartz-jadeite rock, Valley Ford. Sub-rounded crystals of jadeite with strong cleavage and fractures are associated with quartz. Glaucophane, lawsonite, sericite and chlorite also occur, but are not readily distinguished at this magnification. Ordinary light ×7.5.

D. As *C*, nicols crossed. Quartz occurs as relict detrital fragments and as a fine-grained recrystallized mosaic. A fragment of chert lies to the right of the center of the field. The similarity in texture to the graywacke (*A* and *B*) is evident.

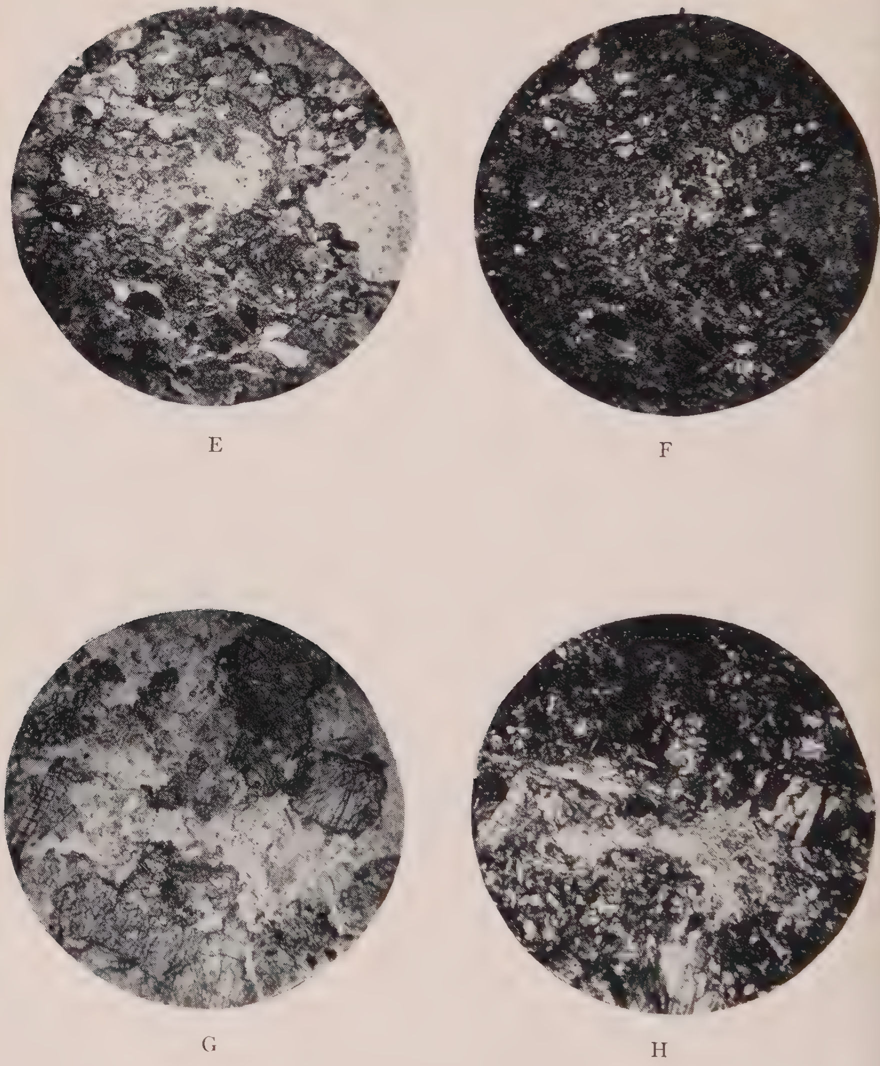

Plate 2

E. Foliated quartz jadeite rock, Valley Ford. An angular fragment of chert is prominent at the right-hand margin of the field. Ordinary light ×7.5.

F. As *E*, nicols crossed.

G. Quartz-jadeite rock, El Cerrito. Jadeite in subradiate clusters, elongate prisms of lawsonite, and quartz mosaic. Ordinary light approx. ×40.

H. As *G*, nicols crossed.

since the glaucophane is developed quite independently of the jadeite.

Lawsonite is a constant associate in the form of cross-fractured elongate prisms scattered throughout the rock and as inclusions in some of the jadeite crystals. Sericite and chlorite form discontinuous aggregates and bands, together with streaks of spongy opaque material which appears to be carbonaceous matter, although some may be ore (ilmenite /leucoxene).

ASSOCIATED GRAYWACKES

The Franciscan sandstones have a texture and mineralogy typical of graywacke; fresh grains of quartz, feldspar, chert and basic rock fragments making up the bulk of the rock (Taliaferro, 1943, pp. 134–135). The feldspar is chiefly a sodic plagioclase (albite/oligoclase) and generally constitutes 30% or more of the rock. The matrix is composed of a colorless mica or clay, chlorite, carbonaceous material and ilmenite/leucoxene.

Chemical analyses show that the Franciscan sandstones contain

TABLE 2

	1	2	3	4	5
SiO_2	70.61	69.14	71.18	71.72	68.84
TiO_2	0.53	0.37	0.44	0.35	0.25
Al_2O_3	11.99	15.08	13.14	13.23	14.54
Fe_2O_3	1.59	1.51	1.05	0.30	0.62
FeO	2.22	0.84	2.37	3.58	2.47
MnO	0.05	0.03	0.06	nil	nil
MgO	2.82	1.08	2.25	1.81	1.94
CaO	2.41	2.79	1.48	1.80	2.23
BaO	—	—	—	—	0.04
Na_2O	2.86	5.31	4.31	2.72	3.83
K_2O	1.64	1.28	1.11	1.29	2.68
ZrO_2	—	—	—	0.04	0.05
H_2O^+	2.81	1.96	1.91	2.53	1.60
H_2O^-	0.20	0.08	0.32	0.15	0.35
CO_2	0.03	0.00	0.15	0.32	0.14
P_2O_5	0.07	0.12	0.08	0.09	0.15
SO_3	—	—	—	—	0.15
	99.83	99.59	99.85	99.93	99.88
S.G.	2.86	2.91	2.70	—	2.72

1. Quartz-jadeite rock (302/*EC*2), Berkeley Hills. Anal. E. H. Oslund, Minnesota.
2. Quartz-jadeite rock (302/138*e*), Valley Ford. Anal. E. H. Oslund, Minnesota.
3. Graywacke (302/74), Valley Ford. Anal. E. H. Oslund, Minnesota.
4. Graywacke, Buckeye Gulch (Taliaferro, 1943, p. 136).
5. Graywacke, Piedmont (David, 1918, p. 22).

rather less total Fe_2O_3, FeO and MgO than many rocks classed as graywacke (Table 2; 3, 4 and 5). Nevertheless their textural and mineralogical characters are those of graywacke (Pettijohn, 1948, pp. 250–251).

ANALYSES

Analyses of quartz-jadeite rock from two localities are given in Table 2; 1 and 2, together with an analysis of graywacke associated with the quartz-jadeite rocks at Valley Ford (3), and two older analyses of graywacke from the Franciscan formation (4 and 5). There is no significant difference in chemical composition between the quartz-jadeite rock and and graywacke. It is also interesting to note the remarkable uniformity in the chemical composition of graywackes from widely separated localities.

In addition to an analysis of jadeite from the metagraywacke (Table 3; 1), two other previously recorded analyses of almost pure jadeite from California are included in Table 3; 2 and 3.

Although the jadeite separated for analyses appeared to be pure under the microscope, an *x*-ray powder photograph revealed strong quartz lines

TABLE 3

	1	2	3	4		5			6
SiO_2	60.64	59.38	61.66	59.44	Si	.801		.831	2.000
TiO_2	1.29	0.04	0.05		Al	.356	.030		
Al_2O_3	18.17	25.82	21.81	25.22			.326		
Fe_2O_3	3.68	0.45	0.32		Fe'''	.046			
FeO	0.53	tr.	0.24		Fe''	.007		.421	1.013
MnO	0.07	nil.	0.05		Mn	.001			
MgO	1.09	0.12	0.98		Mg	.026			
CaO	2.13	0.13	1.38		Ti	.015			
Na_2O	11.36	13.40	12.27	15.34					
K_2O	0.25	0.02	0.57		Ca	.038			
H_2O^+	0.78	0.22	0.44		Na	.367		.410	.987
H_2O^-	0.11	0.16	0.10		K	.005			
Li_2O	0.005	—	—						
Cr_2O_3	—	0.01	—						
	100.10	99.75	99.87	100.00					

1. Jadeite, Valley Ford. Analysis contains 12.55% quartz. Anal. E. H. Oslund, Minnesota.
2. Jadeite, Clear Creek (Coleman, 1954, p. 1241).
3. Jadeite, Cloverdale. Analysis contains 6% quartz (Switzer and Fahey; Wolfe, 1955, p. 258).
4. Theoretical composition of jadeite ($NaAlSi_2O_6$).
5. Metal atoms in 1. Less 12.55% quartz, H_2O and Li_2O.
6. Metal atoms in 1. Less 12.55% quartz, H_2O and Li_2O. On the basis of 6 oxygens.

in addition to those of jadeite. It was not possible to determine accurately the amount of quartz contamination since the difference in grain-size between the jadeite and quartz inclusions was considerable. The true value of density of the jadeite will therefore be higher than that given in Table 1 because of the quartz inclusions.

Allocating atomic proportions to the molecules jadeite, acmite, diopside and ($CaTiAl_2O_6$) resulted in an excess of $SiO_2 = 12.55\%$ (quartz). The analysis corresponds to jadeite $= 77.68\%$, acmite $= 12.39\%$, diopside $= 7.46\%$ and ($CaTiAl_2O_6$) $= 2.47\%$. The presence of Ti in the analysis suggests the possibility of rutile or sphene inclusions in the jadeite. However, further investigation revealed neither of these minerals.

ORIGIN OF THE QUARTZ-JADEITE ROCKS

The fabric and petrographic characters of the quartz-jadeite rocks show that they are derived from the metamorphism of Franciscan graywackes. The preservation of original clastic textures and other features indicate metamorphism at relatively low temperature. Presence of varying amounts of glaucophane and lawsonite suggests that these minerals are stable in the same environment which favors crystallization of jadeite. Absence of feldspar in rocks with abundant jadeite indicates that albite was unstable, its place being taken by jadeite plus quartz, some of the latter appearing as inclusions in the jadeite. However, since the jadeite contains appreciable amounts of diopside and acmite, the relationship is not so simple and involves reaction with Fe, Mg and Ca. It is considered that the diopside represents the anorthite of the original plagioclase, while inclusions of lawsonite in the jadeite may have a similar origin.

The association of quartz-jadeite rock with glaucophane schists, commonly albite-free, is further indication of the instability of albite in the assemblages as a whole. The similarity in chemical composition between associated graywacke and quartz-jadeite rock points to little or no change in bulk composition during metamorphism; the jadeite being derived from clastic albite in the graywacke.

Recently de Roever (1955) has described what appear to be closely similar quartz-jadeite rocks from a glaucophane schist terrane in Celebes. He regards the jadeite "... as having been formed at the expense of original albite by a rather extreme local variety of regional metamorphism in the glaucophane-schist facies" (1955, p. 292).

In California the association of quartz-jadeite rocks and various glaucophane and lawsonite-bearing assemblages with indurated but unmetamorphosed graywackes—the regionally prevalent rocks of the Franciscan—rules out the possibility of metamorphism on a regional scale. We must invoke some physical condition subject to marked fluctuation within short distances (Yoder, 1950, p. 325). A possible factor in the formation of the quartz-jadeite rocks may have been pressure, locally augmented by deformation. Taliaferro (1943, p. 186) has concluded that 25,000 feet is not an excessive estimate for the thickness of the Franciscan. At such a depth pressures of the order of 2,000 atmospheres might be expected. In addition, the composition of the original graywacke (low total, Fe, Mg and Ca) is considered to be a factor favoring the formation of jadeite-rock rather than glaucophane and lawsonite-rich assemblages.

Acknowledgments

This paper is based on studies carried out in the Department of Geology, University of California, during tenure of a Commonwealth Fellowship. The writer wishes to express his thanks to Professor F. J. Turner of the University of California for valuable assistance and criticism during the course of the investigation. The writer is also grateful for help given to him by Mr. C. M. Chesterman of the State Division of Mines, California, and by Mr. R. L. Rose of the University of California. Thanks are also accorded to Professor H. H. Hess of Princeton University and to Colonel K. Saxon of the Presidio, San Francisco, who gave permission for the writer to visit Angel Island.

The writer is indebted to the Commonwealth Fund, New York, for the Fellowship enabling him to pursue research in the United States, and for defraying the cost of chemical analyses.

References

Brothers, N. (1954), Glaucophane schists from the North Berkeley Hills: *Am. Jour. Sci.*, **252,** 614–626.

Coleman, R. G. (1954), Optical and chemical study of jadeite (abstract): *Bull. Geol. Soc. Am.*, **65,** 1241.

Davis, E. F. (1918), The Franciscan sandstone: *Univ. Calif. Pub. Dept. Geol.*, **II,** 1–45.

de Roever, W. P. (1955), Genesis of jadeite by low-grade metamorphism: *Am. Jour. Sci.*, **253,** 283–298.

Maddock, M (1955), Geology of the Mt. Boardman quadrangle, California: Unpublished Ph.D. thesis, University of California, Berkeley, 106–108.

Pettijohn, F. J. (1948), Sedimentary rocks: Harper.

Ransome, F. L. (1894), Geology of Angel Island: *Univ. Calif. Pub. Dept. Geol.*, **I,** 193–235.

Switzer, G. (1945), Eclogite from the California glaucophane schists: *Am. Jour. Sci.*, **243,** 1–8.

Taliaferro, N. L (1943), The Franciscan-Knoxville problem: *Am. Assn. Pet. Geol.*, **27,** 109–219.

Wolfe, C. W. (1955), Crystallography of jadeite from California: *Am. Mineral.*, **40,** 248–260.

Yoder, H. S. (1950), Jadeite problem: *Am. Jour. Sci.*, **248,** 225–248; 312–334.

——— and Chesterman, C. W. (1951), Jadeite of San Benito County, California: *Calif. Div. Mines, Special Report* **10-C.**

Manuscript received Aug. 12, 1955.

A REGULARLY INTERSTRATIFIED CHLORITE-VERMICULITE CLAY MINERAL*§

W. F. Bradley† and C. E. Weaver‡

Abstract

X-ray diffraction and differential thermal data together with a chemical analysis, base-exchange determination, and a one-dimensional Fourier synthesis indicate that a clay residue of the Upper Mississippian Brazer limestone of Colorado contains a regularly interstratified chlorite-vermiculite clay mineral.

The first example of a clay characterized by a specific regularly alternating epitactic intergrowth was rectorite (1) which consists of alternations of one pyrophyllite unit with one vermiculite unit.

Similarly complex chloritic minerals from several English Keuper marls were described by Honeyborne, (2) and by Stephen and MacEwan, (3); others from Japanese clays by Sudo, Takahashi, and Matsui (4). Lippmann (5) reported on an occurrence from a red Keuper clay from Zaiserweiler which he described as a regular alternation of chlorite and vermiculite layers, and for which he proposed the name corrensite. In each of these studies, diffraction diagrams were complicated by the presence of other layer minerals, mainly illite, as accessories. The present intention is to describe an occurrence sufficiently free of accessory minerals for the analyses to be viewed in more intimate detail.

The best example was obtained from the Brazer of Upper Mississippian age, in Juniper Canyon, Moffat County, Colorado. The clay is disseminated through the limestone and can be concentrated as an insoluble residue. Similar though less well-developed clays have been found in the Ordovician limestones of west Texas, and in the Des Moines shales of western Oklahoma.

The Juniper Canyon sample has no significant amount of other clay present but does contain approximately 20 per cent quartz.

X-ray diffraction diagrams of oriented specimens show a regular series

---

* Publication No. 64, Shell Development Company, Exploration and Production Research Division, Houston, Texas. Published with the permission of the Chief, Illinois State Geological Survey, and with the permission of Shell Development Company.

† Illinois State Geological Survey, Urbana, Illinois.

‡ Shell Development Company, 3737 Bellaire Blvd., Houston, Texas.

§ This note was prepared to illustrate that occurrences of corrensite, as named by Lippmann, are not rare, are indeed regularly alternating and justify Lippmann's name. The publication by Earley, Brindley, McVeagh and Vanden Heuvel (*Am. Mineral.*, **41**, 258–267) which arrived with these galleys obviates much of the need for an additional description, but the need still exists to call attention that equivalent geometry characterizes all three cited occurrences. Different choices of descriptive words do not present need for new mineral names.

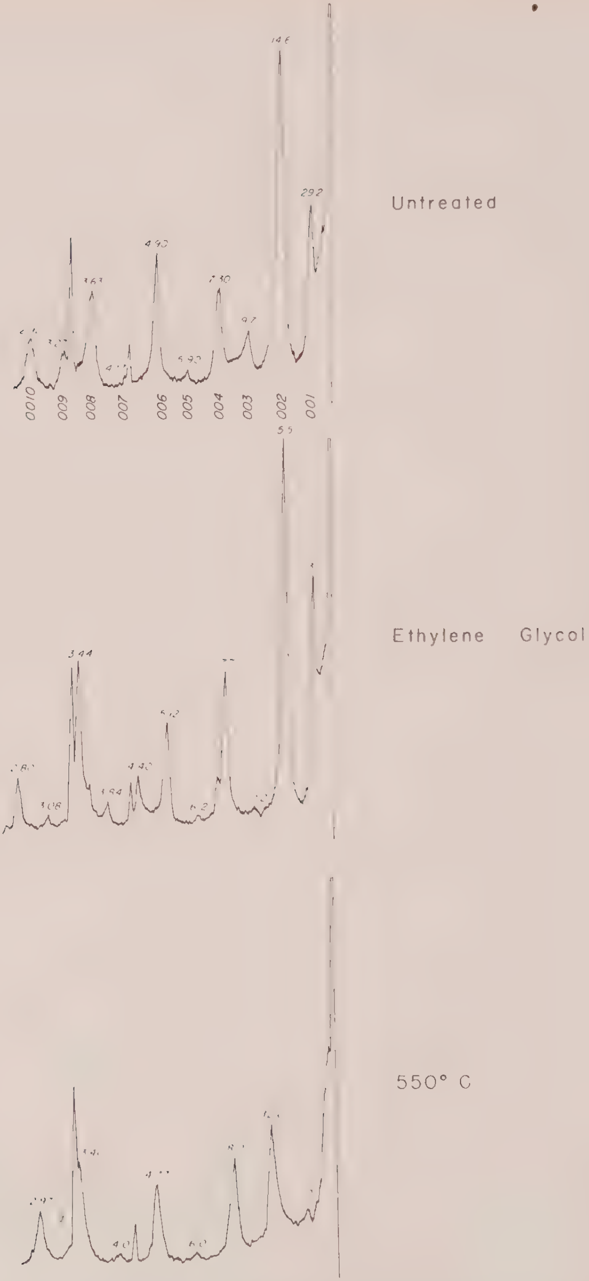

FIG. 1. *X*-ray spectrometer diffraction pattern of oriented slides of Juniper Canyon corrensite. (Peaks proportional to counting rate)

TABLE 1. MEASURED AND CALCULATED 001 SPACINGS OF JUNIPER CANYON SAMPLE

	Untreated		Ethylene glycol		550° C.	
	Calculated (Å)	Measured (Å)	Calculated (Å)	Measured (Å)	Calculated (Å)	Measured (Å)
001	29.2	29	31.0	31	24.0	23
002	14.6	14.6	15.5	15.5	12.0	12.0
003	9.73	9.7	10.3	10.2	8.0	8.0
004	7.30	7.30	7.75	7.7	6.0	6.0
005	5.84	5.90	6.20	6.2	4.8	4.77
006	4.87	4.90	5.16	5.12	4.0	4.0
007	4.17	4.17	4.43	4.40	3.43	3.40
008	3.65	3.63	3.88	3.84	3.0	2.97
009	3.24	3.27	3.44	3.44	2.66	—
0010	2.92	2.92	3.10	3.08	2.40	—

of 00*l* reflections extending from a fundamental periodicity of about 29 Å (Fig. 1). When the sample is exposed to ethylene glycol vapor, a regular 00*l* series with a fundamental periodicity of approximately 31 Å is obtained. After the sample has been heated to 550° C. for two hours, the fundamental periodicity decreases to approximately 24 Å and the remaining 00*l* series is still a very nearly regular sequence of the funda-

TABLE 2. ESTIMATED RELATIVE *F* VALUES FOR JUNIPER CANYON SAMPLE

	Natural after heating to 550° C. 24 Å	Natural 29 Å	Ethylene glycol complex 31 Å
001	+1.6	+3.8	+5.0
002	−6.1	−9.2	−10.0
003	+6.3	+4.0	+1.9
004	+2.0	+6.5	+8.0
005	+6.6	+2.7	+1.7
006	+2.2	+8.6	+7.2
007	+8.1	+2.2	+5.0
008	−5.9	+7.8	+3.4
009		+3.0	+9.8
00·10	−1.8	−5.9	−2.0
00·11			−5.8
00·12	+2.8	−1 (?) (omitted)	−2.0
00·13			−2.3
00·14		+2.1	
00·15			+2.4

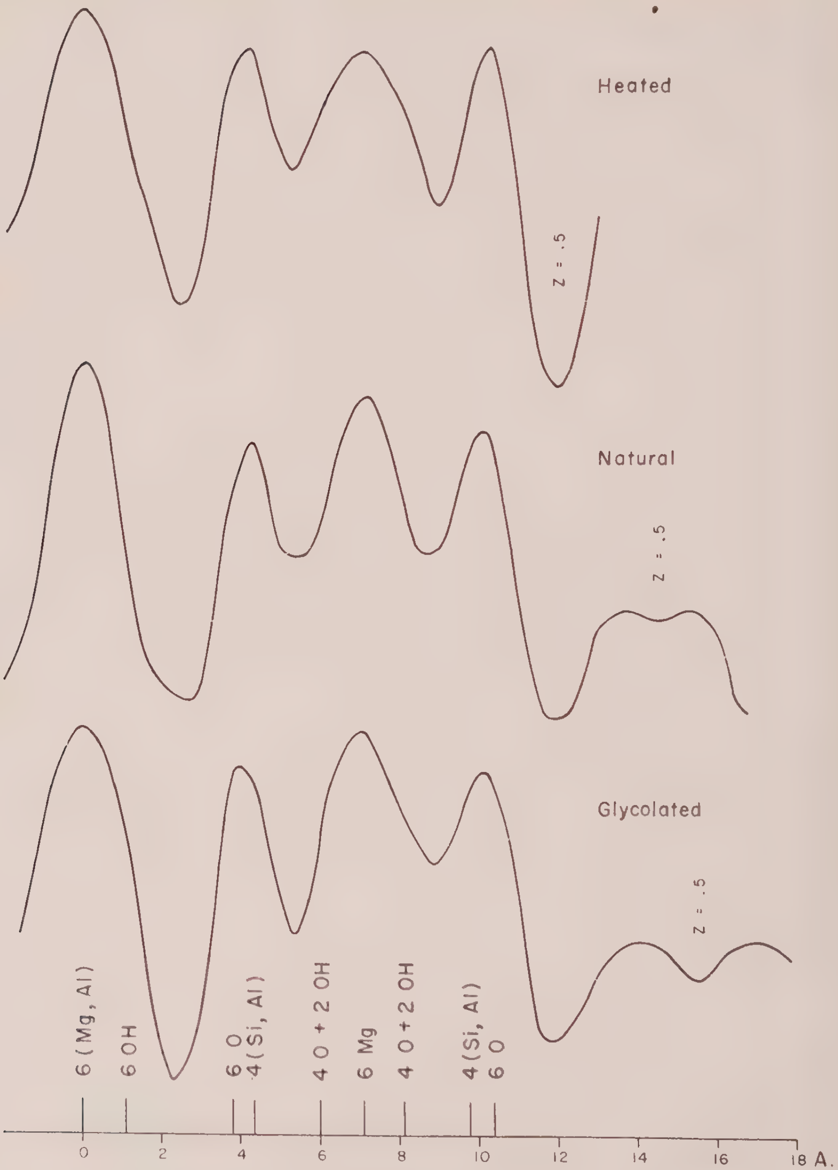

FIG. 2. One-dimensional Fourier syntheses of data from the traces of Fig. 1.

mental period. Table 1 lists the measured and calculated 00*l* values for these three periodicities.

Spectrometer traces of the 00*l* series for the three conditions noted are reproduced in Fig. 1. The successive 00*l* orders and the quartz diagram

TABLE 3. CHEMICAL ANALYSIS AND CATION DISTRIBUTION IN JUNIPER CANYON SAMPLE

	Per cent	Distribution of cations in ideal formula	
SiO_2	41.2 about 20% free 23.2 comb.	5.47	tetrahedral coordination
Al_2O_3	12.1	2.53 .84	octahedral coordination
Fe_2O_3	1.74	.31	
FeO	0.39	.07	
MgO	22.0	7.78	
TiO_2	0.04	—	
CaO	1.4	.71	interlayer (equivalents)
Na_2O	0.07	.03	
K_2O	0.22	.07	
bec	40 *me*/100 gr.	.57	
		Total (+) charge = 50.00	
H_2O (105° C.)	6.80	5.4 mol.	
H_2O (1000° C.)	15.4	12.1 mol.	

appear as the major features. Table 2 lists the relative importance of F values, reduced from the spectrometer curves and modified by an arbitrary temperature factor chosen to equal one-half at 45° 2θ. Although the series are short, the existence of the three sets of values for three different fundamental periods permits one to establish signs and view the major features with some confidence. The three one-dimensional Fourier syntheses illustrated in Fig. 2 are arrived at by application of the signs noted, based on the alternation of layers cited by Lippmann.

The prominence of the maxima representing octahedral levels, as compared with those for tetrahedral, strongly suggests trioctahedral character. The implication is stronger in the natural and glycolated syntheses, in keeping with their clearer conformity to regular alternation.** The implication of trioctahedral character also is supported by the measured (060) diffraction spacing of 1.54. Accuracy of measurement, but not of identity, is limited by incomplete resolution from the almost coincident quartz line.

The chemical analysis of the specimen as collected from an acid medium is listed in Table 3. The diffraction implications cited above permit

---

** It frequently has been demonstrated that even macrocrystalline chlorites suffer some degradation in heating which reduces the scattering power of some octahedral layers and the perfection with which all layers conform to a typical thickness.

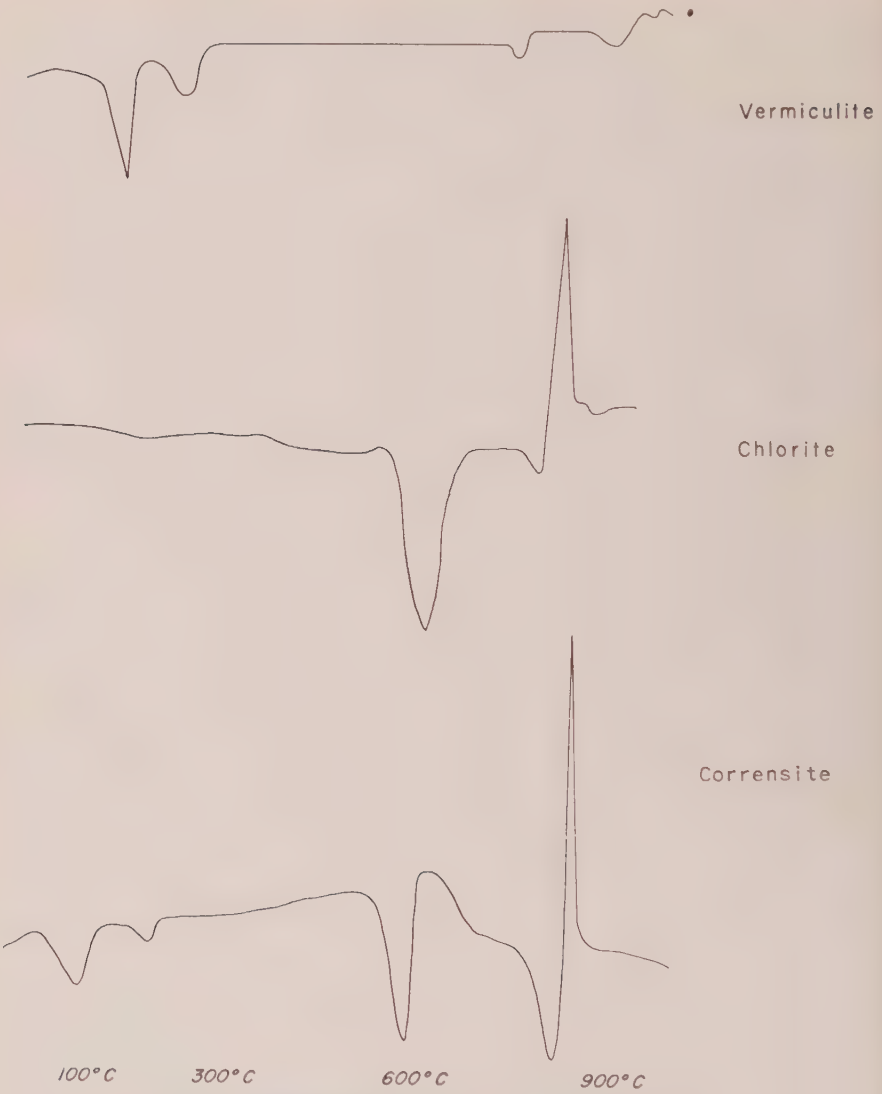

FIG. 3. Differential thermal curves of a typical vermiculite, a typical chlorite, and the Juniper Canyon corrensite.

the following rationalization. It may be assumed that this well-defined complex originally must have been a chlorite, and that it has resulted from replacement of alternate charged "brucite" layers by water and exchange bases. In such case the ideal formula would be

$$Mg_8Al_3Si_6O_{20}(OH)_{10} \cdot 4H_2O + 1 \text{ exchange charge.}$$

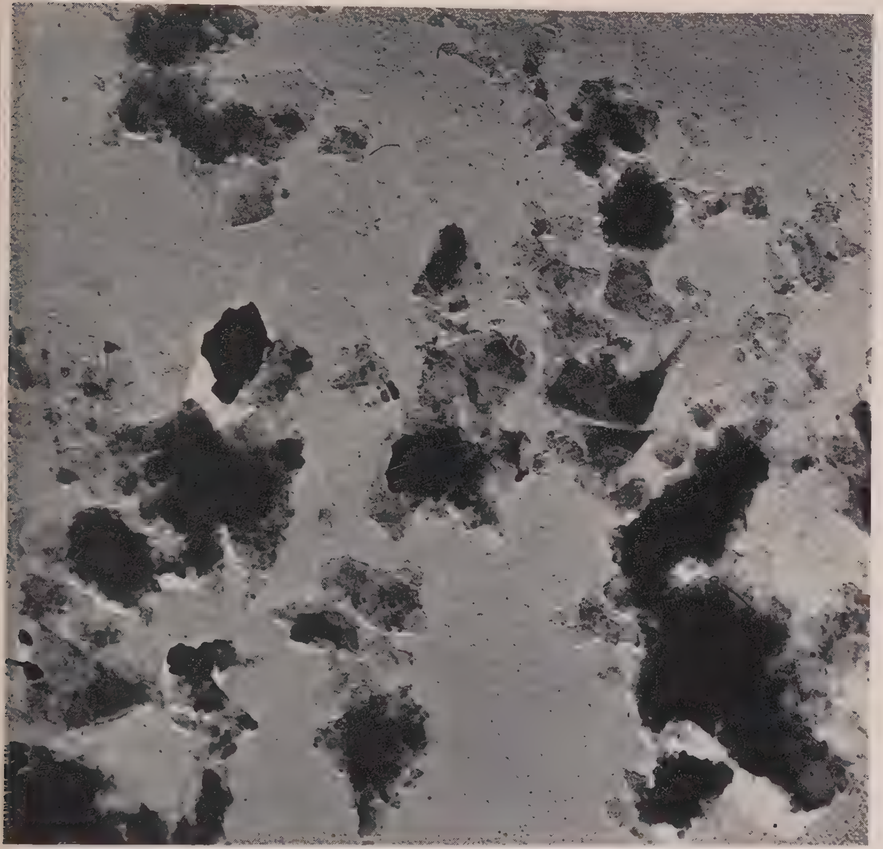

FIG. 4. Electron micrograph of the less-than 2 micron fraction of the Juniper Canyon clay. ×29,000.

For the actual case at hand the sum, in equivalents, of fixed interlayer ions+base-exchange capacity+charge gain by oxidation of iron+octahedral aluminum, must equal the tetrahedral aluminum. This distribution of aluminum affords the allocation of cation populations listed with the chemical analysis. The calculated excess of silica, 18 per cent, compares favorably with the diffraction estimate of 20 per cent free quartz. The proportion of silicon and tetrahedral aluminum is in the range of average compositions of vermiculites and of chlorites. The analyzed H_2O contents are notably higher than the ideal, but this also is commonly true of macrocrystalline vermiculites, and is not considered to be a serious fault.

A differential thermal analysis curve for the Juniper Canyon specimen is compared with curves for a typical vermiculite and a typical chlorite in Fig. 3. The major features qualitatively confirm the foregoing interpretations of the diffraction analysis. Molecular water is lost from the Juniper Canyon specimen in two fractions at about 100° C. and about 210° C. The features do not appear to differ from those of a typical vermiculite to a greater degree than can be attributed to the lesser particle size of the clay. Hydroxyl water features indicate losses in three stages. The first, at about 550° C., is analogous with but of lesser magnitude than the first chlorite hydroxyl feature, commonly attributed to hydroxyl loss from "brucite" layers. The two subsequent features presumably may be attributed to water loss consequent to the proton occupancy of exchange positions, and to the hydroxyl content originally associated with the brucite member of the complex silicate triple layer.

Electron micrographs (Fig. 4) show that the clay consists of thin flakes with sharp, discrete edges.

REFERENCES

1. BRADLEY, W. F., *Am. Mineral.*, **35,** 590–595 (1950).
2. HONEYBORNE, D. B., *Clay Minerals Bull.*, **1,** 150–155 (1951).
3. STEPHEN, I., AND MACEWAN, D. M. C., *Clay Minerals Bull.*, **1,** 157–162 (1951).
4. SUDO, T., TAKAHASHI, H., AND MATSUI, H., *Japan J. Geol.*, **24,** 71–85 (1954).
5. LIPPMANN, F., *Heidelberger Beiträge zur Mineral. u. Petrog.*, **4,** 130–134 (1954).

NOTES AND NEWS

A NOTE ON SOME PROPERTIES OF SYNTHETIC MONTMORILLONITES

Rustum Roy* and L. B. Sand.†

While it has been known for several decades that montmorillonites can be synthesized in the laboratory (1, 2) very little further systematic work has been done to determine either the compositional limits of montmorillonite formation or the properties of the phases obtained. In the meantime the whole field of clay mineralogy has advanced rapidly and has had to contend with the fact that there was relatively little control on the purity or composition of the natural minerals to which detailed attention was given. Hydrothermal investigations (3, 4, 5, 6) recently have encountered montmorillonite phases in the systems Al_2O_3—SiO_2—H_2O, MgO—Al_2O_3—SiO_2—H_2O and Na_2O—Al_2O_3—SiO_2—H_2O, where chemically "known" and mineralogically homogeneous phases were prepared and the equilibrium thermal dissociation temperature determined as a function of decomposition. Other workers (7, 8) have determined the cation exchange capacities of synthetic montmorillonites.

As part of a more detailed investigation of the properties of clay minerals, we undertook to prepare and examine a large number of montmorillonite phases. Roy and Roy (6) already have described some of the results on the 1:1 layer, kaolin-serpentine type structures. Since the more complete cataloguing of properties of a large number of such phases extends over some years, it is considered worthwhile to report briefly the earlier results of such synthetic work. The methods and equipment used have been described in several earlier publications (3, 4). The phases formed are identified in every case by powder *x*-ray diffraction techniques. Equilibrium is presumed on the basis of successively longer runs with given compositions. If the same phase or phase assemblage appears to remain unchanged after a few weeks, and if in each case the total composition may reasonably be fitted in with the composition of the phases present, this is taken as an equilibrium assemblage. In the past we have shown neither patterns nor given the *x*-ray diffraction data for these montmorillonite phases since they are quite analogous to those of natural montmorillonites. However, *x*-ray data are now being compiled for end-member synthetic montmorillonites of known compositions. The crystallinity of the samples is examined under the electron microscope, and has been shown to be as good or better

---

* Contribution No. 54–65. College of Mineral Industries, The Pennsylvania State University, University Park, Pa.

† Dept. of Mineralogy, University of Utah, Salt Lake City, Utah.

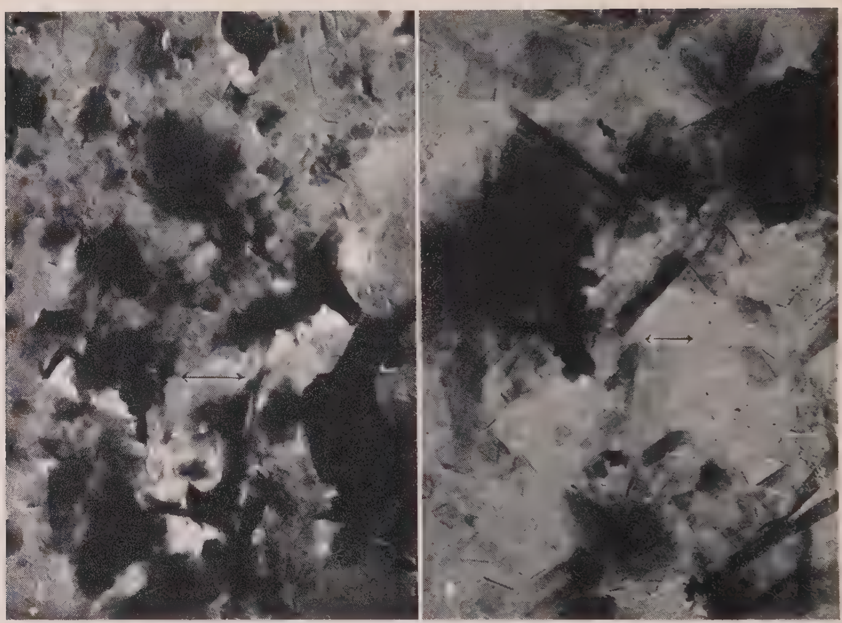

FIG. 1. Electron micrographs of synthetic montmorillonites in the $Na_2O—Al_2O_3—SiO_2—H_2O$ system. (*A*) On the left—typical thin sheets curled at the edges; (*B*) On the right—synthesized at a higher temperature and containing more silica

$$\left(\frac{Na_2O}{6}\cdot Al_2O_3\cdot 4SiO_2 \text{ as compared to } \frac{Na_2O}{6}\cdot Al_2O_3\cdot 3SiO_2 \text{ for } A.\right)$$

shows somewhat greater regularity in habit. Closer comparison will show the presence of the same curled sheets in both.

than that of the natural material (see Fig. 1); the products at the higher temperature giving very much sharper crystal outlines than have previously been observed in montmorillonites. The relation of morphology to both composition and conditions of formation should again prove to be of interest as in the case of the kaolinite-serpentine series. Single crystal electron diffraction studies carried out at the same time did not yield any significantly new data.

Another property which is often difficult to obtain accurately in a natural product is the cation exchange capacity. The fine-grained "amorphous" material (which is frequently a contaminant in natural samples) usually has a very high exchange capacity and the common gangue minerals have low exchange capacities. These contaminants are usually difficult to remove completely. Likewise, dispersions present a problem and a restricted particle size range usually is required for dependable results. These factors are eliminated with the synthetic clays. This has been recognized also by Karsulin and Stubican (8) who have related cation exchange capacity with the substitution of Mg for Al in synthetic montmorillonites. Our determinations have been made by the Bower and Truog (9) method which has been checked for reproducibility and shown in our case to be accurate to about ±3%.

In the table below are listed the properties of one of the many compositions studied and is an example of the program in progress.

TABLE 1

Composition	1/6 $Na_2O \cdot Al_2O_3 \cdot 4SiO_2$.
Conditions of synthesis	400° C., 15,000 psi H_2O, 2 weeks.
Habit	Uniform, clear, well-defined crystals approaching lath-like habit.
Equilibrium decomposition temperature	480° C. at 15,000 psi H_2O.
Decomposition products of above	Paragonite and pyrophyllite+albite.
Exchange capacity (M.e. Mn^{++}/100 g.)	96.
Basal spacing (glycol solvated)	17.0 Å.

The powder *x*-ray diffraction data are listed in Table 2.

TABLE 2. POWDER DATA ON SAMPLE OF TABLE 1

d	*Int.*	*hkl*
17.0	vs	001
8.50	ms	002
5.65	w	003
4.82	w	
4.42	s	
4.23	vw	004
3.73	w	
3.40	ms	005
2.83	w	006
2.57	wd	
1.71	vw	
1.65	vw	
1.50	ms	060(?)
1.34	wd	00, 13
1.24	wd	00, 14

Abbreviations used: vs = very strong, s = strong, ms = moderately strong, w = weak, wd = weak diffuse, vw = very weak.

Montmorillonites have now been prepared by various workers in this laboratory with a wide variety of compositions, some of which are listed in Table 3.

TABLE 3

*Pure	Al_2O_3—SiO_2—H_2O	And with systematic additions of Na and Mg and Ca to yield typical beidellites.
Pure	MgO—SiO_2—H_2O	With systematic additions of Al to yield typical saponites.
	NiO—SiO_2—H_2O	With systematic additions of Al yielding pimelites (?).
	ZnO—SiO_2—H_2O	With systematic additions of Al to yield sauconites.
	Ga_2O_3—SiO_2—H_2O	. . . .
	Cr_2O_3—SiO_2—H_2O	With additions of Al to yield "volchonskoite (?)"- like phases

* The pure members contain no other ions whatever within experimental error, unlike earlier work. The "addition" of Al^{3+} is not, of course, to be taken in the mechanical sense.

It is evident that a wide compositional latitude is possible in montmorillonite structures, especially in systems such as MgO—Al_2O_3—SiO_2—H_2O where several ions can proxy for each other. The only limitation which appears to emerge in addition to the obvious ones of the electrostatic neutrality and the structure appears to be one of the limit on the charge of the layer. Assuming that base exchange capacity is also variable enhances the compositional area over which a single crystalline phase can form, although this point is very difficult to prove experimentally.

ACKNOWLEDGMENTS

The cooperation of W. C. Ormsby in the determination of cation exchange capacities is gratefully acknowledged. Dr. Della M. Roy participated in the hydrothermal syntheses and Mr. J. J. Comer prepared the electronmicrographs.

REFERENCES

1. EWELL, R. H., AND INSLEY, H. (1935), Hydrothermal synthesis of kaolinte, dickite, beidellite and nontronite: *J. Res. Natl. Bur. Stand.*, **15**, 173.
2. NOLL, W. (1944), New investigations in water-silicate systems: *Kolloid Zeits.*, **107**, 181
3. ROY, RUSTUM, AND OSBORN, E. F. (1954), The system Al_2O_3—SiO_2—H_2O: *Am. Mineral.*, **39**, 853–885.
4. ROY, DELLA M., AND ROY, RUSTUM (1955), Synthesis and stability of minerals in the system MgO—Al_2O_3—SiO_2—H_2O: *Am. Mineral.*, **40**, 147–178.
5. SAND, L. B., ROY, RUSTUM, AND OSBORN, E. F. (1953), Stability relationships of some minerals in the system Na_2O—Al_2O_3—SiO_2—H_2O: *Am. Mineral.* (abstract), **39**, 341.
6. ROY, DELLA M., AND ROY, RUSTUM (1954), An experimental study of the formation and properties of synthetic serpentines and related layer silicate minerals: *Am. Mineral.*, **39**, 957–975.

7. Ormsby, W. C., and Sand, L. B. (1953), Base exchange: An analytical tool for mixed layer aggregates: *Proc. Second National Clay Conference*, Publication 327, National Academy of Science-National Research Council, Washington, D. C. (1954).
8. Karšulin, M., and Stubičan, V. (1954), On the structure and properties of synthetic montmorillonite: *Monats. Chem.*, **85**, 343–358.
9. Bower, C. A., and Truog, E. (1940), Base exchange capacity determination of soils and other materials: *Ind. Eng. Chem., Anal. Ed.*, **12**, 411–413.

OPTICAL ANOMALIES IN ARFVEDSONITE FROM GREENLAND

Th. G. Sahama, *Institute of Geology, University of Helsinki, Finland.*

Many alkali amphiboles fail to show complete extinction on (010) between crossed nicols, not even in monochromatic light. The phenomenon was observed by Eskola and Sahlstein (1930) on three amphiboles of the arfvedsonite-riebeckite series, on two alkali amphiboles later called eckermannite by Adamson (1944), on one specimen of hastingsite and one of taramite. The incomplete extinction was found only in sections roughly parallel with (010). On (100), striations parallel with the trace of the *c*-axis were noted.

At that time, no closer experimental study of the phenomenon was made. It was only assumed that the amphiboles, originally crystallized as a homogeneous phase, have later been subjected to exsolution and are now perthitic. The lath-shaped strips are arranged in such a way that the *c*-axis and the (010) plane are common for the exsolved amphibole components.

Later, the incomplete extinction of certain alkali amphiboles, particularly of those belonging to the arfvedsonite-riebeckite series, have been mentioned by a number of Japanese authors (Sato, 1936; Iwao, 1939; Hori, 1942; Inoue, 1950; Yagi, 1953). The phenomenon seems to be very common in alkali-rich amphiboles.

To explain the optical anomalies pointed out above, a specimen of arfvedsonite from Kangerdluarsuq, Greenland (this Institute Collection No. 3436), was studied with more modern equipment. The incomplete extinction on (010) and the striated structure on (100) are very clearly seen on this mineral. Chemical analysis and optical properties of arfvedsonite No. 3436 are given in Table 1.

The material for the chemical analysis was purified by centrifuging in Clerici's solution. The purity of the final powder was tested under the microscope. The optical properties were determined in the usual manner. For determining the optical orientation and for quantitative measurement of the pleochroism and of the degree of non-extinction, thin sections were cut parallel with (010) and (100). On the section (010) it was found that the direction of maximum absorption (=optical α) is parallel with

TABLE 1. CHEMICAL COMPOSITION AND OPTICAL PROPERTIES OF ARFVEDSONITE No. 3436 FROM KANGERDLUARSUQ, GREENLAND

SiO_2	46.61%	Na_2O	6.58%	$\alpha=1.696$ ±0.003
Al_2O_3	4.02	K_2O	2.89	$\beta=1.700$ ±0.003
Fe_2O_3	9.92	TiO_2	0.48	$\gamma=1.705$ ±0.003
FeO	25.79	H_2O^+	1.24	$c\wedge\alpha=0°$
MnO	0.00	H_2O^-	0.00	$b\parallel\gamma$
MgO	0.25	Total	99.84	Absorption:
CaO	2.06			$\alpha>\gamma>\beta$

the trace of the crystallographic c-axis. This is unusual for an arfvedsonite. The relative amounts of transmittance of light vibrating parallel with the three indicatrix axes are given in Table 2. The transmittance of β at 700 mμ was arbitrarily taken as 10.00 and the values of the table were reduced to correspond to that figure. The measurements were carried out with the Leitz microscope photometer and the Leitz monochromator.

TABLE 2. PLEOCHROISM OF ARFVEDSONITE NO. 3436, KANGERDLUARSUQ, GREENLAND. RELATIVE AMOUNTS OF TRANSMITTANCE OF LIGHT VIBRATING PARALLEL WITH THE THREE INDICATRIX AXES. MEASURED WITH THE LEITZ MICROSCOPE PHOTOMETER

Wave length mμ	Relative transmittance of light vibrating parallel with		
	$\alpha(=c)$	β	$\gamma(=b)$
450	0.43	3.30	0.71
500	0.83	5.98	1.06
550	0.55	6.34	0.75
600	0.43	7.40	0.72
650	0.36	9.25	0.80
700	0.27	10.00	0.82

Table 3 gives the degree of non-extinction for light vibrating parallel with optical α (=crystallographic c-axis) on section (010). The amounts of transmittance given in the second column of the table (without analyzer) were taken as 100 and the transmittance values in the third column (with analyzer) were reduced correspondingly. The fourth column indicates the minimum relative amounts of transmittance measurable with the apparatus. As is seen from the table, the analyzer reduces but slightly the intensity of the transmitted light. At 700 mμ the intensity of the transmitted light is not influenced by the analyzer at all. A complete extinction is reached only if the analyzer is turned parallel with the polarizer.

TABLE 3. ARFVEDSONITE NO. 3436, KANGERDLUARSUQ, GREENLAND. RELATIVE TRANSMITTANCE OF LIGHT VIBRATING $\|\alpha(=c$-AXIS). SECTION (010). MEASURED WITH THE LEITZ MICROSCOPE PHOTOMETER

Wave length mμ	Relative transmittance measured on section (010) for vibration $\|\alpha(=c$-axis)		Minimum transmittance still measurable with the photometer
	Without analyzer	With analyzer (nicols crossed)	
450	100	71	10
500	100	91	5
550	100	96	7
600	100	96	10
650	100	98	13
700	100	100	16

The optical anomalies described above are apparently caused by some kind of mosaic structure. To reveal the nature of this mosaic structure, a rotation photograph and a zero-layer Weissenberg photograph were taken of the arfvedsonite, using cobalt radiation with iron filter. The crystal was rotated or oscillated around the crystallographic c-axis. The rotation photograph shows sharp layer lines indicating that the entire crystal is homogeneous with respect to its c-axis. In other words, if there are domains of different orientation in the crystal, these domains must have the c-axis in common. This will hold true within the accuracy attainable by a rotation photograph. On the other hand, the reflections with lower ξ-values on the Weissenberg photograph (that do not normally show separate $\text{Co}K\alpha_1$ and $\text{Co}K\alpha_2$ spots) are very clearly doubled throughout the film. The polar coordinates ξ and ϕ were measured for each reflection and the $hk0$ reciprocal lattice plane was constructed. The doubled $hk0$ pattern is regular and shows no rotation of different domains around the c-axis.

The x-ray data reported above seem to indicate that the arfvedsonite No. 3436 represents a perthitic intergrowth of two amphibole components with slightly differing unit cell dimensions. To test this interpretation, fragments of the same crystal were heated for one hour at 700° C. Microscopic investigation of the heated material revealed the fact that the optical anomalies had disappeared and sections parallel with (010) showed sharp and complete extinction. Of the heated material rotation photograph and zero-layer Weissenberg photograph was taken in the same way as of the unheated material. The Weissenberg photograph of the heated material showed no doubling of the reflections. The crystal had become homogeneous.

It is concluded that an amphibole of the arfevdsonite composition is not stable at low temperatures but will become unmixed. The compositional range of the gap in alkali amphibole solid solutions is not known. The optical properties of the alkali amphiboles, particularly of the arfvedsonite-riebeckite series, must necessarily be influenced by the exsolution.

Acknowledgments. Thanks are due to Mr. Aarno Juurinen and Mr. Kai Hytönen, both of this Institute, for making the chemical analysis of arfvedsonite and for the optical measurements, respectively.

References

Adamson, O. J. (1944), The petrology of the Norra Kärr district: *Geol. För. Stockholm Förh., Bd.* **66,** 114.

Eskola, Pentti, and Sahlstein (Sahama), Th. G. (1930), Ueber die unvollkommene Auslöschung einiger Amphibole: *C. R. Soc. géol. Finlande,* **3,** 89.

Hori, S. (1942), On an abnormal optical phenomenon of alkali-amphibole: *Geol. Soc. Japan Jour.,* **49,** 445.

Inoue, Tami (1950), Amphiboles and biotites from the Fukushinzan alkaline complex, Korea: *Geol. Soc. Japan Jour.,* **56,** 71.

Iwao, S. (1939), Petrology of the alkaline rocks of the Nayosi district, Sakhalin, Japan: *Japanese Jour. Geol. and Geography,* **16,** 155.

Sato, S. (1936), Geology and petrology of Jehol, report of the first scientific expedition to Manchukuo, sect. II, part III, Tokyo, p. 41. (Cited according to Yagi)

Yagi, Kenzo (1953), Petrochemical studies on the alkalic rocks of the Morotu district, Sakhalin: *Bull. Geol. Soc. Am.,* **64,** 769.

UNIT CELL AND SPACE GROUP OF BARYLITE

J. C. Smith, *Department of Mineralogy and Petrography,*
Harvard University, Cambridge, Mass.

The occurrence of barylite, $Be_2BaSi_2O_7$, has been described by Palache and Bauer (1) and by Palache (2) from Franklin, N. J., and by Aminoff (3) from Långban, Sweden. Ygberg (4) made an *x*-ray examination of the barylite from Långban, by the rotation, Laue and powder methods. Aminoff, from morphological investigation, found that barylite belonged to the orthorhombic holohedral class (D_{2h} mmm). The *x*-ray study by Ygberg reduced the space group to two possible choices, D_{2h}^5-Pmma and D_{2h}^{16} $Pnma$, of which he considered the latter to be the more plausible.

An analyzed sample of the barylite from Franklin described by Palache and Bauer (1) was examined using Cu radiation and the Weissenberg method. The lattice type proved to be primitive orthorhombic, and the following extinction criteria were recognized: $hk0$ missing when h is odd; $0kl$ missing when $k+l$ is odd. These establish the space group as

Pnma. The unit cell dimensions obtained from 0-layer photographs are compared to those of Ygberg's, below:

Smith	*Ygberg*
$a_0 = 9.80 \pm .01$ Å	$a_0 = 9.79$ Å
$b_0 = 11.65 \pm .03$	$b_0 = 11.61$
$c_0 = 4.71 \pm .02$	$c_0 = 4.63$

The slightly larger cell dimensions obtained on the Franklin barylite probably are due to a small variation in the chemical composition. This is suggested also by the slight differences observed in the indices of refraction and specific gravities of the Franklin and Långban materials. The reported analyses indicate that the Långban material is relatively rich in calcium, and the Franklin material in lead; both elements substitute for barium. Indexed *x*-ray powder spacing data are given in Table 1.

TABLE 1. *X*-RAY POWDER SPACING DATA FOR FRANKLIN BARYLITE
Cu radiation, Ni filter, in Ångstroms

Index	Meas. *d*	Calc. *d*	Index	Meas. *d*	Calc. *d*
020	5.743	5.810	102	2.300	2.270
210	4.464	4.500	112	2.224	2.229
011	4.263	4.298	241		2.215
220	3.748	3.740	401	2.175	2.168
121	3.389	3.410	022		2.165
201	3.323	3.378	311	2.135	2.129
211	3.206	3.240	202	2.090	2.108
040	3.006	2.905	212		2.098
132	2.881	2.871	421	2.040	2.065
231	2.564	2.550	222	1.998	1.981
240	2.473	2.488	341	1.977	1.970
410	2.412	2.392	302	1.908	1.907
141		2.391	312	1.868	1.870
002	2.367	2.333	042	1.825	1.813

REFERENCES

1. PALACHE, C., AND BAUER, L. H., On the occurrence of beryllium in the zinc deposits of Franklin, N. J.: *Am. Mineral.*, **15,** 30 (1930).
2. PALACHE, C., The minerals of Franklin and Sterling Hill, Sussex County, N. J., *U.S.G.S., Prof. Paper* **180** (1935).
3. AMINOFF, G., Om en association med Barylit och Hedyfan vid Långban.: *Geol. För. Förh., Stockholm,* **45,** 124 (1923).
4. YGBERG, E. R., On the structure of barylite: *Geol. För. Förh., Stockholm,* **134,** 394 (1941).

CONTAMINATION OF THE CHARACTERISTIC *X*-RADIATION OF COPPER BY Fe, Cr AND Ni RADIATION

J. A. Kohn* *U. S. Bureau of Mines, Norris, Tennessee,* and A. A. Levinson, *The Ohio State University, Columbus 10, Ohio.*

During the course of *x*-ray investigations on tungsten carbide and on mica crystals, reflections were noted on Weissenberg photographs which suggested the presence of superlattices. Further study led the authors independently to attribute these reflections to a contamination of the characteristic copper radiation with wavelengths characteristic of iron, chromium, and nickel. Although investigators are quite aware of potential contamination of the target by tungsten, we find only a brief statement in the crystallographic literature of difficulties arising from " . . . iron and other metals . . . ."[1] In addition to the two *x*-ray tubes used by the authors, several other diffraction tubes of the same manufacturer are known to give this effect.

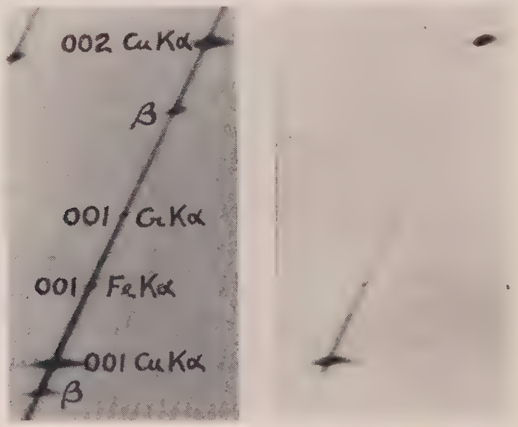

a b

Fig. 1. Portion of Weissenberg photograph showing (00*l*) of WC crystal taken with (*a*) unfiltered Cu radiation, and (*b*) Cu radiation filtered through nickel foil; 35 KVP, 15 MA, 15°-oscillation, 12 hrs. (overexposed for reproduction, 2×.)

Figure 1 shows a portion of the (00*l*) central lattice line of a tungsten carbide (WC) crystal taken with (*a*) unfiltered copper radiation, and (*b*) copper radiation filtered through nickel foil. The (001) reflections due to FeKα and CrKα can be clearly seen in (*a*); that due to NiKα was too weak to reproduce. The nickel filter virtually eliminated the chromium radiation but permitted a considerable portion of the iron radiation to diffract. Misinterpretation of such a pattern as evidence of a superlattice is possible, since the contaminating wavelengths cause reflections to occur for one-quarter and one-half the true Weissenberg spacing. The absence of any such reflections between the undiffracted beam and the spot (001) serves to invalidate a superlattice interpretation.

---

* Present address: Chemical-Physics Branch, Signal Corps, Engineering Laboratory, Ft. Monmouth (Hexagon), New Jersey.

[1] Peiser, H. S., Rooksby, H. P., and Wilson, A. J. C. (1955), *X*-ray diffraction by polycrystalline materials, London, Institute of Physics, p. 62.

The contaminating wavelenghts are primary in origin; that is, they originate at the target of the *x*-ray tube and cannot be attributed to fluorescence. An agent of the manufacturer has stated that " . . . Cr, Fe and Ni . . . emanate from the stainless steel structure comprising the cathode supports and focusing cup." The latter was determined by chemical analysis to consist of approximately 75% iron and 25% chromium. The source of nickel is probably the disc-like shield surrounding the filament leads and located immediately beneath the cathode supporting block. A cursory chemical analysis showed this shield to consist of better than 95% nickel. Two of the *x*-ray tubes mentioned, after only 24 hours of use, gave photographs on which reflections due to iron and chromium were distinctly evident. One of these tubes was checked after 360 hours of operation, and the photograph obtained showed that the reflections due to iron and chromium had increased noticeably in intensity relative to those of copper.

The problem of preventing the migration of elements within a sealed *x*-ray tube operated under conditions of high vacuum, temperature, and applied voltage is at best a difficult one. It is by no means the purpose of this note to point out a "defect" in tube construction but to stress that the supposition of a superlattice must be considered in light of possible contamination of the *x*-ray target. Such diffraction by spurious radiation is not necessarily eliminated by filtering in all cases, and may appear on powder patterns as well as photographs made by single-crystal methods.

Although our tubes were obtained from the same source, some workers in *x*-ray diffraction apparently have been aware of what appears to be similar contamination for some time in tubes of another prominent manufacturer.

A CHART FOR MEASUREMENT OF OPTIC AXIAL ANGLES

A. C. Tobi, *University of Leiden, Holland.*

Introduction

The simple petrographic microscope is the most widely used instrument for the study of the optical properties of minerals. Therefore any method to measure these properties in this way should receive careful attention.

In the interference figure normal to the acute bisectrix the optic (axial) angle (2V) can be determined by measuring the distance (2D) between the melatopes (points of emergence of the optic axes). 2V can now be calculated with the aid of the equation of Mallard:

$$D = K \sin E = KN_Y \sin V = KN \sin H; \qquad (1)$$

where

D = half the distance defined above, measured in scale units of the eyepiece;
K = a constant dependent on the system of lenses used and on the scale of the micrometer eyepiece;
V = half the true optic angle;
E = half the optic angle as measured in air;
H = half the optic angle as measured in a medium with refractive index N;
N_Y = intermediate refractive index of the crystal;
N = refractive index of another medium (e.g. oil below immersion objective).

For further details of this relationship the reader is referred to a textbook on optical crystallography.

The constant K must be calculated or found by measurement of a mineral of known optic angle.

H. Winchell has published a chart[1] based on this equation. Each combination of lenses used (i.e. each value of K) can be plotted on the chart as a straight line. When this is done 2E (or 2V, when N_Y is known) is read directly for any distance 2D (measured in scale units of the eyepiece, using the Bertrand lens).

Especially in cases where several sets of lenses are used in routine work for the measurements of optic angles, the new chart gives a practical solution. Further details are given below.

The chart here suggested

In the construction of this chart the constant K is eliminated by plotting not 2D, but $d = 2D/2R$:

$$d = \frac{2D}{2R} = \frac{2KN_Y \sin V}{2KN \sin a} = \frac{N_Y \sin V}{A}; \qquad (2)$$

---

[1] Winchell, H., A chart for measurement of interference figures: *Am. Mineral.*, **31,** 43 (1946).

where

$2R$ = diameter of interference figure;
N = refractive index of medium below objective (immersion oil or air);
a = angular aperture of the objective;
A = numerical aperture of the objective;
other symbols as in equation (1).

When this is written in another way

$$\frac{d}{N_Y} = \frac{\sin V}{A} \tag{3}$$

the function is derived on which the chart is based. It is constructed in the same way as the well-known birefringence chart of Michel Lévy. The ordinate is divided from $N_Y = 1.00$ to 2.00, the abscissa from $d = 0.00$ to 1.00. Each value of (sin V)/A, for which 2V is a whole number is represented by a line which intersects the horizontal lines $N_Y = 1.00$ and $N_Y = 2.00$ at d = (sin V)/A and d = (2 sin V)/A respectively, and the ordinate at $N_Y = 0.00$. In place of the (sin V)/A values the chart gives directly those of 2V.

The use of the chart

The chart is designed for use when one objective with known numerical aperture (A) is used in routine work.

The chart given here is constructed for objectives with $A = 0.85$, which are widely used for the measurement of optic angles. When an objective of another aperture (A') is used, the chart can be consulted after multiplication of the measured d-value by $A'/0.85$ (which is easily done with a slide rule). When, however, such an objective is used in routine work, it will be worth while to make another chart to meet this special case.

When a definite set of lenses is frequently used for the measurement of optic angles a $2D$-scale can be plotted along the base of the chart for this particular combination. This is done by measuring the diameter of the interference figure in scale units of the micrometer eyepiece. Should this e.g. be 31.5 scale units, then the distance in the chart between $d = 0.00$ and $d = 1.00$ should be divided in 31.5 equal parts. Along this scale $2D$ can now be used in the chart directly.

The chart can also be used with a simple petrographical microscope without a Bertrand lens; d is then directly estimated in the interference figure as seen without an eyepice. For the determination of a mineral this will suffice in most cases.

The reading of the chart

To obtain 2V from d or 2D the chart is used as indicated by Key 1. As the value $N_Y = 1.00$ is included, the chart can be used also to obtain

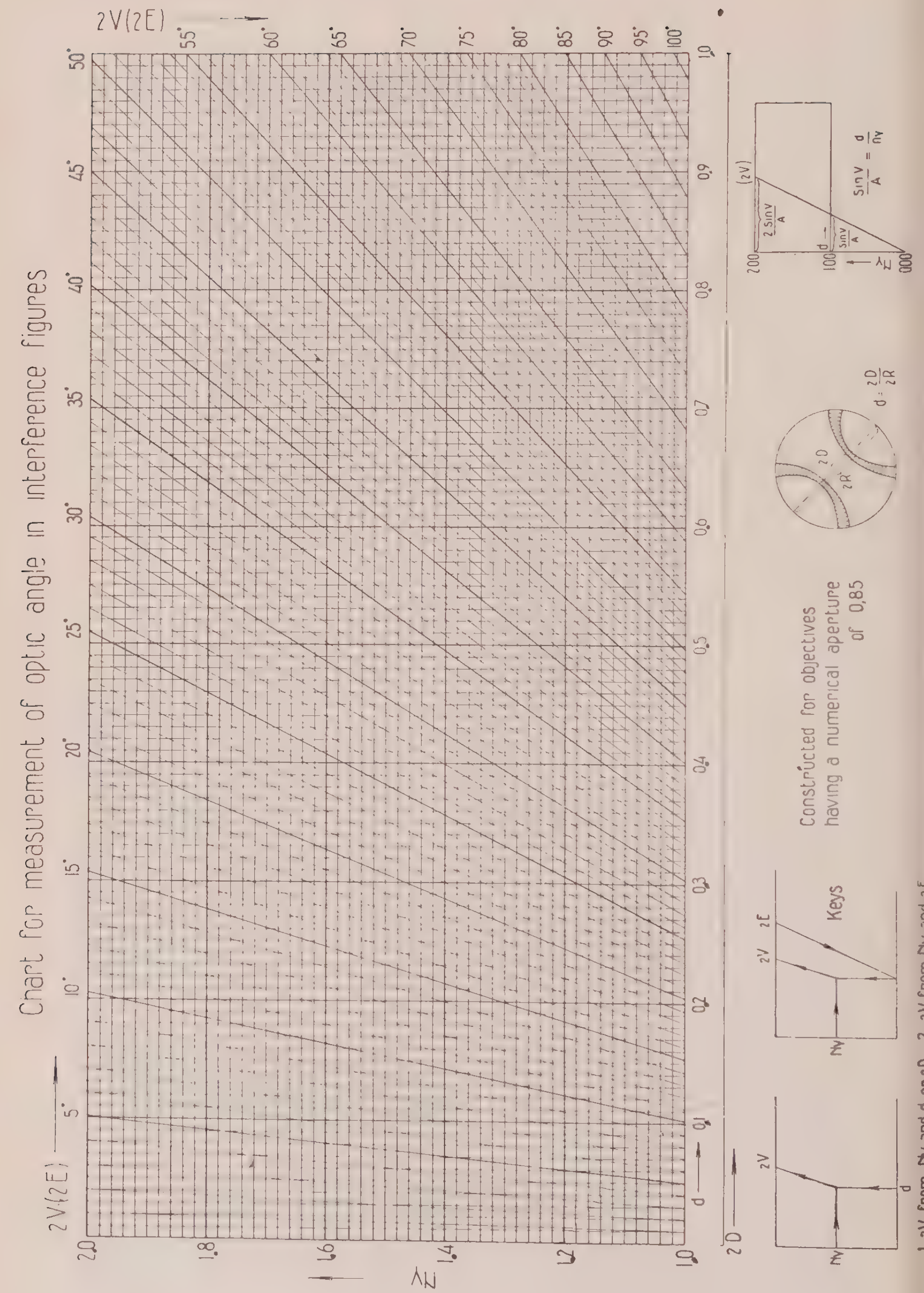
Chart for measurement of optic angle in interference figures
2V(2E)
5°
10°
15°
20°
25°
30°
35°
40°
45°
50°
55°
60°
65°
70°
75°
80°
85°
90°
95°
100°
Nγ
2,0
1,8
1,6
1,4
1,2
1,0
d
0,1
0,2
0,3
0,4
0,5
0,6
0,7
0,8
0,9
1,0
2D
Keys
2V
2E
Constructed for objectives having a numerical aperture of 0,85
2D
2R
d = 2D/2R
(2V)
2 Sin V / A
Sin V / A
200
100
000
Sin V / A = d / Nγ
1. 2V from Nγ and d or 2D 2. 2V from Nγ and 2E

2V from 2E and N_Y, in so far as those values are covered by the graph (Key 2).

As higher and lower values of d (or 2D) are measured with the same degree of accuracy, linear scales are better adapted to the problem than are logarithmic ones.

It will be seen that the reading is of high accuracy, each degree of 2V being represented by a line. Any error made will thus be caused chiefly by the fact that the Mallard equation is an approximation.

The use of oblique interference figures

It is equally possible to measure optic angles in interference figures, in which the acute bisectrix is not well centered. Strictly speaking, the distance between the melatopes should now be measured in two parts, *i.e.* from the center of the interference figure to each of the melatopes. From these two distances $2D'$ and $2D''$ the values 2V′ and 2V″ should then be read separately from the chart and computed afterwards: $2V'+2V''=2V$.

It is seen from the chart however that 2V is almost proportional to d; therefore in practice $2D$ can be measured and used in the chart directly, just as in sections normal to the acute bisectrix. The error will be of the order of 1° or less. The optic plane, however, should be perpendicular or nearly so.

AN EASY METHOD TO OBTAIN *X*-RAY DIFFRACTION PATTERNS OF SMALL AMOUNTS OF MATERIAL

S. A. Hiemstra, *Geological Survey, Pretoria, South Africa.*

It is often desirable to prepare *x*-ray powder diffraction patterns of very small amounts of material. Collodion may be used to work the mineral powder to a small ball between the fingers. It requires much practice to achieve success. The resulting ball may be too large, and some material is often lost.

An easy method to prepare balls which yield good powder diffraction photographs, is as follows: Transfer the small grain, which may weigh less than 0.005 mg., or measure less than 0.1 mm. in diameter, to a clean glass slide. Cover it with a small drop of thin rubber solution (such as can be obtained in a bicycle repair kit) which has previously been placed on another glass slide. The grain can now be ground in the solution between the glass plates without losing any material. Short strokes will prevent the powder from spreading out too much. By inspection under a binocular microscope one can ascertain when the material is fine enough.

Remove the slides from each other for a few seconds to allow the rubber solvent to evaporate. Each slide will show a circular area of clear sticky rubber, with the mineral powder confined to the center of each. The clear rubber can easily be rubbed off with the finger. Put the slides on top of each other again, and with a circular motion, work the powder-rich solution to a small ball, between 0.2 and 0.5 mm. in diameter. Mount this ball on the point of a stiff hair, which has previously been wetted with rubber solution. This ball can now be mounted in the camera with the ball at the middle of the x-ray beam.

In the photograph (Fig. 1) the powder diffraction pattern of pyrite, obtained by means of an 0.2 mm. thick rod, is compared with that obtained by means of a rubber ball. Co-radiation produced at 20 KV and 20 ma., and cameras of 57.3 mm. diameter were used. The upper pattern was obtained by using the rod, and exposing for one hour. In the second pattern a rubber ball was used, exposing for one hour. In the third pattern the same ball was used, but exposure time was increased to two hours.

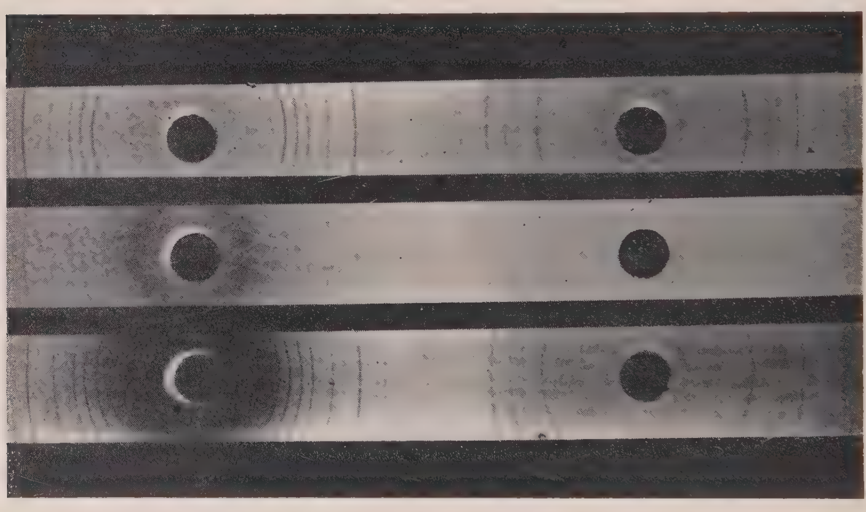

FIG. 1. Powder diffraction patterns of pyrite obtained by means of a rod, above, and rubber balls, in the middle and below.

To compare the accuracy obtainable in the two cases, the upper and lower patterns were measured, and after applying corrections for the film shrinkage, the unit cells were calculated, using the five strongest back reflection lines.

The results are as follows:

$h^2+k^2+l^2$	a_0 (*rod method*)	a_0 (*ball method*)
27	5.417 Å	5.417 Å
29	5.417 Å	5.414 Å
30	5.416 Å	5.417 Å
32	5.417 Å	5.417 Å
36	5.418 Å	5.418 Å

It is evident therefore that, when using very small amounts of material in a rubber ball, the exposure time must be increased. Slightly denser backgrounds are produced. The accuracy may be a little lower.

The method is easy to apply when small amounts of material, such as single grains in heavy mineral fractions, have to be identified. By heating the ball on a platinum plate, all the rubber can be removed, and the material is then available for chemical or spectrographic examination.

A JOINT-FREE SAMPLE SPLITTER*

Charles R. McKinney and Leon T. Silver, *California Institute of Technology, Pasadena 4, California.*

A sample splitter based on the Jones riffle design has been devised which incorporates certain features not found in other splitters heretofore available. The splitter was folded from one piece of sheet metal and as such has neither cracks or joints to hold up material nor joining metal such as solder to contaminate the sample. It is possible to form the splitter from such materials as plastic and paper or to line metal chutes with these materials. Several sizes of 16-chute splitters have been made in this laboratory; the smallest being made from 0.015 inch thick pure aluminum, each chute opening being ½ inch long and ⅛ inch wide. This is a microsplitter comparable to the Otto microsplitter in size. The largest splitter was made from $\frac{1}{32}$ inch thick pure aluminum, each chute opening being 3 inches long and ½ inch wide. An isometric view of a folded 45-degree splitter is shown in Fig. 1. The term "45-degree" refers to the angle between the chute bottom and the horizontal. While 45 degrees is greater than the angle of repose, some hang-up is still experienced and cleaning is required. A 60 degree slope should be much better.

The patterns for 45 degree and 60 degree splitters are shown in Figs. 2 and 3 respectively. Referring to Fig. 2 the distance 2–3 or 5–4 will be the length of the chute opening. The distance *A*, which is the radius of the arcs at the corners, is computed such that the chord of the quarter

---

* Division of Geological Sciences, Contribution No. 784, California Institute of Technology, Pasadena 4, California.

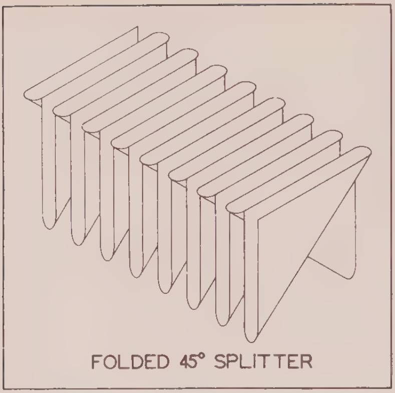

Fig. 1

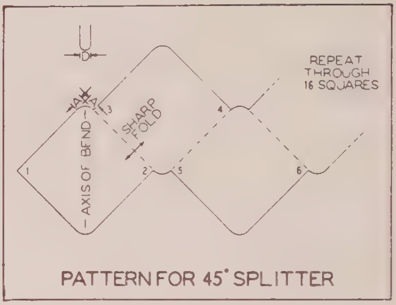

Fig. 2

circle of radius A is equal to half the circumference of a circle whose diameter is D, the spacing of the chutes. Each square is offset from the preceding one by the distance A as shown. If the thickness of the material is kept small compared to the spacing D, no allowance need be made for the length needed for the sharp fold.

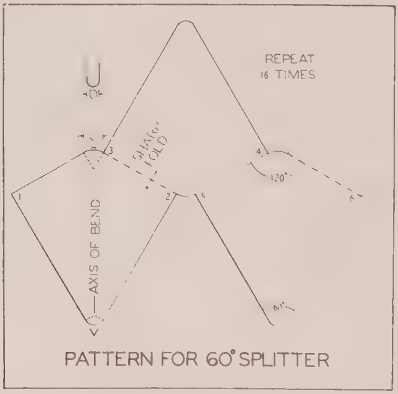

Fig. 3

Folding the splitter begins by bending the first square along the diagonal marked "axis of bend" over a block of thickness D with semicircular edge such that point 1 lies over point 2, as in closing a book. A sharp *reverse* fold is made along line 2–3. The bending block is then placed along the diagonal of the second square, parallel to the first axis of bend, and point 3 is brought over point 4. A sharp reverse fold is made along line 4–5 and the first pair of chutes has been completed. The process is then continued until the desired number of chutes is obtained.

The layout of the 60 degree splitter is similar to that of the 45 degree. The radius of the arcs at the corners being determined such that the chord C is equal to half the circumference of a circle of diameter D, the spacing of the chutes.

The design of the supports, collar and pans is optional. Our splitters are supported at each end with legs made from pure aluminum, fastened together with a single bolt passing under the crotch formed by the chutes. Collars are machined from one piece of aluminum to fit on top of the supported chute assembly. Pouring and receiving pans are also machined from one piece of aluminum to eliminate the need for joining metal. This work was performed under *AEC Contract AT(11-1)-208.*

VALIDITY OF "VEGARD'S LAW"

E-AN ZEN

Vegard and Dale (1928), in their work on binary solid solutions in the cubic system, state as an empirical rule a linear relation between unit cell edge length and composition. Since then, however, this "law" has become accepted by many as of general validity, its soundness being assumed even in non-cubic crystal systems (Chave, 1952, p. 192; Hess, 1952, p. 182). It is taken by some to hold for all ideal solid solutions; and Wasastjerna (1951, p. 2) has employed it as basis for his theory on the heat of formation of binary solid solutions.

In view of this wide publicity, it would be desirable to examine the basis of this "law" theoretically. Consider a binary solid solution in which the volume effects of the two end-members are additive, i.e., the solution shows no volume change upon mixing. Let V_1 and V_2 denote the molar volumes of the two end-members, and N the mole fraction of species 1. We then have for the volume of the solid solution,

$$\begin{aligned} V &= NV_1 + (1 - N)V_2 \\ &= N(V_1 - V_2) + V_2. \end{aligned} \tag{1}$$

In the cubic system and in terms of the unit cell edges R_1 and R_2, equation (1) becomes

$$R^3 = R_2^3\left[1 - \frac{R_2^3 - R_1^3}{R_2^3}N\right] \tag{2}$$

and

$$R = R_2\left\{1 - \left[1 - \left(\frac{R_1}{R_2}\right)^3\right]N\right\}^{1/3}. \tag{3}$$

Now suppose we write "Vegard's Law" in the form

$$R = R_2(1 + \beta N) \tag{4}$$

and compare with equation (3), we see that they are not equal and cannot be made equal by any rearrangement of the factors. The exact equation (3), in fact, is proportional to the cube root of the mole fraction, whereas "Vegard's Law," equation (4), is proportional to the mole fraction itself.

This problem can be formulated in a slightly different way. Writing $\alpha=(R_1/R_2)^3-1$ in equation (3) and expanding the cube root in a series, we get

$$R = R_2(1 + \tfrac{1}{3}\alpha N - \tfrac{1}{9}\alpha^2 N^2 + \cdots). \tag{5}$$

Comparing with (4), we see that $\beta=\frac{1}{3}\alpha$, and the two expressions can be reconciled only when terms higher than the first power in α are negligible, i.e., if

$$\left(\frac{V_1}{V_2}-1\right) \ll 1,$$

which means that the pure end-members do not have very different molar volumes. This fact is intuitively obvious, but equation (5) expresses it analytically and gives a precise relation between allowable difference in end-member volumes and any desired degree of approximation to linearity for the solution (when the other conditions are also satisfied).

REFERENCES

Chave, K. E. (1952), A solid solution between calcite and dolomite: *Jour. Geol.*, **60,** 190–192.

Hess, H. H. (1952), Orthopyroxenes of the Bushveld type, ion substitution and changes in unit cell dimensions: Bowen Volume, *Am. Jour. Sci.*, 173–187.

Vegard, L., and Dale, H. (1928), Untersuchungen ueber Mischkristalle und Legierungen: *Zeits. Krist.*, **67,** 148–162.

Wasastjerna, J. A. (1951), On the theory of the heat of formation of solid solutions: *Soc. Sci. Fenn. Comm. Phys. Math.*, **15,** no. 3.

THE CURVED-CRYSTAL *X*-RAY SPECTROMETER, A MINERALOGICAL TOOL*

Isidore Adler and J. M. Axelrod, *U. S. Geological Survey, Washington 25, D. C.*

Birks and Brooks (1955) have recently described the application of a curved-crystal, reflection-type, focusing *x*-ray spectrometer, using fluorescent *x*-rays, to the determination of microgram quantities of a number of elements. They have reported that the intensities, resolution and line-background ratios for small samples of the order of 1 mg. are comparable to those obtained from a 10-g. sample on a commercial flat-crystal spectrometer.

---

* Publication authorized by the Director, U. S. Geological Survey.

The ability of this type of instrumentation to handle minute samples nondestructively and rapidly makes its application to geochemical and mineralogical problems a natural extension of the method. The technique has been successfully applied in the U. S. Geological Survey to the elemental analysis of *x*-ray diffraction spindles, minute single crystals, and mineral grains in polished ore sections.

Curved-crystal spectrographs have been described by Birks and Brooks (1953) in some detail. The instrument in use in the Geological Survey is also a scanning type spectrograph similar to theirs in principle. A sample holder has been designed which is capable of taking either fibers and single crystals or sections, both thin and polished. The sample holder, which is a modified microscope mechanical stage, permits motion in two directions and makes possible the careful positioning of the sample in the stopped-down *x*-ray beam. For examining *x*-ray diffraction spindles, a narrow slit, approximately 0.5 mm. wide and 5 mm. long, is placed over the *x*-ray tube window. For single crystals or small areas on polished sections the *x*-rays emerge from a pin hole and irradiate approximately 3 square mm. of sample. The area examined may be further reduced by the use of a pin hole in a small section of lead foil which is placed directly on the polished section, with the pin hole directly over the grain to be analyzed.

Successful analyses have been performed with a pin hole approximately 0.5 mm. in diameter.

The area or grain to be investigated is easily located in the *x*-ray beam by the following technique: a small fragment of Patterson screen embedded on a small strip of scotch tape is placed over the grain and the polished section is manipulated by means of the mechanical stage until the fragment of Patterson screen fluoresces brightly. The scotch tape is then peeled off leaving the desired grain in the *x*-ray beam.

Some semiquantitative results obtained on mounted polished sections are illustrated below. Three small areas—chalcopyrite $CuFeS_2$, bornite Cu_5FeS_4, and cubanite $CuFe_2S_3$—were run consecutively. The chalcopyrite was taken as a standard and the iron-copper ratios in the other two calculated. The results of the analysis, all obtained in less than one hour, are shown in the following table.

Mineral	Formula	Ratio of peak intensities CuK:FeK	Calculated atomic ratios
Chalcopyrite	$CuFeS_2$	2:1	Standard (1:1)
Bornite	Cu_3FeS_4	10:1	5:1
Cubanite	$CuFe_2S_3$	1:1	1:2

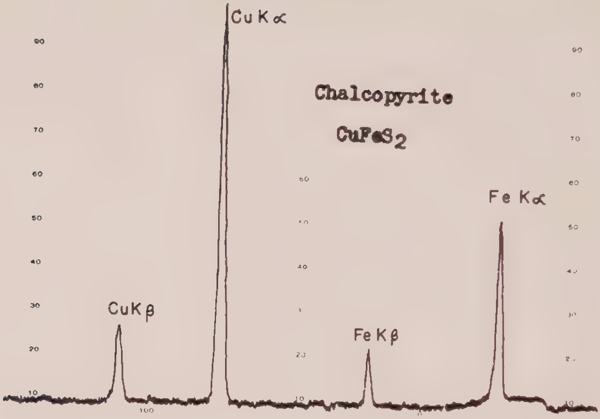
Cu Kα
Chalcopyrite
$CuFeS_2$
Fe Kα
CuKβ
Fe Kβ
90
80
70
60
50
40
30
20
10
100

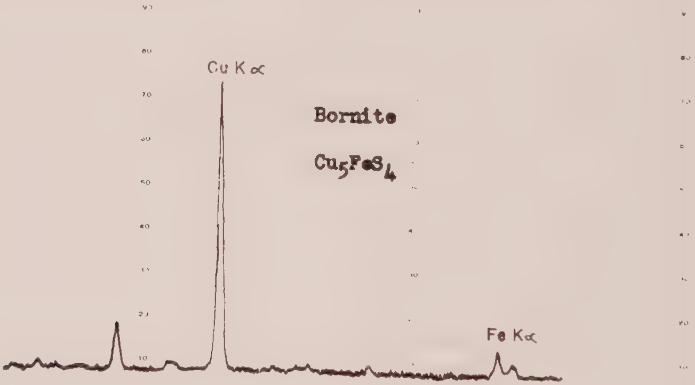
Cu Kα
Bornite
Cu_5FeS_4
Fe Kα
80
70
50
40
20
10

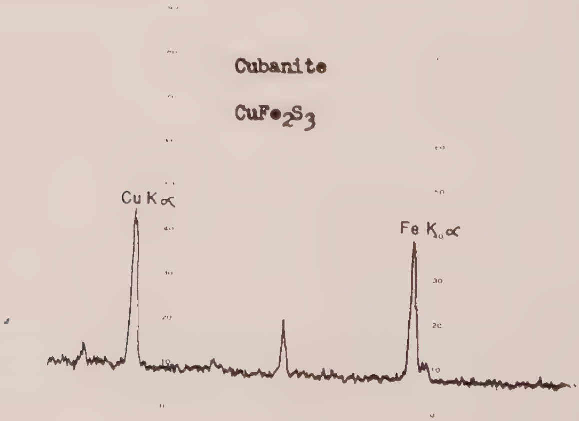
Cubanite
$CuFe_2S_3$
Cu Kα
Fe Kα
30
20
10

The curved, reflection-type x-ray spectrograph is a promising tool in mineralogical research where rapid qualitative or semiquantitative analysis of x-ray diffraction spindles, minute grains, or crystals is needed. The nondestructive character of the method makes it of special value. The present instrument is limited to elements of atomic number greater than 23.

We wish to express our appreciation to Charles Milton of the U. S. Geological Survey for the polished sections and mineralogical data. We also wish to thank L. S. Birks and E. J. Brooks for their help and advice in assembling the spectrometer.

REFERENCES

BIRKS, L. S., AND BROOKS, E. J. (1953), Uniform plastic bending of crystals for focusing x-ray radiation: *Rev. Sci. Instr.*, **24**, 992.

BIRKS, L. S., AND BROOKS, E. J. (1955), Applications of curved-crystal x-ray spectrometers: *Anal. Chemistry*, **27**, 437–440.

INCORPORATION OF IMPURITIES IN SYNTHETIC QUARTZ CRYSTALS

J. M. STANLEY AND S. THEOKRITOFF, *Signal Corps Engineering Laboratories, Fort Monmouth, New Jersey.*

Controlled amounts of selected impurities were incorporated in synthetic quartz crystals during growth to determine their effect on the growth rate, quality and properties of synthetic quartz.

The impurity experiments were carried out under conditions generally used for the growth of quartz from sodium carbonate solutions. The concentration of the solutions was 0.5N and the degree of fill was 70%. The average temperature measured at the top and bottom of the autoclave was 350° C. Temperature gradients between the top and bottom of the autoclaves varied from 20° C. in some runs to 50° C. in others. Observed pressures were 5000–6000 *p.s.i.* The capacity of the autoclaves ranged from 250 cc.–500 cc. The quartz seeds for this work were mostly *AT*-cuts. Growth runs lasted from 8 to 15 days. Resonator plates for evaluation could be cut from the growth obtained in that period of time.

Selection of impurities for addition to solutions for quartz growth was confined to those elements which were believed to be structurally compatible in the quartz lattice with respect to ionic radius and valence. Elements used as additives in these experiments are listed in Table 1 in accordance with their grouping in the periodic table.

Group IV elements were added as oxides; the Group III elements, aluminum and boron as sodium metaborate and sodium aluminate; calcium, the only element tried in Group II, and silver, the only element tried in Group I were added as carbonates. The use of sodium carbonate

TABLE 1

Groups				
I	II	III	IV	V
Na Ag	Ca	B Al	Ti Ge Zr Sn Pb	As

solution in all the experiments made another Group I element available for combination with Group III additives in the quartz lattice. The Group V element arsenic was added as sodium orthoarsenate. The silver ion, although considerably larger than the silicon ion, was tried because spectrochemical analysis has indicated it to be present in certain synthetic quartz crystals.

Of all the elements used in these experiments only aluminum, germanium, lead, tin, and silver were found incorporated in the crystal lattice. The crystals containing lead, tin, and silver were not of the best quality, but those containing germanium and aluminum were of radio-grade. The following table shows the concentration of impurity in the solution, impurity concentration in the crystal and the temperatures at the top and bottom of 12-inch long autoclaves during growth.

No boron was detected in the crystal grown in the run with added boron. Detection of boron by spectrochemical analysis was limited to quantities greater than 300 ppm. It is possible therefore that boron was

TABLE 2

Run No.	Conc. of impurity in sol.	Conc. of impurity in crystal (ppm)	Ionic radius (Å)	Temp. at top and bottom of autoclave	Seed
2636-2	0.2 N Ge^{+4}	Ge-3000	.53	339°–381° C.	Doubly oriented
2636-3	0.2 N Ge^{+4}	Ge-1000	.53	344°–385° C.	Doubly oriented
SN-169	0.5 N Ge^{+4}	Ge-3000	.53	325°–358° C.	*AT* seed
2659-1	0.2 N Ge^{+4}	Ge-1000	.53	287°–344° C.	*AT* seed
2636-1	0.015 N Al^{+3}	Al-100	.51	330°–370° C.	Doubly oriented
SN-138	0.015 N Al^{+3}	Al-200	.51	351°–399° C.	*AT* seed
SN-167	0.03 N Al^{+3}	Al-50	.51	320°–376° C.	*AT* seed
2659-2	0.015 N Al^{+3}	Al-100	.51	332°–348° C.	*Z* seed
SN-132	0.06 N Pb^{+4}	Pb-1000	.84	315°–395° C.	*AT* seed
SN-136	0.05 N Pb^{+4}	Pb-200	.84	345°–378° C.	*AT* seed
SN-165	0.018 N Sn^{+4}	Sn-300	.71	311°–341° C.	*AT* seed
SN-155	0.05 N Ag^{+1}	Ag-200	1.26	350°–365° C.	*AT* seed

present in quantities less than 300 ppm. Boron was the only impurity element which appeared to have an effect on the growth rate.

The crystal containing silver had a rose color.

Overtone *AT* resonator plates prepared from the synthetic quartz crystal containing 100 ppm of aluminum have been investigated by A. R. Chi.[1] This material showed higher inflection temperatures (75° C.) than similar plates cut from both natural quartz (20° C.) and synthetic quartz (40° C.) with no added impurities. The inflection temperature is defined as the point on the frequency temperature curve where the second derivative of frequency versus temperature is zero.

[1] Submitted for publication to *Proceedings of the I.R.E.:* Effects of impurities on resonator properties of quartz, A. R. CHI, D. L. HAMMOND AND E. A. GERBER.

THE GEOCHEMICAL SOCIETY

A new organization known as "The Geochemical Society" was formed on November 7, 1955, during the recent convention of the Geological Society of America in New Orleans. A constitution was adopted which specifies that "the object of the Society shall be to encourage the application of chemistry to the solutions of geological and cosmological problems."

Membership will be worldwide. It is hoped that not only chemists and geologists, but also physicists, biologists, oceanographers, meteorologists, mathematicians and other natural scientists interested in joint attacks on problems in the earth sciences will join in furthering its objectives.

Additional information and membership blanks may be obtained from the Secretary, Professor John C. Maxwell, Dept. of Geology, Princeton University, Princeton, New Jersey.

ANNUAL MEETING

The thirty-seventh annual meeting of the Mineralogical Society of America will be held in Minneapolis, Minnesota, Wednesday through Friday, October 31-November 2, 1956. A series of field trips is being planned for Sunday, Monday and Tuesday preceding the meeting. Detailed notices will be mailed to all members.

Abstracts of papers to be presented at the annual meeting must be received by the Secretary on or before July 15, 1956. Abstract blanks may be obtained from the Secretary.

NOMINATIONS OF OFFICERS FOR 1957

President: D. Jerome Fisher, Department of Geology, University of Chicago, Chicago 37, Illinois.
Vice-President: George E. Goodspeed, University of Washington, Seattle 5, Washington.
Secretary: C. S. Hurlbut, Jr., Harvard University, Cambridge, Massachusetts.
Treasurer: Earl Ingerson, U. S. Geological Survey, Washington, D. C.
Editor: Lewis S. Ramsdell, Mineralogical Laboratory, University of Michigan, Ann Arbor, Michigan.
Councilors (1957–1959): Samuel S. Goldich, Department of Geology, University of Minnesota, Minneapolis 14, Minnesota.
Brian H. Mason, Department of Geology, American Museum of Natural History, New York 24, New York.

BOOK REVIEWS

MICROSCOPY OF CERAMICS AND CEMENTS, INCLUDING GLASSES, SLAGS AND FOUNDRY SANDS, by HERBERT INSLEY AND VAN DERCK FRÉCHETTE (with a chapter on Abrasives, by H. N. BAUMANN, JR.). Academic Press, Inc. New York, 1955. xii+286 pages, 1 fold-in color plate Michel-Levy scale of birefringence). Price $7.50.

Many of the subjects treated in this attractive volume have been covered individually in journal articles, by publications of the *ASTM*, or as chapters in text-books. Such publications cover singly, for example, the microscopy of ceramic glazes, refractories, glass, cement clinker, aggregate for concrete, porcelain enamels, and slags. But the volume under review presents all of these subjects together for the first time, and in addition useful information on microscopic studies of raw materials, structural clay products, foundry sands, and abrasives. It should, therefore, be a most useful textbook in courses dealing with glass technology, metallurgy, cement products, refractories, porcelain, etc., as well as finding wide application as a reference book in research and control laboratories of the corresponding industries.

Perhaps a book that can be highly recommended should simply be recommended and no more said, but rare indeed is a book with no minor faults—and the reviewer can do a service to both reader and author by calling attention to such real or fancied faults as he is able to discern. In the volume under review only 20 pages are devoted to optical mineralogy, obviously not nearly enough to provide an adequate background for the complicated microscopy required to make headway with the difficult materials that form the subject matter of the book. In the opinion of the reviewer, if inadequate space was available, it would have been better to depend on standard textbooks of optical mineralogy for background in this subject, and devote the 20 pages to more details of the microscopic characteristics of raw materials, where many of the mineral descriptions are inadequate. Also, the nomenclature is confusing in some respects. For example, in the table on p. 70 illite is shown as a member of the mica group, as the equivalent of hydrous mica (which is only partly true), whereas in the text the "illite group" is treated as correlative with the montmorillonite group.

There are several usages in the book which are open to question. For example "indices of refraction" is to be preferred to "refractive indices." For symbols of indices of refraction the N_x, N_y, N_z used by Insley and Fréchette are better than nX, nY, and nZ, but the simpler and more generally used α, β, and γ would have been still better. In the footnote on p. 63 "alkaline" should read "alkalic" and the preferred meaning of "presently" (p. 121 par. 2) is still "in a little while" rather than "currently."

In the chapter on optical mineralogy there are a number of statements that do not hold rigidly as written. For example, on p. 18, paragraph 2, lines 14 16, the amount by which E differs from O in an oblique section also depends on their limiting values for a given mineral. The statements concerning extinction angles (footnote, p. 17, and pp. 23 24) are accurate only for principal sections: in others (commonly seen in thin section) the rules as stated are quite misleading, because orthorhombic minerals, for example, can show inclined extinction in oblique sections, and triclinic minerals can show parallel extinction. Also in the footnote on p. 17 the statement is made that tetragonal and hexagonal minerals (are) elongate parallel to *c* only. This is commonly true, but minerals in these systems are by no means uncommonly platy parallel to the basal pinacoid and thus exhibit elongation *normal* to *c*. Less commonly they are elongate parallel to a pyramidal or rhombohedral face and thus oblique to *c*.

In the next to last paragraph on p. 24 the reader is referred to the colored Michel-Levy scale on p. 267, but it is in reality an insert between pp. 268 and 269. In this same paragraph the reader should be told that the grains he is directed to study for flash figures and maximum birefringence are those showing the highest colors.

In the last paragraph on p. 33 a very unsatisfactory method is described for getting a mineral grain in the proper position for measuring a given index. At least two better ones are in common use—embedding the grains in the surface of viscous water glass (Lindberg, *Am. Mineral.*, **29**, p. 317) or on gelatine-coated slides (Fairbairn, *Am. Mineral.*, **28**, p. 396) before the index liquid is added.

On page 63, paragraph 3, the rule for changing volume per cent to weight per cent is incomplete. After multiplying the volume per cents by the respective specific gravities, the figures thus obtained must be recalculated to 100%.

The reference to Austria-Hungary near the middle of p. 83 should probably be just "Austria."

The shorthand method of expressing chemical composition used in the legend of Fig. 10.11, p. 192, should either be explained in the text, or not used.

These minor shortcomings could easily be corrected in a second edition, but even if they are not, they do not detract seriously from what is by all odds the most complete and best treatment of the microscopy of ceramics, cements, and related materials ever attempted.

EARL INGERSON

PRAKTISCHE EDELSTEINPRÜFUNG, a German rendering by W. F. EPPLER of the fifth edition of B. W ANDERSON'S GEM TESTING FOR JEWELLERS. Octavo, 262 pages, 5 colored plates, 64 illustrations in the text, and 12 tables. Rühle-Diebener-Verlag K.G., Stuttgart, Germany, 1955. Price, bound, 24.90 marks.

The first edition of Anderson's GEM TESTING FOR JEWELLERS appeared in 1942 and was reviewed in some detail on pages 60 and 61, Vol. **28**, 1943, of this journal. The book was well received and in subsequent editions was expanded and the illustrations increased. It is now in the fifth edition.

Eppler's rendering in German is exceptionally well done. The English version was closely followed, but in cases where new material became available after the English text was published, Eppler supplied this and other pertinent information in brief footnotes. The book is well printed on good paper. The colored plates—one on absorption spectra, and four showing cut gemstones, not in the English text—are excellent. A worthwhile addition to German gemological literature has been made by Eppler.

EDWARD H. KRAUS,
University of Michigan,
Ann Arbor, Michigan

REPORT OF THE COMMITTEE ON THE MEASUREMENT OF GEOLOGIC TIME, 1953–1954. PUBL. **333** NATL. ACAD. SCI.—NATL. RES COUNCIL, DIV. EARTH SCI. 193 pp. 1955. $1.75.

This will be the last report of the Committee on the Measurement of Geologic Time under the auspices and leadership of the late John P. Marble. Since the death of A. C. Lane the results of the work of the committee have been coordinated by Dr. Marble, who devoted much time to the organization and preparation of the annual reports. These reports have always been informative summaries, and since the enormous expansion of research work on the geology and mineralogy of radioactive materials they have become additionally useful, particularly for the annotated bibliographies they contain. The report for 1953–1954 follows the arrangement pattern of its predecessors, with the following entries: (1) Report of the chairman—a general summary of activities and results in the field of geologic time measurement both for radioactive techniques and other methods;

(2) Annotated bibliography of articles related to geologic time (131 pp.), compiled by Marble; (3) Recent work on natural variations in the ratios of the stable isotopes by Marble—an eight page summary with a 76-entry bibliography; (4) A translation by Marble and Dr. Taisia Stadnichenko from the Russian of an article by G. R. Rik and G. V. Avdzyeliko, entitled "On the question of the variation of the isotopic composition of common lead" (*Dokl. Akad. Nauk, U.S.S.R.*, **90,** 829–831, 1953); and (5) Reports from overseas collaborators.

As has been the case for previous reports, this summary, too, will be a valuable reference tool for anyone in mineralogy or geology interested in age determination methods or "radioactive geology" in general.

E. Wm. Heinrich,
University of Michigan,
Ann Arbor, Michigan

A DESCRIPTIVE GLOSSARY OF RADIOACTIVE MINERALS, by James W. Crosby III. Washington State Institute of Technology, Bull. **230.** 148 pp. Paper cover, multigraphed. 1955. State College of Washington, Pullman, Washington (no price indicated).

This bulletin presents brief mineralogical descriptions of about 200 radioactive minerals (exclusive of varieties and synonyms) under the four major categories originally used by Frondel and Fleischer (*U. S. Geol. Survey, Circ.* **74,** 1950):

I. Minerals containing uranium and thorium as major constituents.
II. Minerals containing uranium and thorium as minor constituents.
III. Minerals that, if investigated by modern analytical methods, might show uranium or thorium content (a category abandoned by Frondel and Fleischer in *U. S. Geol. Survey, Bull.* **1009-F**).
IV. Minerals that are non-uranium or non-thorium bearing, but that have been reported to contain impurities or intergrowths of uranium, thorium, or rare-earth minerals.

Each of the species is described in capsule form under numerous entries including: name, composition, crystal system, habit, radioactivity, cleavage, color, luster, specific gravity, hardness, fracture, optical (properties), occurrence, tests, varieties, remarks, and references. The bulk of the data has been obtained from Dana's System of Mineralogy, 6th and 7th ed.; U. S. Atomic Energy Commission **RMO-563** by D'Arcy George; Dana-Ford Textbook of Mineralogy; Winchell's Elements of Optical Mineralogy, 3d ed., Part II; and U. S. Geol. Survey Circulars **74** and **194** by Frondel and Fleischer. In the introduction it is stated that the " . . . bulletin is designed primarily to meet the needs of the geologist or mining engineer . . . not to fill the requirements of the highly skilled mineralogist . . . or the prospector and amateur. . . . "

Compilations of this type can be useful and informative, provided that the data are listed accurately and have been chosen with discrimination. There is little purpose, however, in a book that purports to aim at such an *intermediate* level in describing in detail all of the numerous rare mineral species whose radioactivity is very minor and whose occurrences are severely limited (lovozerite, melanocerite, rinkolite, etc.). Nor does it seem worthwhile to describe the properties of minerals of markedly questionable validity in a glossary of this type (medjidite, hokutolite, randite, uraconite, etc.), when a mere listing of invalid species would suffice.

The glossary also contains many errors, and for some species the information is incomplete or outdated; e.g., aldanite does not contain V; bassetite is not a monoclinic modification of autunite; the most significant occurrence of brannerite, that in the Blind River Ontario region is not mentioned; djalmaite is a synonym of microlite and is not a valid species; the composition of gummite cannot be represented by a formula and hardly by $UO_3 \cdot nH_2O$; studtite does not contain Th; no mention is made of meta-tyuyamunite; the description of metazeunerite is incomplete; davidite is not a mineral with *minor* U content; Khabina for Khibina; no description is included of uraniferous collophane-francolite; and the "Bulletins of the Mineralogical Society of America," referred to in the introduction, are non-existent; what is meant, of course, is *The American Mineralogist.*

E. W. Heinrich,
University of Michigan,
Ann Arbor, Michigan

THE MICROSTRUCTURES OF DIAMOND SURFACES, by S. Tolansky, N.A.G. Press, Ltd., 226 Latymer Court, Hammersmith, London, W. 6, 1955, 67+viii pages, 9 Figures, 143 Plates, Price, 40 s.

Professor Tolansky's The Microstructures of Diamond Surfaces presents a summary of his work on the nature of irregularities of crystal faces, cleavage surfaces, and polished and etched surfaces of diamonds. The techniques are those developed by the author—multiple-beam interferometry and the light-profile.

After an introductory chapter, a qualitative description of the methods employed is given. A more thorough treatment was published in "Multiple-Beam Interferometry of Surfaces and Films," Oxford, 1948. Some characteristics of diamond are briefly dealt with in the third chapter. The nature of the surface markings on octahedron faces, especially the characteristic trigons, are described in Chapters 4, 5, and 6. It is interesting to note that diligent search over a period of years has failed to disclose on diamond the appearance of growth spirals which are so prevalent on some crystals.

The linear discontinuities which Professor Tolansky considers may be due to slip, although he suggests twinning as an explanation, are described in Chapter 7. It seems to the reviewer that these lines are more likely thin twin-lamellae. None of the "perfect" diamond crystals on which hardness studies have been made at the University of Michigan has been free of twinning, which often manifests itself as lines (similar to those illustrated) on polished surfaces. Since these lines are parallel to octahedron planes, the distribution of trigons along such lines may be associated with other structural disturbances which are characteristic of twin boundaries in the diamond.

Etching is described in Chapter 8. In the chapter on cleavage (Chapter 9), it is pointed out that the mineralogical texts describe the cleavage of diamond as "perfect," whereas from an interferometric point of view the cleavage is far from perfect. Of course, the term "perfect cleavage" in the mineralogical sense is a relative one used to describe semiquantitatively the relative completeness of specular reflection of broken surfaces of crystals as determined by inspection with the unaided eye. Actually there are various degrees of perfection within this category. Since these terms are used primarily in the identification of minerals (cleavage is probably the most constant of the easily determined properties of crystals) much as hardness is used, a more precise statement is unwarranted. In this sense diamond does have a perfect cleavage.

The interesting fact that the two parts of a cleaved diamond do not match in detail is illustrated. Examples of a much better match of parts of cleaved topaz and mica are given. Possibly other substances could be found which behave as does the diamond.

Shadow casting, a less sensitive method for the study of larger features, is described in Chapter 10. In Chapter 11 are described both natural and induced percussion cracks.

In the final Chapter (12) studies on polished surfaces are described. The limit of attainable flatness on a diamond surface is discussed. It is concluded from the studies that no Bielby layer exists in diamond polishing, a conclusion which seems most reasonable.

Directional hardness measurements of E. M. Wilks, using the Grodzinski and Stern hardness microabrasion method, are described. The sensitivity of symmetry to orientation is in agreement with the reviewer's published findings. The multiple beam interferogram of a diamond hemisphere ground on Grodzinski's apparatus shows a high degree of perfection over the small area shown in the photograph. The tremendous directional hardness variation in diamond makes such accuracy quite difficult to attain.

The core of the work is a truly remarkable series of 143 plates, most of which are multiple-beam interferograms of diamond surfaces. Many of these rival in beauty the extraordinary photographs of interference phenomena of an entirely different nature published early in the century by Hauswaldt.

The general format and the quality of presentation are excellent. Reading would be made more pleasant if the plates were located closer to their textual references. Page references in the table of contents would facilitate the location of specific material.

This book is a must for all investigators whose work deals with diamond surfaces. It should be of general interest to mineralogists and crystallographers.

Reynolds M. Denning,
University of Michigan,
Ann Arbor, Michigan

SMALL-ANGLE SCATTERING OF X-RAYS, by André Guinier and Gérard Fournet, translated by Christopher B. Walker. John Wiley and Sons, Inc., New York, N. Y., 1955. 268 pages, 78 figures, bibliography of 569 references. Price $7.50.

The authors deserve much credit both for recognizing the need for such a book and for satisfying it so admirably. As they state in the preface: "Since the late 1930's many theoretical works have appeared in this field; starting from different points of view, these have occasionally arrived at different, but non-contradictory, results. In a parallel manner, apparatus based on quite varied principles have been used in experimental methods. We believed that it was now time to collect and evaluate the results that have been obtained from the different approaches."

The key role played by Professor Guinier in the development of small-angle scattering methodology and its applications qualifies him singularly for the task of writing the first monograph on the subject. His co-author, Dr. Fournet, is well known for substantial theoretical contributions in the field. The number of workers employing the small-angle scattering technique is growing rapidly as the fields of its application are extended, and it is these new recruits who will feel particularly grateful for this book. At the same time experienced workers are sure to regard it as an indispensable reference work.

After a short introductory chapter, the authors devote the 78 pages of chapter 2 to a comprehensive treatment of the present theoretical state of the subject. Lack of space precludes presentation of many of the mathematical derivations, but all the significant formulas are given together with a thorough appraisal of their meaning and accuracy. The reader is referred to appropriate original papers for any details necessarily omitted.

The third chapter describes the kinds of equipment employed and the proper choice of experimental conditions to yield different types of information, such as long spacings, radius of gyration, and specific surface. The fourth chapter shows how the theory is applied to the interpretation of the experimental data. Chapter 5 compares particle sizes measured by small-angle scattering with values obtained by other physical methods.

Chapter 6 is devoted to applications in chemistry, biology, and metallurgy, which gives it special practical importance. Included are descriptions of studies of such subjects as virus molecules, proteins, hemoglobin, natural and synthetic fibers, catalysts, adsorbents, and heterogeneities and age-hardening in metals. The usefulness of the book is enhanced by the inclusion of an extensive bibliography of small-angle scattering literature consisting of 569 references. This is a revision of a 398-title bibliography compiled by K. L. Yudowitch and issued in 1952 by the American Crystallographic Association.

The authors and translator have produced a lucid, readable text; however, it is understandable that a thorough grasp of the theoretical portions requires both painstaking attention and occasional reference to the original literature. The reviewer found a few typographical and grammatical errors and a number of more consequential errors in the references at the chapter ends. However, these defects are trivial in relation to the high quality of the book in all major respects.

LEROY E. ALEXANDER,
Mellon Institute,
Pittsburgh 13, Pennsylvania

ANNOUNCEMENT OF A SPECIAL DOUBLE NUMBER OF GEOCHIMICA ET COSMOCHIMICA ACTA, JULY–AUGUST, 1956

This issue will contain the following papers:

(1) Silica in Hot-Springs Waters
Donald E. White, W. W. Brannock, and K. J. Murata, U.S.G.S.
(2) Dissolution and Precipitation of Silica at Low Temperatures
Konrad B. Krauskopf.
(3) Potassium-argon Dating
R. E. Folinsbee.

Subscribers who wish extra copies of this special issue may obtain them for $4.20; non-subscribers for $7.00. For $2.80 additional non-subscribers may obtain the entire current volume of 6 numbers. Orders may be sent to:

Pergamon Press, Inc.,
122 East 55th Street,
New York 22, New York

and should be received by early July so that the proper number of copies can be printed.

Kandites, Smectites

G. Brown, Report of the clay minerals group subcommittee on nomenclature of the clay minerals. *Clay Minerals Bull.*, **2**, No. 13, 294–302 (1955).

Tentative proposals on nomenclature include the following:

"Smectites is the name proposed for the minerals at present variously known as the montmorillonoids, montmorins, minerals of the montmorillonite group, or frequently even montmorillonites. Smectites are defined as minerals composed of 2:1 or triphormic layers, which, when the readily exchangeable cations are replaced by Na^+ and the material is saturated with glycerol, give a basal spacing of 18 Å, approximately. Such minerals have a cation exchange capacity of 70–120 m.e./100 g. for readily exchangeable cations."

"Kandites is proposed for what are presently known as the minerals of the kaolinite group or the kaolin minerals. These are the minerals composed of 1:1 (diphormic) layers with essential chemical composition close to $Al_2O_3 \cdot 2SiO_2 \cdot 2H_2O$."

"The group names are plural but an individual member of the group may be called for example 'a smectite.' The group names can also be used as adjectives, for example 'the smectite content.'"

Discussion: I think that the proposed names are bad ones and I hope that they are never used. New names for minerals or mineral groups should not be introduced unless absolutely necessary. The terms "kaolinite group minerals" and "montmorillonite group minerals" have been in general use for many years and are understood by all workers in the field, and this is an advantage that far outweighs the use of fewer words. The resurrection of the long abandoned smectite, which had been used for both montmorillonite and halloysite, is particularly unfortunate.

I hope that all who are concerned with clay minerals will send comments on these and other problems of nomenclature to the British Clay Minerals Group and to the Committee on Nomenclature of the Mineralogical Society of America, so that these will have a basis for future discussion of the problems.

Michael Fleischer

Ledikite

G. Brown, *op. cit.*

The name ledikite is proposed for the material described by G. F. Walker, *Mineralog. Mag.*, **29**, 72–84 (1950), as a hydrous mica bearing the same relation structurally to biotite as dioctahedral illite does to muscovite.

The name is for the locality, East Ledikin, Aberdeenshire.

Discussion: Walker (1950) wrote: "In spite of these difficulties, however, it is not proposed to introduce a new mineral name at this time, since it is felt that this would be likely merely to add to the existing confusion in the nomenclature of the clay micas, especially since data on the trioctahedral clay mica itself are still rather scanty."

Yoder and Eugster, *Geochimica et Cosmochimica Acta*, **6**, 182–183 (1954), discussed Walker's data and stated, "An examination of the diffuse *x*-ray pattern and the accompanying table of indexed reflections published by Walker suggests that this material is a 1 *Md* trioctahedral mica."

The status of this material and, indeed, the whole nomenclature of the hydrous micas therefore require reconsideration. Dr. Walker's statement of 1950 quoted above is still a good one, and I regret that he has not agreed to the subcommittee's proposal of this new name.

M. F.

Ordonezite

G. Switzer and W. F. Foshag, *Am. Mineral.*, **40,** 64–69 (1955).

Rabbittite

M. E. Thompson, A. D Weeks and A. M. Sherwood, *Am. Mineral.*, **40,** 201–206 (1955).

Navajoite

A. D. Weeks, M. E. Thompson and A. M. Sherwood, *Am. Mineral.*, **40,** 207–212 (1955).

Goldichite

A. Rosenzweig and E. B. Gross, *Am. Mineral.*, **40,** 469–480 (1955).

Hawleyite

R. J. Traill and R. W. Boyle, *Am. Mineral.*, **40,** 555–559 (1955).

Cerianite

A. R. Graham, *Am. Mineral.*, **40,** 560–564 (1955).

Neomesselite

C. Frondel, *Am. Mineral.*, **40,** 828–833 (1955).

Beta-Roselite

C. Frondel, *Am. Mineral.*, **40,** 828–833 (1955).

Paramontroseite

H. T. Evans, Jr., and M. E. Mrose, *Am. Mineral.*, **40,** 861–875 (1955).

Murdochite

J. J. Fahey, *Am. Mineral.*, **40,** 905–906 (1955).
C. L. Christ and J. R. Clark, *Am. Mineral.*, **40,** 907–916 (1955).

Tavorite

M. L. Lindberg and W. T. Pecora, *Am. Mineral.*, **40,** 952–966 (1955).

Barbosalite

M. L. Lindberg and W. T. Pecora, *Am. Mineral.*, **40,** 952–966 (1955).

Gonyerite

C. Frondel, *Am. Mineral.*, **40,** 1090–1094 (1955).

M. F.

NEW DATA

Fischerite (=Wavellite) (?)

N. G. Sumin, Are fischerite and wavellite identical minerals? *Trudy Mineralog. Muzeya, Akad. Nauk. S.S.S.R.*, No. **5,** 146–152 (1950); from an abstract by Wilhelm Eitel in *Chem. Abs.*, **49,** 15649 (1955).

Emil Fischer. Über die Selbständigkeit des Minerals Fischerit. *Heidelberger Beitr. Mineral. Petrog.*, **4**, 522–525 (1955).

Fischerite was described in 1844 by R. Hermann. Wherry (*Am. Mineral.*, **2**, 32 (1917) suggested that it was identical with wavellite. Sumin examined material from Nizhnii Tagil (type locality) and from Mednorudyansk, Urals. Fischer examined a sample from Nizhnii Tagil in the Humboldt University collection, marked "Coll. G. Rose" and 5 similar samples from the Freiberg collection, labelled as having been sent from Russia to Breithaupt in 1838.

Goniometric data gave $a:b=0.594:1$ (Sumin), $0.5505:1$ (Fischer). Wavellite has $a:b=0.5577:1$ (Dana, 7th Ed., Vol. 2, p. 962, as the average of rather discordant values). *X*-ray powder patterns of fischerite and wavellite appear to be identical (Sumin) (Fischer). G. (fischerite) 2.43 (Sumin), 2.32–2.36 reported for wavellite. Hardness (fischerite) 4–5 (Sumin); $3\frac{1}{2}$–4 reported for wavellite. Fischerite is optically biaxial, positive with α 1.531, β 1.540, γ 1.552, 2V 65° (Sumin, who states that these are higher than the data for wavellite. (However, even higher indices have been reported for wavellite, see Dana, p. 963.)

The original analysis of fischerite corresponds to $6\ Al_2O_3 \cdot 3\ P_2O_5 \cdot 24\ H_2O$, whereas the accepted formula of wavellite corresponds to $6\ Al_2O_3 \cdot 4\ P_2O_5 \cdot 26\ H_2O$. New analyses (Fischer) gave: P_2O_5—wavellite 34.7, fischerite 35.3, fischerite (green crust) 35.7%; ignition loss—wavellite 28.2, fischerite 27.5, fischerite (green crust) 24.7%. The crust contains a little copper. Fischer states that the low H_2O and the Cu of the crust indicate the presence of callaite or chalcosiderite, and this was confirmed by the *x*-ray powder photographs.

From his data, Sumin concludes that fischerite is an independent species; from his own data, Fischer concludes that fischerite is identical with wavellite.

Discussion: The *x*-ray data seem to me to be decisive in favor of Fischer's conclusion.

M. F.

Scawtite

J. Murdoch, *Am. Mineral.*, **40**, 505–509 (1955).
J. D. C. McConnell, *Am. Mineral.*, **40**, 510–514 (1955).

Hewettite, Metahewettite

W. H. Barnes, *Am. Mineral.*, **40**, 689–692 (1955).

Niggliite

W. O. J. G. Meijer, *Am. Mineral.*, **40**, 693–696 (1955).

Kutnahorite

C. Frondel and L. H. Bauer, *Am. Mineral.*, **40**, 748–760 (1955).

M. F.

DISCREDITED MINERALS

Beyrichite

C. Milton and J. M. Axelrod, *Am. Mineral.*, **40**, 767–769 (1955).

Schizolite (=manganoan pectolite)

W. T. Schaller, *Am. Mineral.*, **40**, 1022–1031 (1955).

Melanolite (=delessite)

C. Frondel, *Am. Mineral.*, **40**, 1090–1094 (1955).

M. F.